THE UNIVERSITY OF MICHIGAN

INDUSTRY PROGRAM OF THE COLLEGE OF ENGINEERING

STRESS ANALYSIS AND DESIGN OF FIXED DENTAL STRUCTURES BY TWO DIMENSIONAL PHOTOELASTICITY

Mohamed K. El-Ebrashi

A dissertation submitted in partial fulfillment
of the requirements for the degree of
Doctor of Philosophy in
The University of Michigan

March, 1968

IP-814

ACKNOWLEDGMENTS

The author wishes to express his appreciation to:

Professor Robert G. Craig for his advice, assistance and guidance during the entire course of this investigation.

Professor Samuel K. Clark for his suggestions involving the photoelastic experiments.

Professor George E. Myers for his suggestions concerning the application of the findings to dentistry.

Professor Floyd A. Peyton for his encouragement and advice concerning the applications of engineering methods to dental research.

Professor Edwin H. Young for his advice involving the experimental design and presentation of results.

In addition, acknowledgment is due to the Ministry of Higher Education, the United Arab Republic Government, for support throughout the graduate program through several grants, which were administered by the School of Dentistry, University of Alexandria, Alexandria, U.A.R.

The aid of the Industry Program of the College of Engineering in the final preparation of the manuscript is much appreciated.

TABLE OF CONTENTS

TABLE OF CONTENTS (CONT'D)

TABLE OF CONTENTS (CONT'D)

LIST OF TABLES

LIST OF FIGURES

LIST OF FIGURES (CONT'D)

LIST OF FIGURES (CONT'D)

LIST OF SYMBOLS

d	Width.
D	Diameter.
E	Modulus of elasticity.
E_m	Modulus of elasticity of a model.
E_p	Modulus of elasticity of a prototype.
f	Stress optical coefficient.
F	Force.
h	Thickness.
I	Moment of inertia.
K	Stress concentration factor (theoretical or geometrical).
K_f	Fatique stress concentration factor.
l	Length.
M	Bending moment.
m	Mass.
N	Integer, order of extinction, number of fringes.
p	Probability.
P	Load.
r	Replication in factorial design.
$S_{\bar{x}}$	Standard error of the mean.
t	Thickness.
x	Abscissa of a point.
x, y, z	Cartesian coordinates.
α, β, θ	Angles.

ϵ	Normal strain.
λ	Scale factor in dimensional analysis.
μ	Poisson's ratio.
ν	Degrees of freedom.
σ	Normal stress component.
σ_n	Normal component of the resultant stress.
$\sigma_x, \sigma_y, \sigma_z$	Normal stresses on planes perpendicular to the x, y, and z axes.
$\sigma_1, \sigma_2, \sigma_3$	Normal principal stresses.
σ_{max}	Maximum stress.
σ_{nom}	Nominal stress.
τ	Shear stress component.
τ_n	Shear stress component of the resultant stress.
$\tau_{xy} = \tau_{yx}$ $\tau_{yz} = \tau_{zy}$ $\tau_{xz} = \tau_{zx}$	Shear stress components in cartesian coordinates.
τ_{max}	Maximum shear.

GLOSSARY

Analyzer

A prism or a sheet of polarizing material which allows only those rays of light to pass through, whose plane of vibration is parallel to the axis of the analyzer.

Axial Wall

It is the wall in the cavity prepared in a tooth, which is parallel to the long axis of that tooth.

Birefringency

It is a property of certain transparent materials; plates made of this material have the property or resolving the light into two components and transmitting it in planes at right angles.

Brittle Coating Method

The method is based on the perfect adhesion of a coating with brittle characteristics to the component being studied. When loads are applied, strains developed in the substructure are transmitted to the coating, and ultimately the stresses cause the coating to fail in tension by cracking.

Buccolingual Section

It is "radial" section through the tooth from the buccal side (pertaining to or adjacent to the cheek) to the lingual side (pertaining to the tongue).

Chamfer

In extracoronal cavity preparations, a marginal finish that produces a curve from an axial wall to the junction of the wall of the cavity with the surface of the tooth.

Circular Polarized Light

It is a beam of polarized light in which the tip of the vector representing the wave motion moves in a helix along the beam.

Crossed Polariscope

It is a polariscope in which the planes of polarization of the analyzer and the polarizer are placed at 90°.

Fringes

Fringes are black lines seen in the field of a polariscope when monochromatic light is used to illuminate a loaded model, or colored lines when white light is used.

Gingival

Pertaining to or in relation to the gingiva.

Isochromatic Fringe Pattern

Isochromatics are a family of fringes, along which ($\sigma_1 - \sigma_2$) equals a constant, depending on N , the order of the fringe.

Isoclinic Fringe Pattern

Isoclinics are a family of fringes, along which the principal stresses have a constant inclination, to some arbitrary reference.

Isotropic Point

It is a location where the two principal stresses are equal ($\sigma_1 = \sigma_2$). In the photoelastic model this is represented by the zero order of interference.

Mesiodistal Section

It is a section through a tooth, from the mesial surface (toward the center line of the dental arch) to the distal surface (away from the center line). It is perpendicular to the buccolingual section.

Mohr's Circle

It is the most commonly used method of representing stresses and strains at a point, where stress or strain quantities appear as rectangular coordinates.

Oblique Incidence Method

It is a method for separating the principal stresses, commonly used in stress analysis.

Occlusal

Pertaining to the contacting surfaces of opposing teeth.

Polarized Light

When the vibration pattern of the electromagnetic waves of light exhibit a preference as to the transverse direction of vibration, then the light is considered to be polarized.

Plane Polarized Light

It is obtained by restricting the light vector to vibrate in a single plane known as the plane of polarization, which has a constant inclination to an arbitrary reference plane.

Polariscope

It is an apparatus used to provide the light rays used and to hold the model to be analyzed. Two general groups of polariscopesare known, transmission polariscopes and doubling or reflection polariscopes.

Polarizer

The same as analyzer, used to convert a beam of ordinary light to plane polarized light.

Principal Directions

There are three mutually perpendicular directions at a point in a three dimensional stress system. No shear stresses act on planes perpendicular to these directions.

Principal Stresses

These are normal stresses acting in the principal directions.

Proximal

Pertaining to the surface of a tooth or the portion of a cavity that is nearest to the adjacent tooth. The mesial or distal surface of a tooth.

Quarter Wave Plates

These are sheets of polarizing material which provide a retardation of one-quarter wave. Such a plate generates circularly polarized light, and two in sequence are used to suppress isoclinics.

Reflected-Light Polariscope

This is a polariscope used and designed for birefringent coating analysis. Observation of the birefringent coating by means of this polariscope gives a fringe pattern which is related to the surface strains of the specimen.

Retardation

If a doubly refracting plate is placed in a field of plane polarized light, the light vector is resolved into two components, which travel through the plate with different velocities, and the two components will emerge from the plate at different times.

Shear-Difference Method

It is a method to completely determine the state of stress at interior points in the model, and used in two-and three-dimensional photoelasticity.

Three-Dimensional Photoelasticity

This is a method where stresses are frozen into the model, and the fringe pattern remains in the model when the load is removed.

Time-Edge Effect

When a photoelastic model is machined from a sheet of plastic and examined under no load condition as a function of time, it is noted that a stress is introduced on the boundary which produces a fringe parallel to the boundary.

Two-Dimensional Photoelasticity

This is a method where a suitable model is fabricated, loaded, and placed in a polariscope and the fringe pattern is examined and photographed.

White Light

When the components of the light vectors are of different frequencies, the colors of the components are mixed and the eye records this mixture as white light.

CHAPTER I

INTRODUCTION

For many years, the problem of structural design of fixed dental restorations and their failures has been the topic of intensive clinical research. Little attempt has been made, however, to "design" cavities prepared in teeth and restorations to correspond with the principle of reduction of local stress concentrations. Since the early work of G. V. Black in 1908, cavity design has not changed basically, and the current concepts used in dentistry still depend upon clinical experience and empirical practices. Quantitative testing of these old "rules" was rarely attempted, due to the complicated and irregular morphology of the teeth which defies mathematical analysis.

Three main factors usually encountered in dental design, are namely, biological, esthetical and mechanical. The mechanical factors are the only ones considered and investigated in this thesis, keeping in mind the biological and esthetical limitations encountered in restorative dentistry. The limit of mathematical methods of stress analysis is quickly reached when dealing with dental problems, hence they represent a classical example of the problem for which no theoretical solutions have yet been reached.

In contrast, experimental stress analysis technics could be used in the determination and improvement of the mechanical strength of structures. Experimental methods do not remain, however, as mere counterparts of theoretical methods of stress analysis but encompass those, utilizing all the conclusions reached by theoretical considerations, and go far beyond them in maintaining direct contact with the true physical nature of the problems under consideration.

Photoelasticity is the most versatile method of experimental stress analysis, and variations of this method rank among the oldest as well as the newest of the methods. Among the chief advantages of the method are: (1) It provides a means of obtaining an overall picture of the shear stress distribution throughout the body, (2) Measuring stresses at a point with consequent possibility of finding actual peak values of the principal stresses even in regions of high stress gardient, and (3) Determining stresses in problems that could not be solved analytically, with accurate stress determination in models of irregular geometry which would lead to accurate computations of stress concentration factors. For these reasons, the photoelastic method of stress analysis was chosen for the investigation of structural analysis and design of dental structures, since it will provide accurate information about these analytically indeterminate problems in all stress fields. Pursuant to this aim, an attempt is made in this research to assess the overall

stress picture in different dental designs and compare them through computations of geometrical stress concentration factors, as well as by statistical inference techniques.

In summary, it is the purpose of this study to investigate the stresses in the various components of dental bridges restoring the posterior teeth of the lower jaw (lower posterior three-unit fixed bridges), and to measure quantitatively the effects of design modifications of the different preparations on the stresses in the restorations. The determination of the optimum design of several preparations on the abutment teeth is also one of the objectives of this investigation. This study should serve as a basis for further investigations of other types of dental restorations such as partial and complete dentures, and orthodontic appliances.

CHAPTER II

REVIEW OF LITERATURE

A. History

The discovery of artificial double refraction, i.e., the production of double refraction effects by stress applied to an isotropic transparent material, was made by Brewster in 1816.[12] When a piece of glass was stressed and viewed by polarized light transmitted through it, a brilliant color pattern due to the stress was seen. The possibility of valuable engineering applications, however, was not immediately recognized, and few practical problems were investigated with photoelasticity prior to 1900. The theory of photoelasticity was further developed by many physicists, notably Neuman[168] (1841) and Maxwell[154] (1853). Both of them discovered the stress-optical law independently. It was not until 1891, however, that an actual application of the photoelastic method was made. At that time, Wilson[227] published the results of a photoelastic investigation of a simply supported beam subjected to a single point load. Mesnager[157] made further applications in 1901.

These early workers were seriously handicapped by the lack of a suitable material for the construction of models. Glass, a very insensitive material, was the only one available for this purpose. The introduction of Celluloid gave impetus to the development of photoelasticity. It was not

until 1920, long after the theory of elasticity had become well accepted, that definite progress was made in photoelasticity. At this time, Coker started the publication of a series of pioneering articles which led to the publication of the treatise by Coker and Filon in 1931.[29] Alexander,[2] Mindlin,[160] and Frocht[75,76] followed their leading treatise. The photoelastic method was the first precise method developed in experimental stress analysis for the solution of plane stress problems.

B. General Survey of Photoelasticity Literature*

1. Optics Related to Photoelasticity.

The generally accepted theory of light is Maxwell's electromagnetic theory.[107] According to this theory, light is an electromagnetic disturbance, represented by two vectors, an electric vector and a magnetic vector, perpendicular to each other, and to the direction of wave propagation. The most recent theory is the quantum theory which can be considered as a combination of a corpuscular theory and a wave theory.[196]

Applications of the principles of optics to the polariscope have been investigated for many years. The details of removal of isoclinics prior to photography were discussed by Mindlin.[159] The employment of a large source of light and

*Under this title, general brief reference will be made to the most important contributions in the last twenty-five years. No attempt was made to present an exhaustive review, as it is beyond the scope of this dissertation.

a collimating lens to collect parallel rays from the model was a significant contribution to improve the optics in photoelasticity.[110] It was shown in 1948 that the size of the light source and the thickness of the model directly affects the sharpness of the recorded fringes.[166] Accurate calibration of quarter-wave plates was presented by Jerrard in 1952,[109] and an easy practical way was suggested for eliminating the isoclinics in 1954.[130]

2. Theory of Photoelasticity.

Two-dimensional stress-optic law, in terms of absolute retardations, was used to determine the individual principal stresses by means of a Mach-Zender interferometer.[70] In 1939, Mindlin[160] published two important articles reviewing the theory and the corresponding separation technics. The theory was developed further by Frocht in 1941-1948,[77-79] and by Jessop and Harris[112] in 1950, demonstrating its wide applications in engineering design. Detailed separation of stresses in beams supplemented by examples, were published by Timoshenko and Goodier in 1951.[214]

Photography technics in photoelasticity[72] were refined in 1958, followed by an investigation of stresses in composite models with notches and holes in the same year.[199] A detailed analysis of the isochromatics in photoelasticity, correlated to the theory of elasticity appeared in 1958.[59] The accuracy and limits of applications were discussed in great length in 1961,[162] showing that the error does not exceed two percent.[81]

In 1962, a method was presented to sharpen and double isochromatic fringes,[44] by the superposition of ordinary light- and dark-field isochromatic fringe patterns (mixed field). The new mixed-field pattern represents an increase by a factor of two in the number of countable fringes. The stress-optical coefficient was established to be independent of the wave length of light in 1964,[220] after much controversy about the correlation. Again in 1967, the accuracy of two-dimensional experiments was checked, and good agreement was reported between theoretical and experimental technics. The error was estimated to be about five percent when uniform edge loading was employed.[201] In the same year, a new multiple-exposure photographic method was described, which would produce isotatics along with isochromatics in the same photograph.[94]

3. Materials Used for Photoelastic Models.

The word "model" as used throughout this investigation will mean the specimen built to study the stress or strain distribution in a prototype, usually geometrically similar to the prototype and usually scaled up or down. The criteria for selection of model materials were discussed in detail.[45]

The time-edge effect was explained in 1942, to be a result of absorption, or evaporation of moisture from the surface of the model.[132] Castolite was preferred to Bakelite, due to its insensitivity to time-edge stresses.[82]

At the same time, Columbia Resin (CR-39) was introduced,[25,32] but it was found to creep, hence the material fringe value must be determined as a function of time.

Epoxy resins were first introduced in the mid 1950's, when they were employed as materials for three-dimensional photoelasticity.[43,140] Although the epoxies are susceptible to time-edge effects, the rate of diffusion of water into epoxy is sufficiently high to permit a saturation condition to be achieved in about two months. The modulus of elasticity of epoxy at room temperature is about 300,000 - 550,000 psi, and at the critical temperature (about 270°F) is about 2,000 psi. The tensile strengths at the two temperatures are 12,000 and 200 psi respectively, and the material fringe value, about 65 and 0.70 psi/in/fringe.[45,63]

4. Techniques of Analysis in Photoelasticity.

In conventional two-dimensional photoelastic stress analysis a suitable model is manufactured, loaded, and placed in a polariscope, and the fringe pattern is examined and photographed. The interpretation of the isochromatic and isoclinic fringe patterns, and compensation and separation techniques have been detailed in several publications. (References 42, 53, 76, 81, 129 and 179).

The Tardy method of compensation was developed in 1929,[111,212] to determine the order of isochromatic fringe at any arbitrary point in the model. The method is considered to be superior over other methods, since no auxiliary

equipment is necessary, and the analyzer of the polariscope serves as the compensating device. Fractional fringe orders obtained by this method are accurate to two decimal points, and are often quoted in the literature.[45]

The shear-difference method was developed in 1939,[122] and refined in 1941.[77] The method is used to determine the principal stresses at interior points in the model. Decreasing the size of the intervals in the grid system employed in the shear-difference method, would lead to greater accuracy of the results.[99,219]

Other methods of separation of stresses were developed, which include the interferometer methods,[169,178] and the oblique incidence method;[53,54] only the second method is comparable in its accuracy to the shear-difference method.[54]

The interpretation of the experimental data depended on the fact that the stress distribution in the model could be transferred to the prototype, except in the immediate vicinity of the point of load application.[27] The application of dimensional analysis techniques was established in stress-analysis.[134] Langhaar showed that the difference between the number of original variables and the number of dimensionless products in a statical problem of stress-analysis is usually two, since these problems involve only two dimensions, force and length.[131]

C. Applications of Photoelasticity

The photoelastic method of stress analysis was used to solve numerous problems in engineering and dentistry. The engineering applications of photoelasticity will be discussed briefly, while those in dentistry will be presented in greater detail.

1. Applications of Photoelasticity to Engineering.

The problem of localized stresses in regular geometric shapes lends itself to the photoelastic method. Fillet profiles,[6] circular discontinuities,[57] elliptical discontinuities,[62] stresses in gear teeth,[52,98] curved beams,[51] and the effect of holes and notches in shafts,[80,104,193] were investigated using photoelasticity. The determination of stress-concentration factors is usually attained by the photoelastic approach. (References 58, 69, 73, 75, 80, 83, 101, 105, 118, 144, 172, 173 and 221).

The design of machine parts has been studied in many instances experimentally, using the appropriate scaling factors.[60,100,102,171] Stresses in structures, with emphasis in automotive and aeronautical engineering are numerous.[50,61,65,141,181]

In all two-dimensional problems, several results could be obtained from these applications, namely, differences of principal stresses at every point, secondary maximum shear at every point, stress tangential to free boundaries, the positive acute angle between a principal stress (either

σ_1 or σ_2) and a given reference axis, isostatics could be drawn, directions associated with σ_1 and σ_2, stress ratios and stress concentration factors, shear stress at any point, and individual values of the principal stresses.[59,81]

2. Applications of Photoelasticity to Dentistry.

In 1949, Noonan published the first paper in dentistry. (Reference 170). Different shaped cavities made in Bakelite models, were packed with silver amalgam. The load used was about 55 lbs., applied to the center of the restoration. He found that a flat floor exhibited less stress concentration than the one that is rounded. Castro published her work,[21] Comparing four types in cavity preparations for primary teeth. Four Bakelite models were constructed, and she found that flat or rounded floors were better than double sloping floors or a flat floor with central notch. King[124] investigated three types of occluso-proximal restorations in aluminum molds. He did not rank the three structures, but concluded that the photoelastic method is suitable for dental research. In Japan, Yajima[231] found high stress gradients behind anterior upper teeth. In 1954, Haskins, Haack, and Ireland[93] studied the effect of rounding axio-pulpal line angles, as well as the stress distribution associated with the variations of vertical axial walls. They used Catalin models mounted in matrices made of low fusing models. They found that less stress concentration existed in deep cavities (15 mm), while rounding and sloping of the axial walls did

not have any influence. There was a marked reduction of stress when the pulpal wall was rounded and sloped. Walton and Leven presented a three-dimensional photoelastic study of an anterior jacket crown.[224] Four slices were investigated, and they came to the conclusion that the thicker the walls of the jacket, the greater its strength. They also found that greater strength is obtained by providing a generous bevel of the lingualproximal line angles.

In 1955, Mahler and Peyton[148] reviewed the general applications of photoelasticity as a research technique for analyzing stresses in dental structures. In Belgium, Massa (Reference 153) published an extensive photoelastic study of the femur bone along with an elementary study of two mandibular incisors in occlusion. Also he presented the first photoelastic study of the human mandible, showing the different areas of tension and compression.

In 1956, Mahler[149] published his findings on the resistance form of a disto-occlusal amalgam restoration in a primary mandibular first molar. He found the failure of the restoration in the isthmus was due to the presence of tensile stresses, and maximum stress being at the occlusal surface of the restoration. The tensile stresses could be reduced if the isthmus was placed as close to the axial wall as possible. The least tensile stress in the restoration was found for the sloping axial wall in combination with the flat pulpal wall. In 1958, Guard et al.[88] studied buccolingual sections of Class II cavity restoration.

Five different forms were studied, and the cavity preparation containing the "gently rounded pulpal wall" and "gently rounded line angles" showed the lowest value of the maximum fringe order around the boundary of the model.

In 1959, Miyauchi[161] published a three-dimensional study of anterior abutment teeth. The published report was rather qualitative in nature, and no attempt was made to compare the different restorations. In 1960, Sato[192] published a report, investigating traumatic occlusion as a cause of alveolar pyorrhea. No tentative conclusions were achieved.

In 1961, a study was published showing the difference between shoulder and shoulderless jacket crowns with incisal loading,[174] and it was found that a short preparation exhibited a higher stress concentration factor than a longer one, due to the larger exerted moment. No computations were made to substantiate the results. A study of strain patterns in jacket crowns on anterior teeth was published by Lehman and Hampson in England (1962).[135] Araldite crowns were constructed for stress freezing, and eight slices were compared in a table, showing that the stress increased from 661 psi near the incisal edge of the crown to 6,042 psi near the gingival part of the crown, which helps explain why crescent shaped fracture lines occur near the gingival part of the crown. Dimensional analysis was used in arriving at the cited values.

The midline fracture of upper dentures was investigated in Germany by Klotzer in 1963,[126] using three-dimensional photoelasticity. Maximum tensile stresses were shown dorsally to the upper incisors. The author concluded that the possibility of breakage could be reduced by good molding, by avoiding notches or cracks, and by the use of acrylic resin reinforced by fiber-glass.

Colin et al.[30] investigated stress concentrations in full crown restorations, and they found that sharp angles at the gingival shoulders ought to be avoided, since such areas are more prone to failure than restorations with rounded line angles. Klotzer[127] used three-dimensional photoelasticity to study the stability of complete upper dentures. He demonstrated high stress gradients in the midlines of dentures.

Buccolingual sections of ten different Class II cavities were studied by Guard.[89] He reported that rounded line and point angles are better in cavity design, and the obtained results could be adapted to Class I preparations. The stresses produced by expansion of dental amalgam were described by Robinson,[183] where he built two Araldite models, having parallel walls versus undercuts. Control models were left unfilled with amalgam. Distributed loads were used, and the author found out that "no great stress was set up in the tooth model by a well-made amalgam filling."

Comparative investigations of Class II cavity restorations of dental amalgam were reported by Granath in 1965.[87] He inferred that an experimental cavity with a semi-circular floor and inclined walls (7°), was slightly superior to an inverted cone cavity with a plane pulpal floor, rounded internal line angles, and similarly inclined walls. He also mentioned that greater proximal depth and "Bronner-inclination" increased the maximum compressive stress at the inner vertical border with a one-point concentrated load, thus indicating increased retention of the proximal portion. He showed that a slightly rounded pulpal-axial line angle is recommended, in order both to facilitate the packing of the amalgam and to avoid the risk of irregularities of the isthmus.

Rumetsch, Schreiber and Motsch[189] reported their studies of statics of jacket crowns using two-dimensional photoelasticity. It was shown that the worst direction of stresses resulted from a shoulder which had a rounded inside corner; sharply cut shoulders showed more favorable results, indicating that the best distribution of stresses resulted from the shoulderless preparation. In the same year, Johnson[113] showed the inclusion of irregularly shaped pulp chambers in three-dimensional models of lower molars, did not effect the load distribution in the models, but slightly modified the stress distribution at the base of the cavity. He mentioned that the stress concentration factors were "not conclusive, but they did exhibit a trend, which agreed with that to be expected from normal engineering practice." Johnson *et al.*[114] studied Class I cavities and reported

that those with rounded line angles do reduce stress concentrations by about 30 percent, and those with a continuously rounded pulpal wall by over 50 percent.

In England, Robinson[184] studied the wedging effect of dental restorations using two-dimensional photoelasticity. He found that the greatest stresses were produced when there was a wedging effect, i.e., when there was a protuberance on the restoration or on the cavity in such a way that when the restoration was seated, the walls were forced apart. He postulated that this wedging effect might cause dental pain.

Klotzer[128] in Germany, studied three-dimensional photoelastic models of upper jaws, to be restored with partial dentures. He published detailed isoclinics and isostatics of the intact models, showing directions of principal stresses, without any numerical analysis. In England, 1966, Lehman and Meyer[136] studied the relationship of dental caries and stress concentrations, using three-dimensional photoelastic models. The results have shown that mechanical stresses in contact areas of teeth might be the direct cause of initiation and propagation of early carious lesions. They also concluded that "crowning" of teeth intended to be used for partial denture clasping would be the safest measure, from both the mechanical and biological viewpoint.

Craig, El-Ebrashi, and Peyton[38-40] examined several sections of teeth which had inlays and crowns, using two-dimensional photoelasticity. They found that compressive

stresses could be reduced near the pulpal floors of certain cavities, if the applied load was moved mesially or distally. It was found that rounded axio-pulpal line angles lowered the stress-concentrations, in occluso-proximal restorations. In crowns, it was established that multiple point contact on abutments reduced stress concentrations near the central fossa of the restored teeth. Increasing the bulk of proximal restorations near the cervical margins, and rounding the reduced cusps on the preparations improved the structural design and strength of crowns.

D. Structural Design in the Dental Literature

The improvement of engineering design is often accomplished first by some method reducing the cross-sectional area of low-stressed regions, and second by increasing the cross-sectional area in the regions of maximum stresses, thus allowing the concentration of stresses to be distributed over a greater area.[69] This is not the case, however, in structural design in dentistry. Much of mechanical dentistry is founded on artistic technics, which are carefully followed without reasonable comprehension of the reasons for the various steps. Thus a dental restoration or appliance, for a specific purpose, has been developed by trial and error methods. Actually, through the process of "clinical" failure and resulting change, the form and dimensions of dental restorations have become serviceable. The end result may approach that which would have been produced by

support is transmitted to the embedded portion of the beam, and the proximal part would tend to bend or rotate out of the cavity. Gingival retention with a moment equal to the dislodging one was needed to prevent the unwanted rotation, and he defended a gingival bevel or a seat on that basis. In 1957, however, Kanders[119] reported that the basic consideration to the periodontal health "is to maintain a knife or a feather edge" in dental restorations. In the same year, Bartels[5] recommended a lingual and proximal right angle shoulders, and a labial chamfer, to improve the strength of full porcelain veneer crowns. Smith,[202] in 1957, also asserted that the knife-edge margin of the shoulderless crown was ideal for periodontal health, because "the finishing line is definite, unbroken by irregularities and is superior for fitting." Lucca in 1959,[147] felt that the chamfer preparation for crowns was "ideal" periodontally, because" it is easily prepared and easily finished on teeth."

Tylman and Tylman[216] discussed the different types of margins encountered in restorative dentistry. They emphasized the importance of the width and angle of shoulders, and concluded that as a general rule the width of shoulders should not exceed 0.5 mm, and the angle may vary between acute and right angles, considering an obtuse angle to be similar to the chamfer in morphology. It therefore was considered to be a modified shoulderless preparation. Their treatise was almost in complete agreement with that of Conod.[31]

Johnson et al.[116] discussed bridge failures in detail, and attributed looseness of bridges to marginal failures, as a result of excessive "torque" that would break the cement bond. They correlated this failure to insufficient retention in abutment preparations.

In 1962, Wilson and Lang[228] reported that the knife edge margin is the most generally used in restorative dentistry "because it provides a definite marginal finish line with a minimum of removal of tooth structure, and it has adequate strength and even greater retention hence more tooth structure is circumscribed." Herlands et al.[97] added that the chamfer margin has the advantage of "a tapered finishing line rather than a square edge, as in the case of full shoulders." Colin, Kaufman and Papirno[30] did agree with the later statement, because they found photoelastically that sharp angles at the gingival shoulder exhibited higher stress gradients than those with rounded line angles.

Rosner[187] (1963) presented the rationale for beveling margins in gold castings. He reported that the bevel could serve four functions, namely, to reduce inherent defects in castings and cementation, to pretect enamal rods at margins, to allow for burnishing after cementation, and to augment circumferential retention. Fusayama et al.[85] showed that the magnitude of exposed cement varied with the types of cervical margins, and the best seating of a casting

was that of the chamfer type, and for that reason they concluded that it is the optimum design (based on the degree of misseating and the extent of the exposure of the cement).

Rosentiel[186] (1964) reported that marginal fit and retention were the two main criteria for a good restoration. He asserted that the bevel angle should be between 30° and 45° to ensure good "edge strength". In 1965, Miller and Belsky[158] published an extensive report, discussing the advantages of full shoulder preparations for periodontal health, because "it had a definite and clearly defined finishing line, and less tooth structure is removed in the area of pulpal horns."

2. The Concept of Parallelism of Axial Walls.

Parallelism of axial walls is important in retention of dental restorations. Tylman[216] reviewed the relationship, and concluded that a slight divergence of 2° to 5° from parallelism would furnish the required resistance to displacement by bucco-lingual torque. Jørgensen[117] concluded that the relationship between the retentive force and the angle of convergence in cemented veneer crowns to be a hyperbola, with parallel axial walls showing the highest retention. Schwartz[195] evaluated axial walls, and found that pulpal and axial walls should be flat and at right angles to one another.

The retention of inlays and crowns was analyzed as a function of geometric form by Rosentiel.[185] He agreed and confirmed Jørgensen's work, and interpreted the decrease

in retention as taper of axial walls increase, because inlays and crowns can move into the preparation in one definite path, or "path or insertion." Geometry and mechanics were used by Lewis and Owen[142] to evaluate the degree of convergence of axial walls. They reported that by increasing the slope of axial walls, their length increases and the retentivity decreases. They assumed in their hypothesis that both the crown and the tooth were rigid bodies, i.e., the distance between every pair of points remained fixed, and that the adjoining sides of the crown and the prepared tooth were frictionless.

In France, LeHuche[139] estimated the angle of convergence of anterior abutments to be about 5°, and that for posterior abutments to be 10°. Convergence of axial walls was discussed by Kaufman et al.[121] They found that every unit area of a prepared tooth surface having the same degree of convergence, has the same retentiveness regardless of the height of the inclined planes of the axial walls. They also established that the areas closer to the gingival termination contributed the greater proportion of retention, due to "larger diameter, more contact and reinforcing effect." Pickard[177] interpreted the convergence of axial walls as the real source of retention, asserting that an occlusal convergence of 5° was "acceptable".

3. The Concept of Occlusal Reduction.

There has always been a great deal of controversy about the extent of covering of occlusal surface by gold. Keyes[123] was concerned with rounding of reduced cusps and elimination of sharp point angles, rather than studying the exact extent of occlusal reduction, due to lack of precision of casting procedures of dental golds at that time (1943). "Tipping the cusps" was discussed by Smyd,[203] to place safely the inlay margin on enamel supported by dentin, when a cusp is undermined by caries. Weinberg[226] applied the law of sines to study the components of forces on occlusal surfaces of posterior teeth. He established the unpolished gold restorations would cause high coefficient of friction where it is least needed.

LeHuche[139] reported that occlusal reduction of cusps, and extension of gold margins to cover them, is especially indicated to protect pulpless teeth, where the risk of fracture is eminent. He reported that one millimeter of gold was adequate to serve that function. Roucoules[188] asserted that in occlusal reduction, the tips of the cusps should be flattened mesiodistally, but buccolingually, occlusal reduction should conform anatomically to the height of the cusp and of the fossa depth, with an optimum occlusal thickness of the restoration between 1-2 millimeters. Cuspal protection by gold, was claimed by Brass[11] to facilitate full protection of lingual cusps of upper and buccal cusps of lower teeth, hence both

are involved in masticatory function. He stated that "gold replacing the reduced area must be of sufficient bulk to resist any change in form and prevent the opening of the margins under masticatory forces."

Johnston et al.[116] reviewed the indications of occlusal coverage, and stated that if cusps exist, then occlusal surface should be prepared to reproduce roughly the contour of uncut surface. They summarized the three fundamentals of retention, namely, 5° - 7° convergence of axial walls, circumferential irregularity to prevent rotation around the long axis of the crowns, and "enough metal thickness" to protect the occlusal surface. Protected cusp restorations were discussed by Schultz et al.;[194] they claimed that gold extended to cover reduced cusps does provide for "greater structural strength of the casting" itself. The extent of reduction of tooth structure was not evaluated.

4. Vertical Pins in Restorative Dentistry.

In recent years, the pendulum has been swinging toward conservation of tooth structure and maintaining gingival health. Full coverage no longer is considered as the only concept of retention. Pins were introduced to augment the retentivity of intracoronal retainers, so as to avoid disturbing the gingival margin.[163,200]

Jeanneret[106] was the first to apply elementary statics to pins in restorations. He established that combining pins with onlays, would supply a significant increase to any displacing tensile force, thus augmenting the anchorage of the restoration. Morrant[163,164] confirmed this interpretation in usage of pins in periodontal splints.

The introduction of multiple parallel pins in extensive occlusal rehabilitation is credited to Karlstrom[120] in Sweden. Sanell[191] concluded that pins were indicated whenever a minimum removal of tooth structure was desirable. He stated that no ledge was necessary if the path of insertion exceeded 45°.

In 1965, Embrell[67] reported the retentive qualities of pin-retained castings. He established the retention of cemented castings increases as the diameter and length of pins were increased. Mann, Courtade and Snell[152] found that parallel pins were better than tapered pins, because the former provided continual retention during attempted dislodgement, while with the latter, any slight dislodgement would result in loss of the retention of the pin in its tapered channel. Wagner[222] maintained that pins engaged in remaining sound dentin, could act in conjunction with either limited retention from the internal wall or external sleeve.

Burns[20] reported that there was no significant differences when three basic designs were tested; five parallel-sided pins, three parallel-sided pins, and three tapered pins. These results maintained that reliance on pins as the sole source of retention was hazardous, and some extracoronal retention should be included in the preparations. Dumont[56] felt that pins do supply enough retention in restorative dentistry. Lorey et al.[146] showed that the retention of cemented castings increased significantly as the diameter and length of pins were increased. They found that castings with threaded, 4.0 and 0.75 millimeter diameter, pins registered the greatest retention.

5. Proximal Design in Compound Restorations.

Clinical experience would often insinuate which type of proximal reduction, the slice, or the box with parallel walls or diverging walls, is the appropriate design. The decision is often arbitrary concerning the form and shape of proximal designs in compound restorations.

As early as 1934, Wylie[230] compared the slice and box preparations in posterior teeth, by the weight loss method. He found the amount of tooth substance saved through the slice preparation gave it "slight preference" over the box type. Klaffenbach[125] felt that slices were better because "they increase retention, save time and conserve tooth structure." Hendrick[96] agreed with Wylie[230] and he also used the weight difference method.

He observed that greater extension of margins is an advantage rather than a disadvantage. Thom[213] maintained that the slice preparation displayed an unnecessary amount of gold buccally, and the margins were not extended "far enough" bucco-lingually at the gingival third to include a very susceptible area where decay might begin later. His objection to the design was purely esthetical and biological, rather than mechanical, and he believed that box preparations were superior.

Symd[205] discussed the slice preparation, and felt that its usage in all indirect technics of metal inlays was rather hazardous. Tylman[216] recommended the incorporation of either a lock or a channel in the slice, to increase its retentivity. Brunel[18] was the first to use auxiliary slices buccally and lingually, as an external retention form.

The main advantages of the slice restoration were cited by Hampson,[91] namely, assurance that enamel prisms at the cavity margin are well protected, and conservation of tooth structure. Schultz et al.[194] observed that the decision, to which form the proximal design should be shaped, depends mainly on tooth form. They stated that "in general, a broad proximal contact both bucco-lingually and occluso-cervically will dictate the use of the slice preparation." They maintained that this slice preparation

provided external support of weakened tooth tissues or areas subjected to high stresses during function. It was advocated that auxiliary slices would serve as a source of external retention.

6. Structural Design of Dental Bridges.

The fundamentals of structural design of dental bridges require a thorough knowledge of the principles of engineering design, as well as with the biological, mechanical, and esthetical restrictions of the oral cavity.[223] The conventional structural design is primarily concerned with the analysis of given structures.[4,17] The usual design procedures in engineering, involve a repetition of the process of informed experimental and theoretical testing of the structural geometry by analyzing the corresponding stresses and deflections, and by modifying the sections which have either insufficient or excessive integrity. The process continues until the designed structure is both safe and economic. It is important to consider that all fatigue failures occur at points of stress concentration, or stress raisers such as grooves, fillets, holes, threads, keyways, etc.

In dentistry, redundant geometry and continuous variations of the forces applied to the structures, impose a serious challenge for the practitioners. Considerations of both forces, and materials used in the construction of dental bridges, should be a required accompaniment to

the planning and construction of dental bridges. The primary objective of a dental bridge is to receive the forces of mastication and occlusion, and to transmit them through the abutments to the supporting tissues. If the transmitted forces were large enough, or if the bridge was improperly designed, damage to the supporting tissues, and/or the bridge would follow. Precise knowledge of the mechanical and physical properties, of both dental golds and the hard dental tissues is axiomatic for the determination of proper design.

Bending moments in models representing dental bridges were studied by Smyd.[204] Bending moments of semifixed bridges (fixed at one end only) were found to be higher than those estimated for fixed bridges at both ends. It was shown that deflection varied with the cube of the length, i.e., doubling the span of the bridge would increase deflection by a factor of eight. Deflection also was inversely proportional with the cube of the depth.[203]

Load carrying capacities were theoretically determined by Brumfield.[16,17] He established the load carrying capacity varied directly as the first power of the width of the beam (bucco-lingual), directly as the square of the depth (occluso-cervically), inversely as the first power of the length of the span (mesiodistally), and directly as the proportional limit of the alloy used in bridge construction. He asserted the most important

factor in the design of bridges was depth, but unfortunately, it was beyond control for biological reasons. Partial denture gold was recommended for longer span bridges, because they would have progressively lower load carrying capacities. Soldered joints should be as deep occluso-gingivally as possible. He advocated in planning, the maximum stress allowed in dental bridges should not exceed 60 percent of the proportional limit of the alloy used. (25,000-60,000 lb./in.^{2}).

Idealization of dental beams as long blocks was attempted, and equations for computations of moments of inertia, section modulus, and maximum stresses were presented. (Reference 15).

Measurement of oral forces was tried by Howell,[103] Ledley,[133] and Tylman.[217] The range of functional forces, in the oral cavity, was found to be 37.5 to 128 pounds, from the anterior to the posterior portions of the oral cavity, respectively. Telemetry was recently used, for measuring vertical and lateral occlusal forces,[26] and it was found that the transmitted force was less than the total applied force on models.

The physical properties of human enamel and dentin were also investigated,[34-36] and recently the tensile strength of dentin was established to be about 6,000 psi,[137] while its compressive strength was previously reported to

be 35,000 ± 8,000 psi.[209,210] A detailed discussion of these properties will appear later in the present investigation.

The types of ends of dental bridges were generally studied by few authors[1,15,91,116,139,216] and it was interesting to find less emphasis on cantilever bridges in dentistry.[68] It was claimed that posterior cantilever bridges would function "as a neutralizing force against the anterior component of force, thus reducing the ever present tendency for a forward tooth movement."

The design of pontics always was treated ambiguously in dental literature. Ante[3] suggested that the bucco-lingual width of the occlusal surface of a pontic of a bridge should not exceed 90 percent of the bucco-lingual width of the tooth which is being replaced. No evidence has been presented to substantiate this empirical statement. Many terms were used to justify the narrowing of the pontic, such as decreasing leverage, torque, stress, force and thrust on the abutment teeth.[92,115,165,229] Sometimes it was even claimed that this modification of design would be mandatory to "decrease the load" carried by the abutment teeth in function.[92,115] The progressive reduction in width of the pontic as the span length increases was based on the notion that "deflection is proportional to the cube of the length of the restoration." (References 165 and 229). The normal width concept was advocated by other authors[7,216] because "nature should

be reproduced." The relationship of design to restorative materials was generally discussed.[150,151,217] Until recently, no accurate reporting about tooth statics was attempted. Dempster and Duddles[48] found that two static systems may be contrasted; one which is involved principally with the action of a force couple on the crown, and the other results from oblique or transverse forces on the crown. They concluded that the force vectors on the different parts of the roots attack them at specific angulations, at particular regions and with varying magnitudes. The first report concerning the measurement of stresses in fixed bridges using a brittle coating technique, was published in 1965.[37] The posterior bridges when loaded deflected in a typical transverse manner, since little if any tipping occurred. The stress and directions of strain were found to be function of load, position of force application, and mass and shape of the restoration. Strain gages were used to study the stress distribution on gold and chromium alloy bridges.

Summary

The preceding review of the literature is an extremely brief account of the technical concepts concerning the design of fixed dental restorations. It is by no means intended to be an all-inclusive presentation. Omitted from this review are the voluminous numbers of reports concerning the different theories and approaches to occlusion,

functional disturbances of the masticatory system, diagnosis and treatment planning of functional disturbances of occlusion, cutting instruments and technics of tooth reduction, casting procedures or corrective measures of bridge failures, and other conditions that have indirect effects on the design of dental restorations.

It was interesting to note, after making such an extensive survey of the literature, that little mention was made of engineering principles of design. The concepts of todays dentistry are mostly empirical and lack scientific documentation. The controversial technics backing many of the design concepts are even questionable. In dental technology, emphasis is placed on the "how" rather than on the "why". There is no evidence in the literature to indicate a rational concrete approach to the eternal excuses usually made in dental technics, "they work in my hands". There is usually no data or analysis to substantiate the basis of (guesswork or notions) in the structural design of dental structures.

CHAPTER III

EXPERIMENTAL DESIGN

More attention has been paid recently by research workers to the principles of experimental design. Evidence of this change can be seen in the medical and social sciences, in physics and chemistry, and in industrial engineering research.

The work of Fisher[71] had paved the grounds toward the present methodology of experimental design in statistics, in particular the development of factorial experimentation. The most useful of the experimental designs were presented extensively by Cochran and Cox.[28]

A. Factorial Design

Factorial experiment is the name commonly applied to an experiment wherein several factors are controlled, and their effects are investigated at two or more levels.[167] The advantages of a factorial design can be summed up as:[46]
(1) Factorial design gives the maximum efficiency in the estimation of the effects, when there are no interactions, (2) When interactions exist, their nature being unknown, a factorial design is necessary to avoid misleading conclusions, and (3) The effect of a factor is estimated at several levels of the other factors, and the conclusions hold over a wide range of conditions.

The term factor is used to denote any feature of the experimental conditions which may be assigned at will from one trial to another. There are two main types of factors: qualitative and quantitative. A qualitative factor is one in which the different levels cannot be arranged in order of magnitude, e.g. different dental designs tested in the present report. A quantitative factor is one whose values can be arranged in order of magnitude, e.g. concentrated loads applied to different dental designs in this investigation (Table 1 and 2). Table 1 shows a three-factorial design, Factor A refers to tested designs (in this case they were proximal margins), Factor B refers to sites of loads i.e., four sites of concentrated loads (b_1 to b_4), and Factor C represents two loads C_1 and C_2 (C_3 was excluded to fulfill the requirement of equal replications) applied at each b_i to each a_i. Table 2 shows a four-factorial design, which was used for testing the effect of pins and occlusal reduction on stress distribution. These tables will be used, and referred to in Chapter IV. The various values of a factor examined in an experiment are known as levels, and the term has been extended by analogy to both qualitative and quantitative factors. In the analysis of factorial experiments, two terms are usually used, main effects and interaction effects.[13,28,211] Main effects of a given factor are always functions of the average response or yield at the various levels of a factor. The interaction is the mixed

TABLE I

FACTORIAL DESIGN TABLE FOR ONE DESIGN EXPERIMENTS, FACTOR A = TESTED DESIGNS, FACTOR B = SITES OF LOADS, AND FACTOR C = LOAD MAGNITUDES.

B	C \ A	a_1	a_2	a_3	a_4	a_5	a_6	a_7
b_1	c_1	$a_1b_1c_1$	$a_2b_1c_1$	$a_3b_1c_1$	$a_4b_1c_1$	$a_5b_1c_1$	$a_6b_1c_1$	$a_7b_1c_1$
	c_2	$a_1b_1c_2$	$a_2b_1c_2$	$a_3b_1c_2$	$a_4b_1c_2$	$a_5b_1c_2$	$a_6b_1c_2$	$a_7b_1c_2$
b_2	c_1	$a_1b_2c_1$	$a_2b_2c_1$	$a_3b_2c_1$	$a_4b_2c_1$	$a_5b_2c_1$	$a_6b_2c_1$	$a_7b_2c_1$
	c_2	$a_1b_2c_2$	$a_2b_2c_2$	$a_3b_2c_2$	$a_4b_2c_2$	$a_5b_2c_2$	$a_6b_2c_2$	$a_7b_2c_2$
	c_3	$a_1b_2c_3$	$a_2b_2c_3$	$a_3b_2c_3$	$a_4b_2c_3$	$a_5b_2c_3$	$a_6b_2c_3$	$a_7b_2c_3$
b_3	c_1	$a_1b_3c_1$	$a_2b_3c_1$	$a_3b_3c_1$	$a_4b_3c_1$	$a_5b_3c_1$	$a_6b_3c_1$	$a_7b_3c_1$
	c_2	$a_1b_3c_2$	$a_2b_3c_2$	$a_3b_3c_2$	$a_4b_3c_2$	$a_5b_3c_2$	$a_6b_3c_2$	$a_7b_3c_2$
b_4	c_1	$a_1b_4c_1$	$a_2b_4c_1$	$a_3b_4c_1$	$a_4b_4c_1$	$a_5b_4c_1$	$a_5b_4c_1$	$a_7b_4c_1$
	c_2	$a_1b_4c_2$	$a_2b_4c_2$	$a_3b_4c_2$	$a_4b_4c_2$	$a_5b_4c_2$	$a_6b_4c_2$	$a_7b_4c_2$

TABLE II

FACTORIAL DESIGN TABLE FOR TWO COMBINED FACTORS, PINS AND OCCUSAL REDUCTION.

B	C \ D	A					
		A_1			A_2		
		D_1	D_2	D_3	D_1	D_2	D_3
B_1	C_1	$a_1b_1c_1d_1$	$a_1b_1c_1d_2$	$a_1b_1c_1d_3$	$a_2b_1c_1d_1$	$a_2b_1c_1d_2$	$a_2b_1c_1d_3$
	C_2	$a_1b_1c_2d_1$	$a_1b_1c_2d_2$	$a_1b_1c_2d_3$	$a_2b_1c_2d_1$	$a_2b_1c_2d_2$	$a_2b_1c_2d_3$
	C_3	$a_1b_1c_3d_1$	$a_1b_1c_3d_2$	$a_1b_1c_3d_3$	$a_2b_1c_3d_1$	$a_2b_1c_3d_2$	$a_1b_1c_3d_3$
B_2	C_1	$a_1b_2c_1d_1$	$a_1b_2c_1d_2$	$a_1b_2c_1d_3$	$a_2b_2c_1d_1$	$a_2b_2c_1d_2$	$a_2b_2c_1d_3$
	C_2	$a_1b_2c_2d_1$	$a_1b_2c_2d_2$	$a_1b_2c_2d_3$	$a_2b_2c_2d_1$	$a_2b_2c_2d_2$	$a_2b_2c_2d_3$
	C_3	$a_1b_2c_3d_1$	$a_1b_2c_3d_2$	$a_1b_2c_3d_3$	$a_2b_2c_3d_1$	$a_2b_2c_3d_2$	$a_2b_2c_3d_3$
B_3	C_1	$a_1b_3c_1d_1$	$a_1b_3c_1d_2$	$a_1b_3c_1d_3$	$a_2b_3c_1d_1$	$a_2b_3c_1d_2$	$a_2b_3c_1d_3$
	C_2	$a_1b_3c_2d_1$	$a_1b_3c_2d_2$	$a_1b_3c_2d_3$	$a_2b_3c_2d_1$	$a_2b_3c_2d_2$	$a_2b_3c_2d_3$
	C_3	$a_1b_3c_3d_1$	$a_1b_3c_3d_2$	$a_1b_3c_3d_3$	$a_2b_3c_3d_1$	$a_2b_3c_3d_2$	$a_2b_3c_3d_3$

A=PINS **B**=SITES of LOADS **C**=LOADS **D**=OCCLUSAL REDUCTN.

effect of two (or more) main factors, and the relationship is a symmetric one; i.e., the interaction of A with B is the same as that B with A . If the interaction is significant the factors are not independent of one another, but if it is nonsignificant, it is concluded that the factors under consideration act independently of each other.[14]

It has been shown that in a complete exploration of the effects of varying two or more factors, it is not sufficient to vary one factor at a time, but that all combinations of the different factor levels must be examined in order to elucidate the effects of each factor and the possible ways in which each factor may be modified by the variation of the others. In the analysis of the experimental results in factorial designs, the effects of the factors and their interactions can be estimated mathematically, by using the analysis of variances technics.

B. Analysis of Variance

The analysis of variance was a method developed by Fisher for agriculturists,[71] and its applications are now extended to various experimental sciences. The main objective of the analysis of variance (ANOVA) is to test the hypothesis that a number of population means are equal, or the levels of a tested factor have the same effect.[90] Student "t" test could not be used in this instance, because of the increased level of significance (α) , and loss of precision in estimation of the variance.[14,211] ANOVA depends on a separation of the variance of all the observations into parts,

each part measuring variability attributable to some specific source, e.g., to internal variation of several populations, to variation from one population to another, etc. The term ANOVA refers to this breakdown of the sample variance to its components.[24]

There are different classification of ANOVA. The one-way classification is mainly concerned with testing the null hypothesis that several population means are equal, versus the alternative hypothesis that at least two means are not equal.[49] In this instance, the total variation is divided mathematically into variation due to differences "among groups", and variation due to differences "within groups".[14,90,211] In the present investigation, the previous general classification was not used. Two-factor, three-factor, and four-factor analysis were used to test for variations due to restorative design, to different loading sites, and to different applied loads, at each loading site, and to each restorative design. All the cells were measured in Table I and II, and no missing cells were estimated. Thus it would be feasible to test for the main effects of different modifications of cavity design and restorative morphology, on the dependent factor, stress distribution. This particular approach included planned grouping, randomization and replication, to help free the comparisions of interest from the effects of uncontrolled variables, and to simplify the analysis of the results. Replication

provided the measure of precision, while randomization assured the validity of the measure of precision.

The statistic encountered in analysis of variance has an F distribution. It is important to indicate that there is an equivalence of the F and t tests when r = 2 (because t^2 has an $F_{(1, \upsilon)}$ distribution).(90)

* denotes a weakly significant difference, $0.01 < p < 0.05$

** denotes a significant difference, $0.001 < p < 0.01$

*** denotes a highly significant difference, $p < 0.001$

where p = probability.

1. The Problem of Multiple Comparisons.

An F test as performed in the analysis of variance, may reject the null hypothesis that the means are equal; but it would not indicate which means are significantly different. A single prechosen pair may be compared by an ordinary "t" test.(49) If more than two comparisons are made, the significance level would become hopelessly incorrect. Several procedures have been proposed for this problem, especially those offered by Duncan.(55)

The new multiple range test was developed by Duncan(55) to rank the treatment means, and is used especially for non-independent comparisons. The standard error of the experiment ($S_{\bar{x}}$) could be computed from Equation (1),

$$S_{\bar{x}} = \sqrt{\text{error mean square}/r} \qquad (1)$$

where the error mean square could be obtained from the ANOVA table, and r is the replication in every cell, in the factorial design tables.[24,46] Significant studenized ranges (SSR) for the five percent and one percent levels were given by Duncan in his paper. The least significant ranges (LSR) for the number of the means involved in a comparison can be computed from Equation (2),

$$LSR = SSR \cdot S_{\bar{x}} \qquad (2)$$

Another method was used in conjunction with Duncan's test, to compare treatments. Linear orthogonal contrasts[143] were written for means to compare the different levels of a given factor. The procedure is simply a division of the treatment sums of squares into individual components, each with a single degree of freedom, then using the $F_{(1, \upsilon \text{ error})}$ to test for significance. Orthogonal contrasts were written to detect subtle differences between means. In all statisical procedures, equal replications of the treatments was the adopted procedure, (equal sample sizes), in order to avoid modifications of the procedures of ANOVA, or those used in multiple comparisons.

2. Estimate of the Experimental Error

In the present investigation, several assumptions about the error were considered. First, errors in the constructed models are independent, second, in experiments to compare group

means, the variance of the errors is the same in each group, and third that errors are normally distributed.[23]

The experimental error was estimated, using the estimate of the error variance, obtained from the analysis of variance tables. The standard error could be computed from the estimate of the error variance[211] [Equation (1)]. The error of the first type was discussed under the different levels of significance. Detailed discussion of the experimental error, which will include tolerances in the photoelastic models, will be presented in the following chapters.

CHAPTER IV

METHODS AND MATERIALS

A. Photoelastic Analytical Principles and Equations

The conventional two-dimensional photoelastic method involves the fabrication of a suitable model, which is loaded and placed in a polariscope, and the fringe pattern is examined and photographed. The fundamentals of photoelasticity will not be presented, although the interpretation of the photoelastic data will be discussed. The fundamental photoelastic data consist of the isochromatic fringes and their orders, the isoclinic parameters and the stress optical coefficient. The latter is determined by testing a calibration specimen, which will be presented later in this chapter.

The isochromatic fringe pattern obtained in photoelasticity represents all points exhibiting the same relative retardation (or the same maximum shear stress) for a certain load, and the computation of the principal stress difference ($\sigma_1 - \sigma_2$) will be equal to a constant along each isochromatic fringe.

It is now important to present the different types of stress fields (Figure 1) and the representation of the cartesian components of stress (Figure 2), in order to correlate them with the isochromatics ($\sigma_1 - \sigma_2$). A typical example of isochromatics is presented in Figure 3. The upper half of Figure 3 represents an isochromatic fringe pattern observed in a light field, which would facilitate the progressive computing of the half-order fringes, while the lower half of

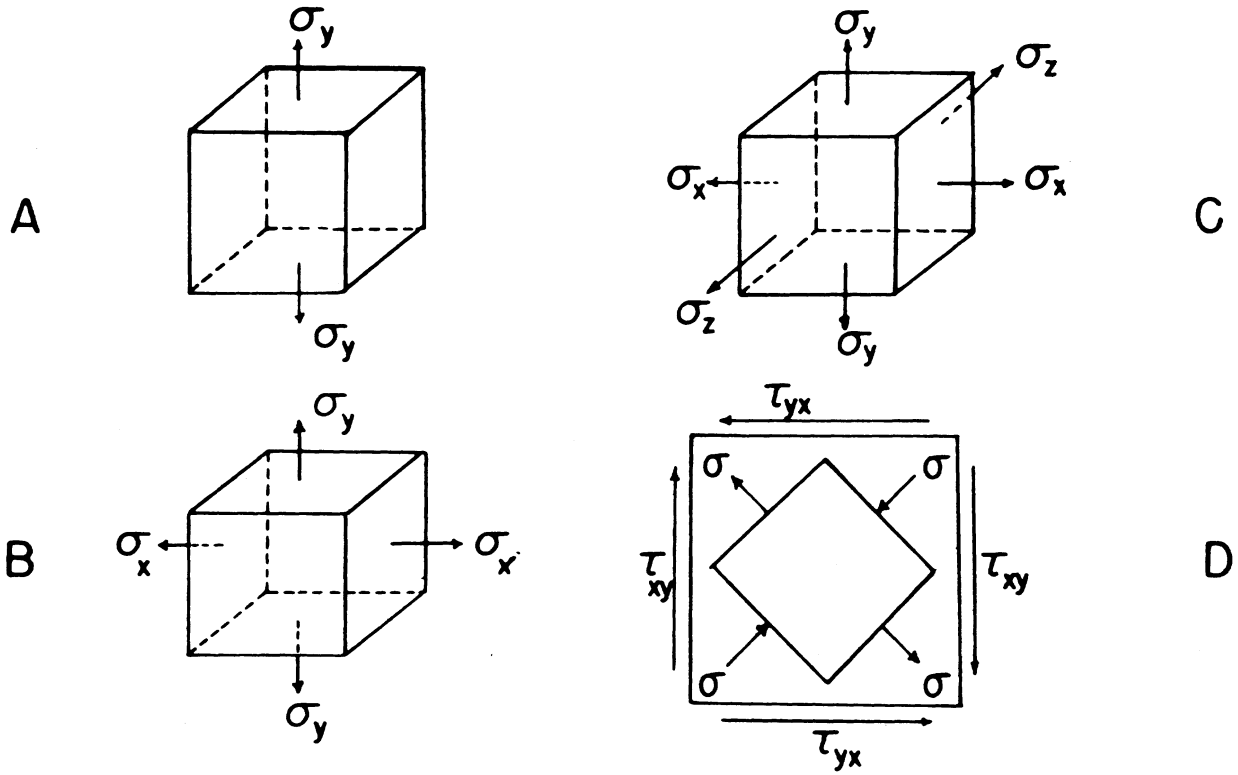

A - Uniaxial stress field.

B - Biaxial stress field.

C - Triaxial stress field.

D - Pure shear stress field.

Figure 1. Different Types of Stress Fields, A-Uniaxial Stress Field, B-Biaxial Stress Field, C-Triaxial Stress Field, D-Pure Shear Stress Field.

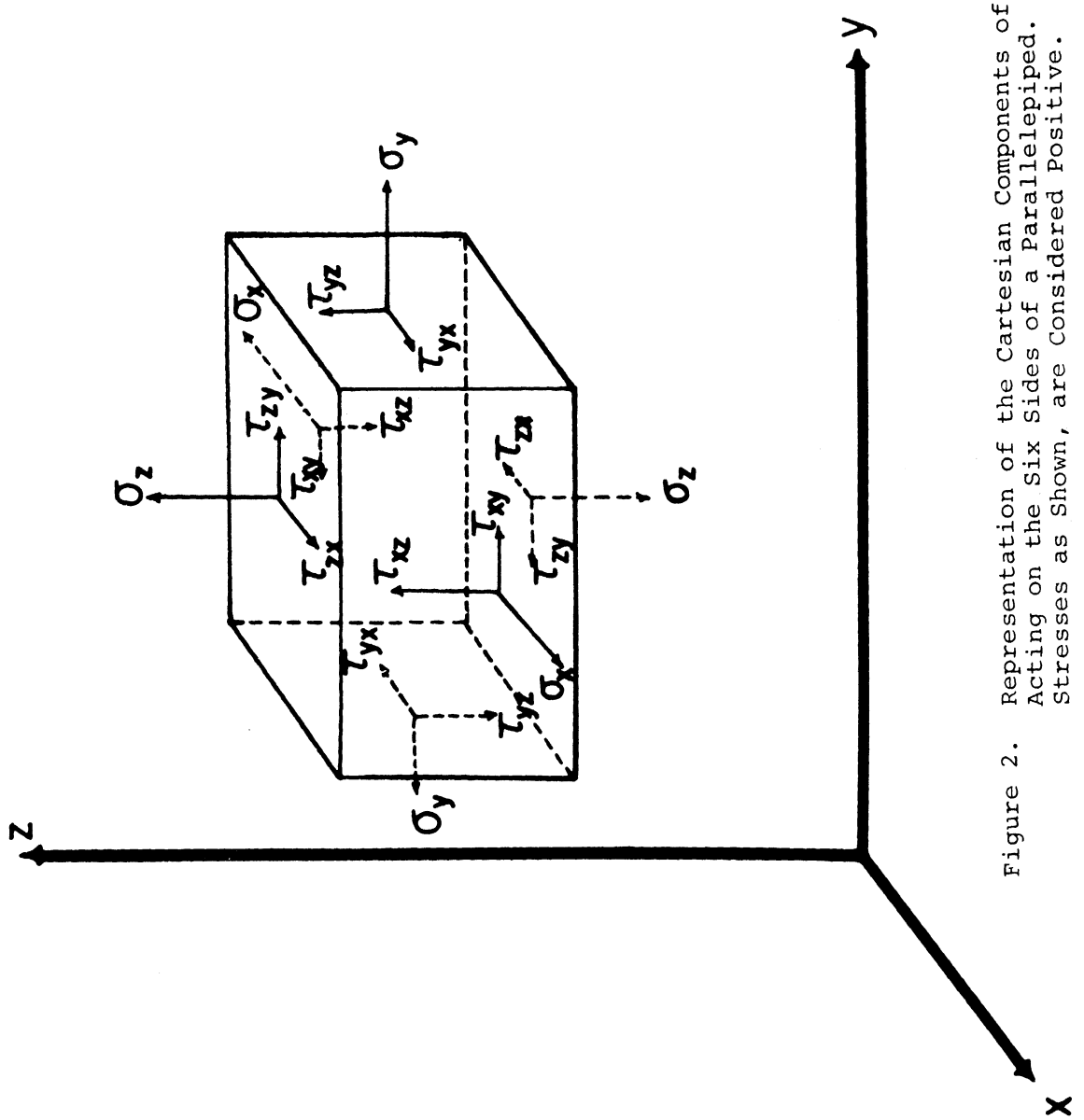

Figure 2. Representation of the Cartesian Components of Stress Acting on the Six Sides of a Parallelepiped. All the Stresses as Shown, are Considered Positive.

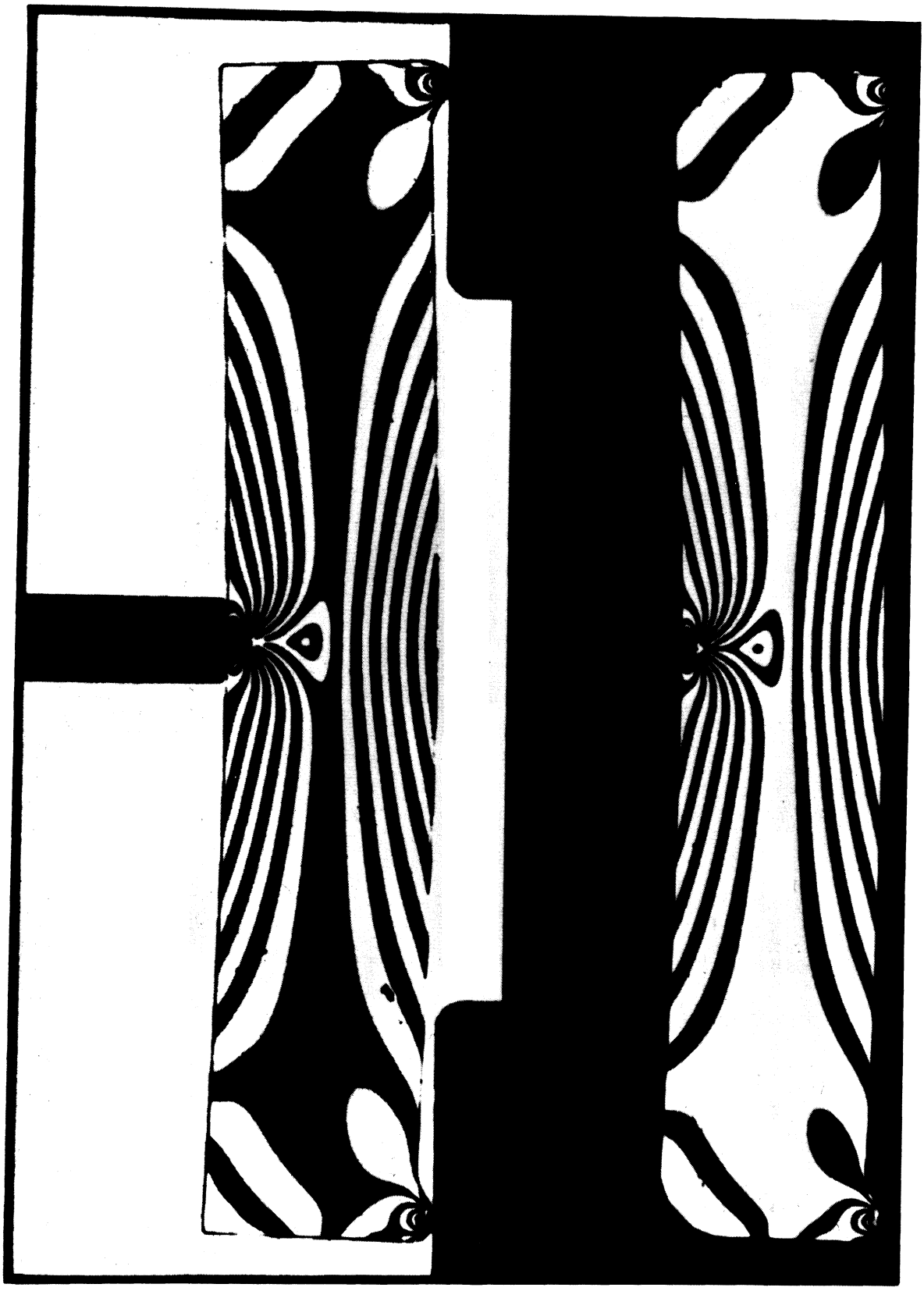

Figure 3. Beam in Simple Bending, Upper Picture: Light-Field Photography, Lower Picture: Dark-Field Photography.

Figure 3 shows an isochromatic fringe pattern, observed in a dark field, which would facilitate the progressive counting of the full-order fringes. Fringes in both light field and dark field can be obtained by arrangement of the optical elements in the polariscope.

The relationship between stress components can be graphically represented by using Mohr's circle of stress, as illustrated in Figure 4. In this diagram, normal stress components σ are plotted horizontally, while shear stress components τ are plotted vertically. Tensile stresses are plotted to the right of the τ axis, while compressive stresses are plotted to the left of the τ axis. For shear stress components which tend to produce a clockwise rotation of a small element the points are plotted above the σ axis, while those tending to produce a counterclockwise rotation are plotted below. When plotted in this manner, the stress components are associated with each plane though the points are represented by a point on the circle. The diagram thus gives an excellent visual picture of the state of stress at a point. Equations (3 and 4) and Mohr's circle are often used in experimental stress analysis work when stress components are transformed from one coordinate system to another.

$$\sigma_1, \sigma_2 = \frac{\sigma_X + \sigma_Y}{2} \pm \sqrt{\left(\frac{\sigma_X - \sigma_Y}{2}\right)^2 + \tau_{XY}^2} \qquad (3)$$

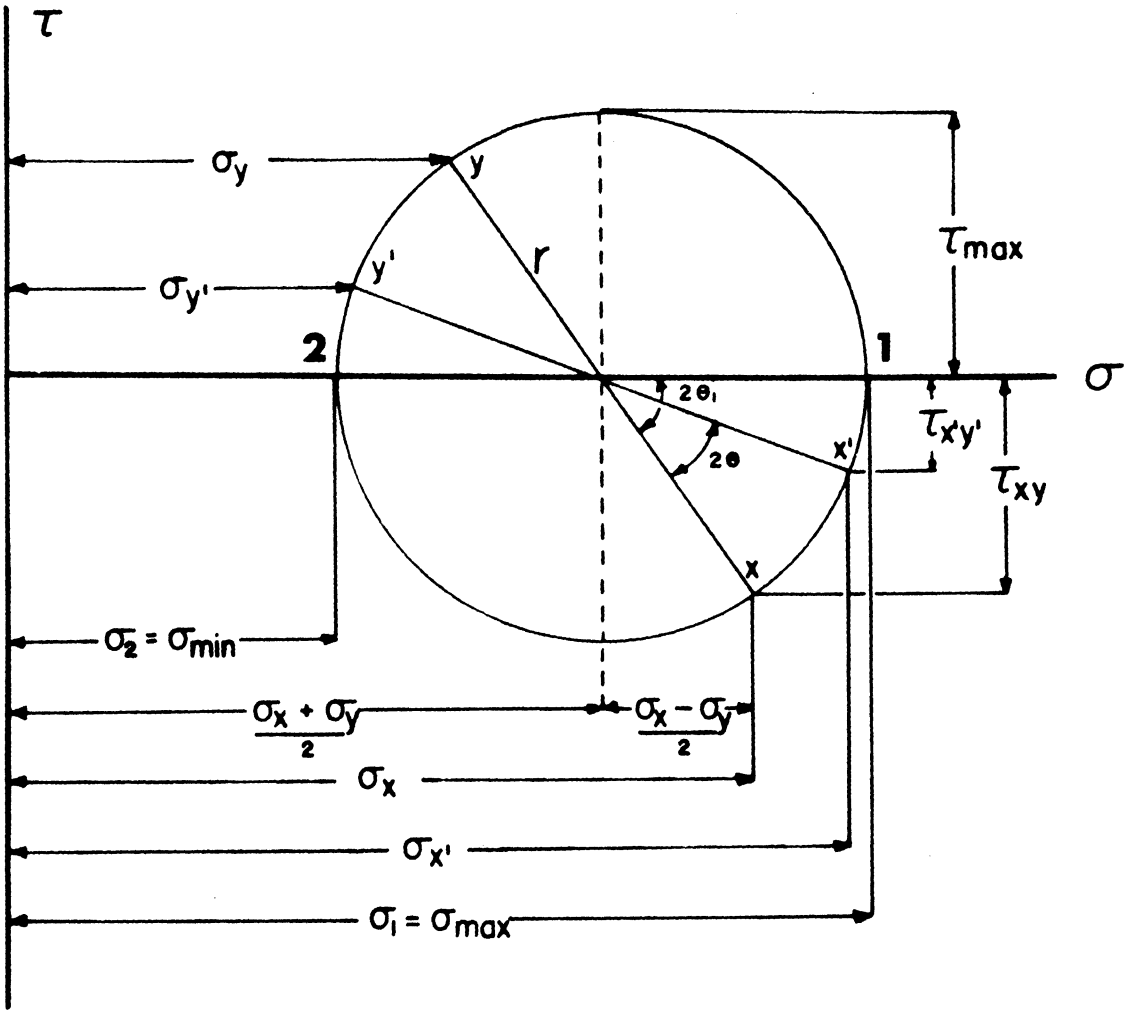

$$\sigma_1, \sigma_2 = \frac{\sigma_x + \sigma_y}{2} \pm \sqrt{\left(\frac{\sigma_x - \sigma_y}{2}\right)^2 + \tau_{xy}^2}, \quad \sigma_3 = 0$$

$$\tau_{max} = \sqrt{\left(\frac{\sigma_x - \sigma_y}{2}\right)^2 + \tau_{xy}^2}$$

Figure 4. Mohr's Circle Representation for Plane Stresses.

$$\tau_{max} = \sqrt{\left(\frac{\sigma_X - \sigma_Y}{2}\right)^2 + \tau_{XY}^2} \qquad (4)$$

For two dimensional stress fields, $\sigma_Z = \tau_{ZX} = \tau_{YZ} = 0$.
The applications of the stress optic law, and combining it with basic elasticity theory, would yield the basic equation of photoelasticity, Equation (5).

$$\sigma_1 - \sigma_2 = \frac{N \cdot f}{h} \qquad (5)$$

Actually the function of the polariscope is to determine N , the isochromatic fringe order at each point in the photoelastic model, σ_1 and σ_2 are the principal stresses, f is the stress optical coefficient (PSI/fringe/inch), and h is the thickness of the model in inches. If a photoelastic model exhibits perfectly elastic behavior, the difference in the principal strains ($\epsilon_1 - \epsilon_2$) can also be measured by establishing the fringe order N . The maximum shear is given by Equation (6),

$$\tau_{max} = \frac{1}{2}\left(\sigma_1 - \sigma_2\right) = \frac{N \cdot f}{2\,h} \qquad (6)$$

provided σ_1 and σ_2 are of opposite sign and $\sigma_3 = 0$; otherwise

$$\tau_{max} = \frac{1}{2}(\sigma_1 - \sigma_3) = \frac{1}{2}\sigma_1 \quad \textit{if } \sigma_1 \& \sigma_2 \textit{ are positive}$$

$$\tau_{max} = \frac{1}{2}(\sigma_3 - \sigma_2) = \frac{1}{2}\sigma_2 \quad \textit{if } \sigma_1 \& \sigma_2 \textit{ are negative} \tag{7}$$

On the free boundary of the model, either σ_1 or σ_2 is equal to zero, hence the stress tangential to the boundary can be determined directly from Equation (8).

$$\sigma_1, \sigma_2 = \frac{N \cdot f}{h} \tag{8}$$

The sign usually can be determined by inspection, particularly in the critical areas where the boundary stresses are a maximum. If the boundary is not free, but the applied normal load is known, then the tangential boundary stress can be interpreted by applying Equation (9);

$$\sigma_1 - \sigma_2 = \sigma_1 + P = \frac{N \cdot f}{h} \quad \text{or} \quad \sigma_1 = \frac{N \cdot f}{h} - P \tag{9}$$

where $\sigma_2 = -P$, since the applied normal load P is considered as a positive quantity.

It is frequently necessary or desirable to obtain individual values of the principal stresses throughout the interior regions of the model. The technique used in the present investigation for separation of σ_1 and σ_2 was the shear difference method. The method is based on equations of equilibrium and a numerical integration process, and is shown in Figure 5. A grid system is often employed in the application of the shear difference method. All the information necessary for its execution, is readily available from the basic photoelastic data. The isoclinic parameters, θ, can be obtained readily from the isoclinic fringe patterns, as will be explained later. Equations (10) and (11) represent the two final equations of the shear difference method.

$$\sigma_1 = \frac{1}{2}\left(\sigma_x + \sigma_y + \frac{N \cdot f}{h}\right) \tag{10}$$

$$\sigma_2 = \frac{1}{2}\left(\sigma_x + \sigma_y - \frac{N \cdot f}{h}\right) \tag{11}$$

These two equations will be used to separate the stresses along any selected arbitrary line in the photoelastic models.

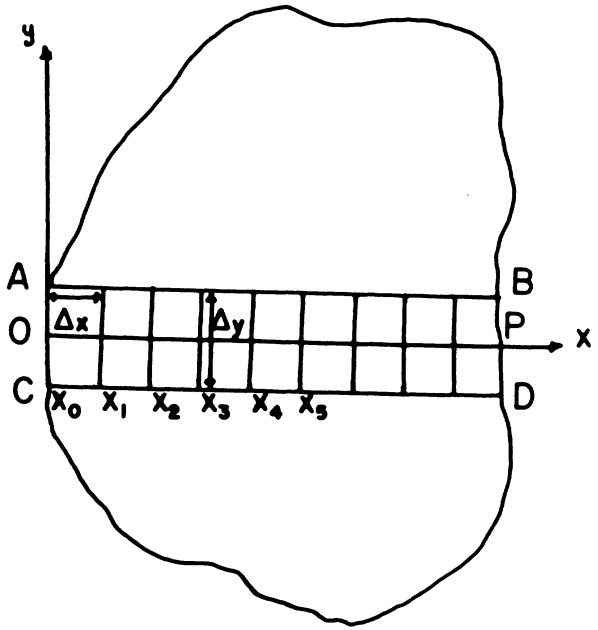

Adapted from "EXPERIMENTAL STRESS ANALYSIS" by J. W. DALLY & W. F. RILEY

$$\tau_{xy} = \frac{\sigma_1 - \sigma_2}{2} \sin 2\theta = \frac{N \cdot f}{2h} \sin 2\theta$$

$$\Delta \tau_{xy} = \tau_{xy}\Big|_{AB} - \tau_{xy}\Big|_{CD} \quad \text{at positions:}$$

$$\frac{X_0 + X_1}{2}, \frac{X_1 + X_2}{2}, \frac{X_2 + X_3}{2}, \text{ etc.}$$

$$\sigma_{xx}\Big|_{X_1} = \sigma_{xx}\Big|_{X_0} - \Delta \tau_{xy}\Big|_{(X_0 + X_1)/2},$$

$$\sigma_{xx}\Big|_{X_2} = \sigma_{xx}\Big|_{X_1} - \Delta \tau_{xy}\Big|_{(X_1 + X_2)/2}, \ldots\ldots$$

$$\sigma_{yy} = \sigma_{xx} - (\sigma_1 - \sigma_2) \cos 2\theta$$

$$= \sigma_{xx} - \frac{N \cdot f}{h} \cdot \cos 2\theta$$

$$\sigma_1 = \frac{1}{2} \left(\sigma_{xx} + \sigma_{yy} + \frac{N \cdot f}{h} \right)$$

$$\sigma_2 = \frac{1}{2} \left(\sigma_{xx} + \sigma_{yy} - \frac{N \cdot f}{h} \right)$$

Figure 5. The Shear Difference Method for Separation of Principal Stresses.

The direction of the principal stresses could be established from the isoclinic fringe. An isoclinic is defined as a line along which the principal stresses (σ_1 and σ_2) have a constant inclination. Isoclinics can be distinguished from isochromatics when white light is used in the crossed plane polariscope, and the isoclinics will appear as dark bands superimposed on an otherwise colored pattern. The positive acute angle between a principal stress (σ_1 or σ_2) and a given reference axis can be determined from the isoclinic parameter, θ . The isoclinics can be obtained by rotation of the analyzer and polarizer together to produce maximum darkness at a certain reference point. The angle of rotation producing the extinction is the isoclinic parameter, θ . The directions of the principal stresses are usually presented in the form of an isostatic or stress trajectory diagram where the principal stresses are tangent or normal to the isostatic line at each point. Figure 6 represents the plot of the stress trajectories from the composite isoclinic pattern, by utilizing the procedure outlined graphically. Stress distribution in a semi-infinite plate subjected the concentrated normal load is shown in Figure 7. The left part shows the isochromatics and their order, while the right part shows the isostatics constructed from the isoclinics.

B. The Photoelastic Bench

A circular transmission polariscope is the instrument which is usually used to record the isochromatic and isoclinic fringes.

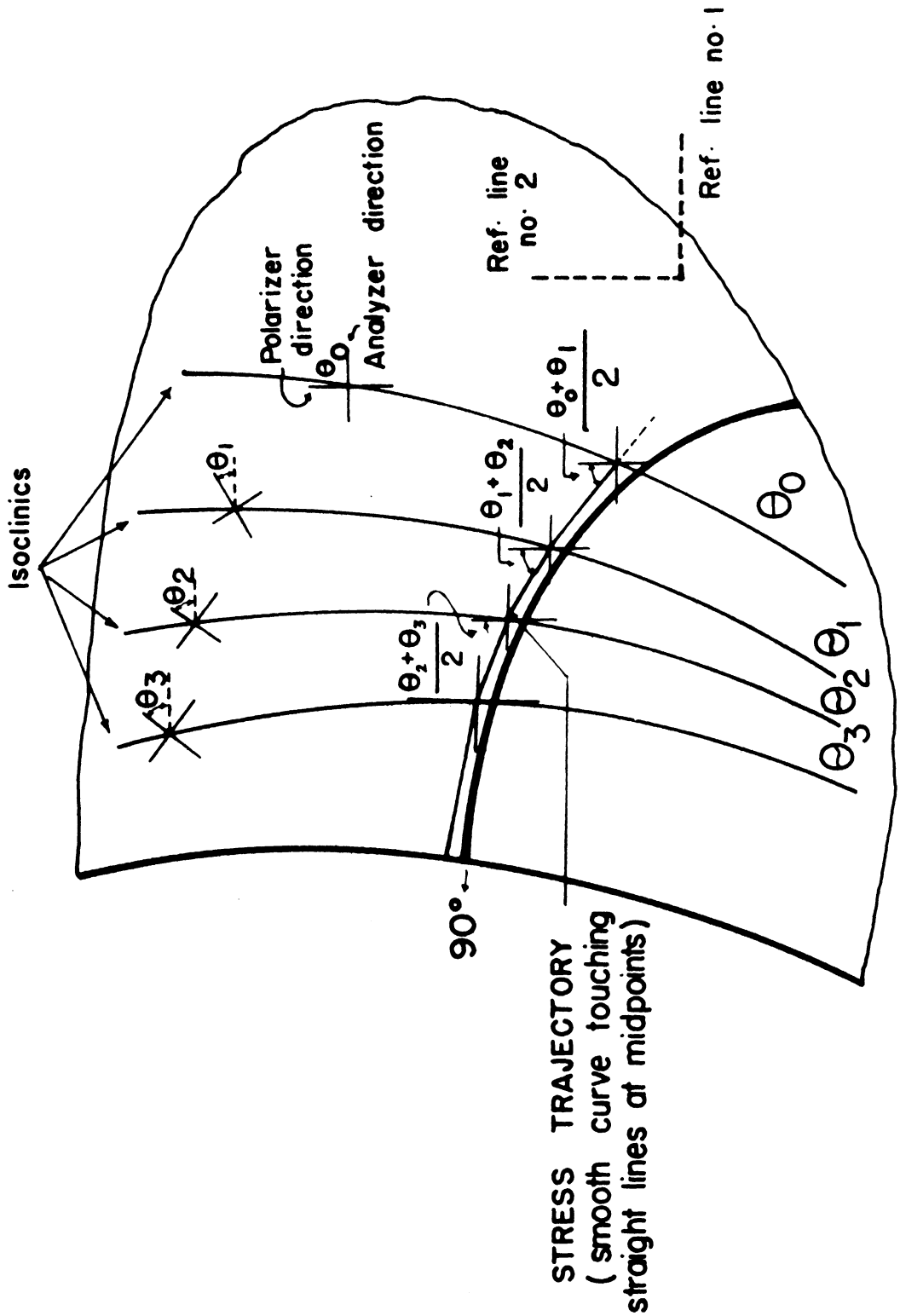

Figure 6. Construction of Stress Trajectories, Tangential to One of the Principal Stresses and Perpendicular to the Other.

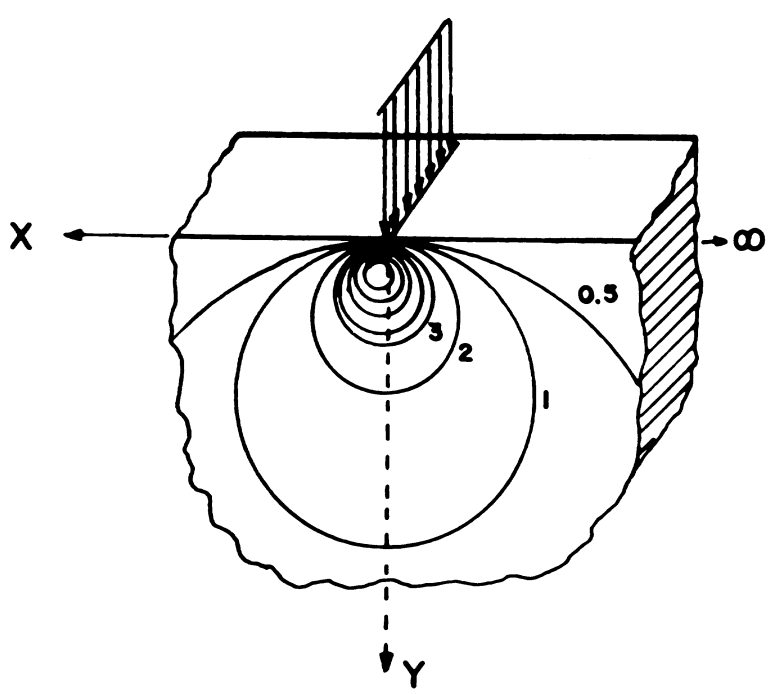

ISOCHROMATICS

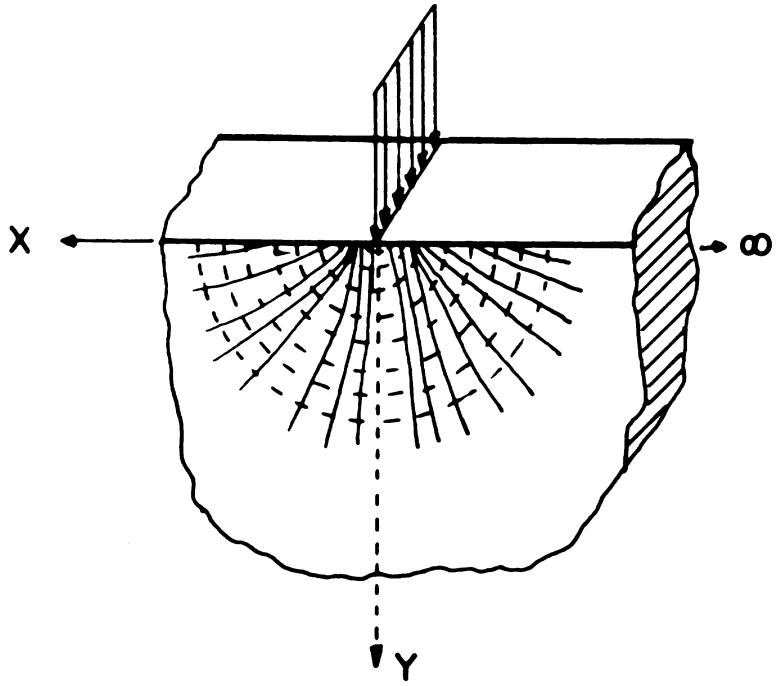

ISOSTATICS, solid lines represent the σ_2 family, dotted lines represent the σ_1 family.

Figure 7. Stress Distribution in a Semi-Infinite Plate Subjected to Concentrated Normal Load.

The circular polariscope used in this study is shown in Figure 8, and consists of the following components, from right to left along the optical components. The numbers in Figure 8 are the same numbers used for the components of the polariscope.

1. Light Source.

A ventilated lamp housing which surrounds a 500-watt General Electric Mercury Vapor Lamp (G.E.Ft 15 T 8-C). A lens in the front of the light source focuses the light into the aperture, which is a one-eighth inch hole in a thin plate of brass. The center of the light source is focused onto this aperture. The aperture is set as the focal length of the condensing lens. This arrangement would ensure parallel light rays emerging from the condensing lens.

2. Monochromatic Filter.

A corning color combination (No. 4-102) is used to produce monochromatic light. This filter allows for 12 percent transmission of the mercury green line (5461 Angstrom) and practically zero for everything else.

3. Condensing Lens.

A five inch lens, with a focal length of 40 inch (f/8) is positioned between the light source and the polariser, in such a way that parallel waves of light will pass through the model.

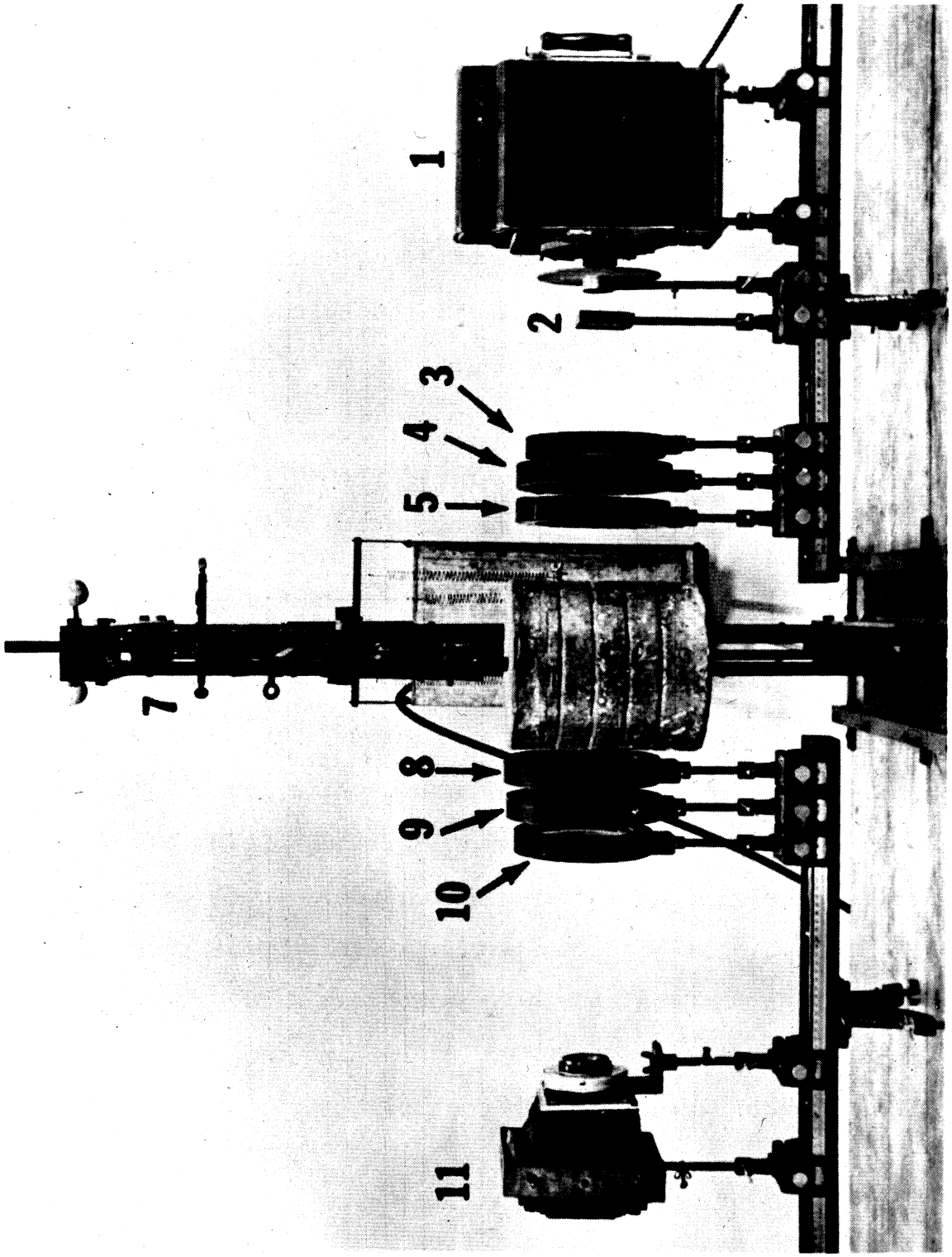

Figure 8. The Photoelastic Bench.

4. Polarizer.

A five-inch diameter polaroid plate, which is placed between the condensing lens and the first quarter-wave plate. The polarizer transforms the ordinary light into plane polarized light.

5. First Quarter-Wave Plate.

A five-inch diameter plate, which is placed between the polarizer and the model. The first quarter-wave plate transforms the plane-polarized light into circularly-polarized light, by producing a phase difference of one-quarter of the mercury green line. Insertion of the two quarter-wave plates will eliminate the isoclinics, and thus allows for accurate recording of the isochromatics only.

6. Photoelastic Model.

It will be discussed in detail in Section C.

7. Loading Mechanism.

The load is applied by a second-class lever, which could be balanced in the zero-load position. Loads are applied at a short distance from the fulcrum. Loads were read directly from a dial gage mounted on a dynamometer ring, which is placed between the lever and the model. Vertical and horizontal control of the entire loading mechanism was possible through the use of two control screws.

8. Second Quarter-Wave Plate.

The plate is the same as the first, and its function is to restore the original plane-polarized light or rotate it through 90°, depending on whether it is crossed or parallel to the first plate.

9. Analyzer.

A five-inch diameter polaroid plate, which blocks out or transmits the plane-polarized light according to the desired background. Both quarter-wave plates, the polarizer and the analyzer may be rotated in their mountings, and a scale is provided which indicates the degree of rotation.

10. Collecting Lens.

It is a five-inch diameter lens having a forty inch focal length. It is used to converge the light onto the camera.

11. Camera.

The stress pattern may be viewed on the ground-glass plate of the camera. The used camera was a No. 4 - Universal, made by Ilex Optical Company. The ground glass plate could be replaced by a 4 x 5 Polaroid Land Film holder to record the fringe patterns. Polaroid film type 55 P/N was used throughout this investigation.

12. Arrangement of the Optical Elements In a Polariscope.

The optical elements can be arranged to produce to different transmission polariscopes, plane and circular. A plane polaricsope is one which does not have any quarter-wave plates. It is used for photographic recording of isoclinics. In the circular polariscope, circularly polarized light is employed to record the isochromatics. There are two arrangements used where light or dark backgrounds are produced. Light background (field) is produced when both quarter-wave plates are crossed, while the analyzer and the polarizer are parallel. Dark background (field) is produced when both quarter-wave plates are crossed, and both analyzer and polarizer are crossed. A complete schematic view of the transformations undertaken by the light as it goes through the complete polariscope and model is shown in Figure 9. The settings of the circular polariscope in Figure 9 will produce dark field in photography. Indeed, the circular polariscope is employed solely to eliminate the isoclinic fringe pattern from the superimposed isoclinic-isochromatic fringe pattern obtained with a plane polariscope.

The isochromatic fringe order can be determined to the nearest half-order by employing the light and the dark-field arrangements. Fractional orders less than half can be obtained using the Tardy method of compensation. The accuracy of the Tardy compensation is one-hundredth of a fringe, and since it was used, no auxiliary equipment was needed to supplement the optical elements of the polariscope.

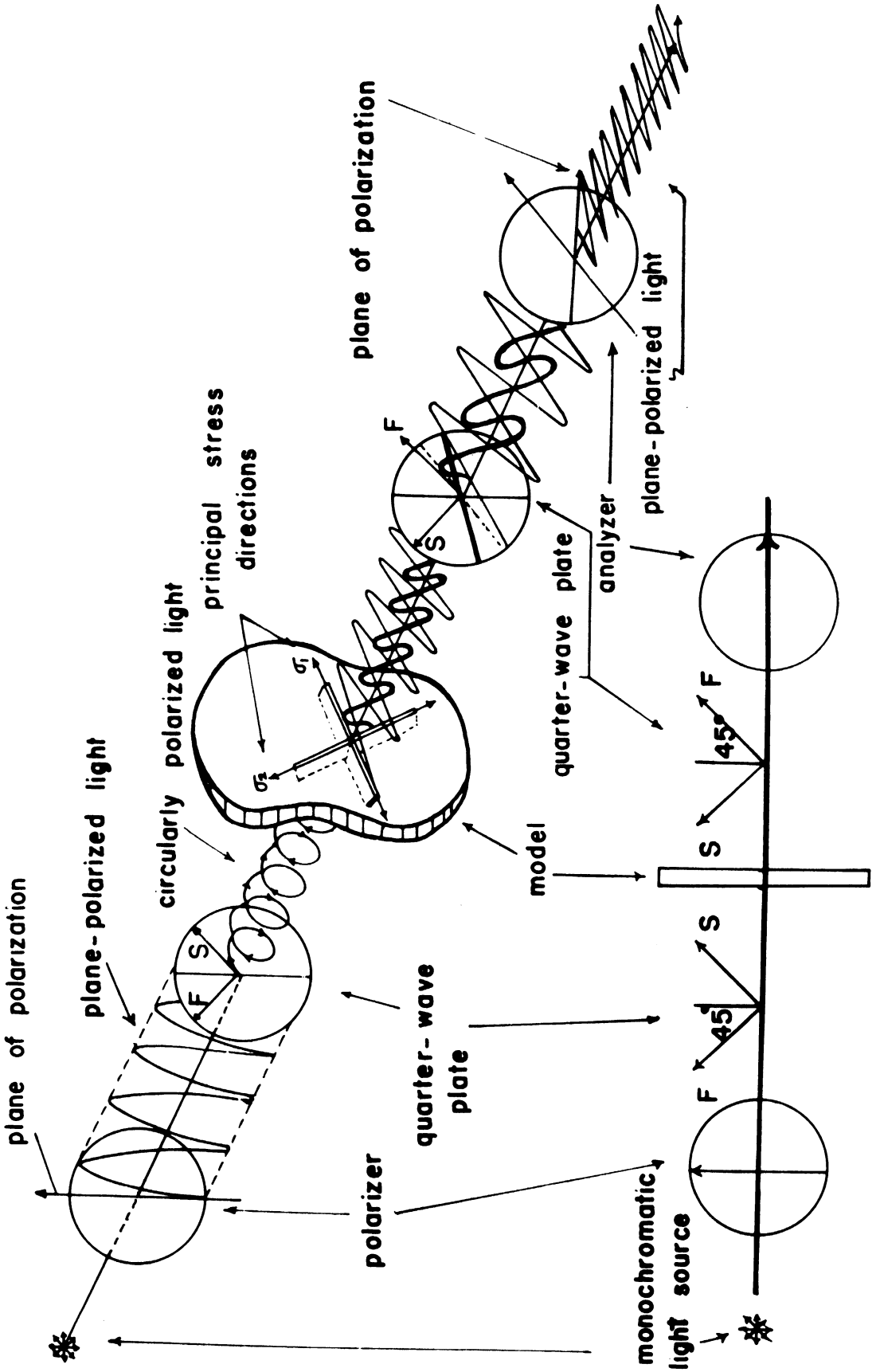

Figure 9. Schematic Diagram of Optical Transformations in a Circular Polariscope Set For Dark Background.

C. Photoelastic Model Materials and the Construction of the Models.

Sheets for models were supplied by Photoelastic, Inc.* The sheets were ten inches by ten inches, with protective coatings on both sides, for tracing of the shape of the model without scratching the plastic. Two birefringent materials were used in this study, PSM-1 (I)* and PSM-5 (II)* Material (I) is a clear polyester sheet, free of creep and edge effects. It has a nominal thickness of 0.250 $\pm$ 0.002 inch. Material (II) is a clear epoxy resin, exhibiting higher modulus of elasticity and higher sensitivity. The modulus of elasticity of material (I) was 340×10^3 psi, and that of material (II) was 450×10^3 psi. Material (I) was used in constructing the substructure which has the appropriate cavity preparation, in accordance with conventional dental procedures, and material (II) was used in making the restorations to be investigated. The two materials were used in the construction of composite photoelastic models. Improved dental stone** was used in luting the composite photoelastic models to represent dental cement.

In scaling the composite models, Equation (12) was used,

$$\frac{E_{gold}}{E_{tooth\ structure}} = \frac{E_{material\ (II)}}{E_{material\ (I)}} \qquad (12)$$

* Photoelastic, Inc., Lincoln Hwy, Malvern, Pa.

**Duroc, Ransom and Randolph Company, Toledo, Ohio.

where E for gold is about 12 x 10^6 psi,[176] E for tooth structure will be the average of E for enamel and dentin. E for enamel is about 13 x 10^6 psi,[33-35] and that for dentin is about 4 $\pm$ 1 x 10^6 psi.[33-35] The average E for tooth structure is considered in this presentation to be about 8.5 $\pm$ 0.5 x 10^6 psi.

The left side of Equation (12) would yield a ratio of about 1.40 while the right side of the equation would yield a ratio of about 1.31. The error in the scaling is about 6.3 percent due to the discrepancy between the two ratios. No photoelastic materials were found to satisfy the 1.40 relationships, therefore, materials having the ratio of 1.31 were used in the construction of the models in this investigation.

1. Calibration.

A beam was cut of both materials (I) and (II), five inches by one inch by 0.25 inch and was used as a beam simply supported and centrally loaded, as shown in Figure 10. The bending moment, M, was computed, and f stress optical coefficient was computed as shown in Figures 10 and 11.

The Crites Equation,[42] which uses the fringes on the upper or lower fibres,

$$f = \frac{6\ M}{N\ w^2} \qquad (13)$$

and the Hetenyi Equation,[98] which uses the total number of fringes,

$$f = \frac{12\ M}{N\ w^2} \qquad (14)$$

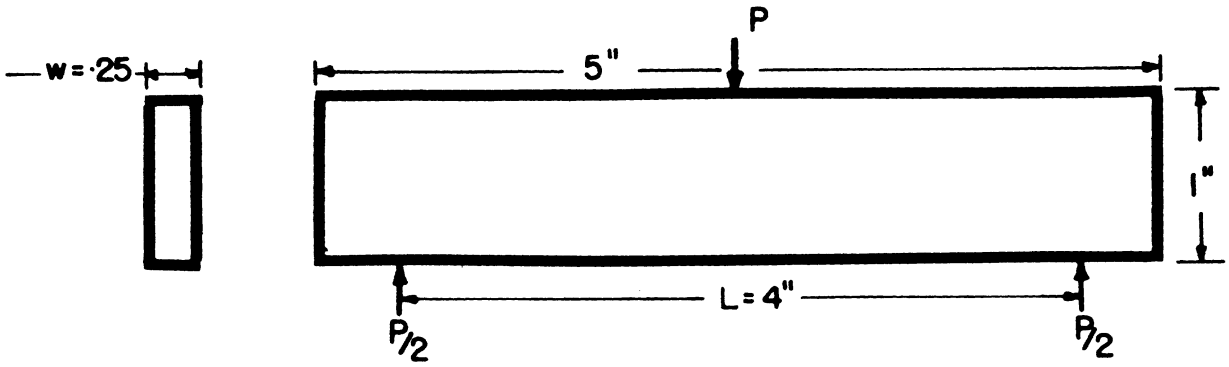

$$M = \frac{PL}{4}, \qquad f = \frac{6M}{nw^2}$$

WHERE: M = BENDING MOMENT, P = LOAD

n = NO. OF FRINGES AT UPPER OR LOWER BORDER

f = STRESS OPTICAL COEFFICIENT (PSI/FRINGE/INCH)

W = WIDTH

Figure 10. Calibration of Beams Made of Photoelastic Materials, to Compute Stress Optical Coefficient.

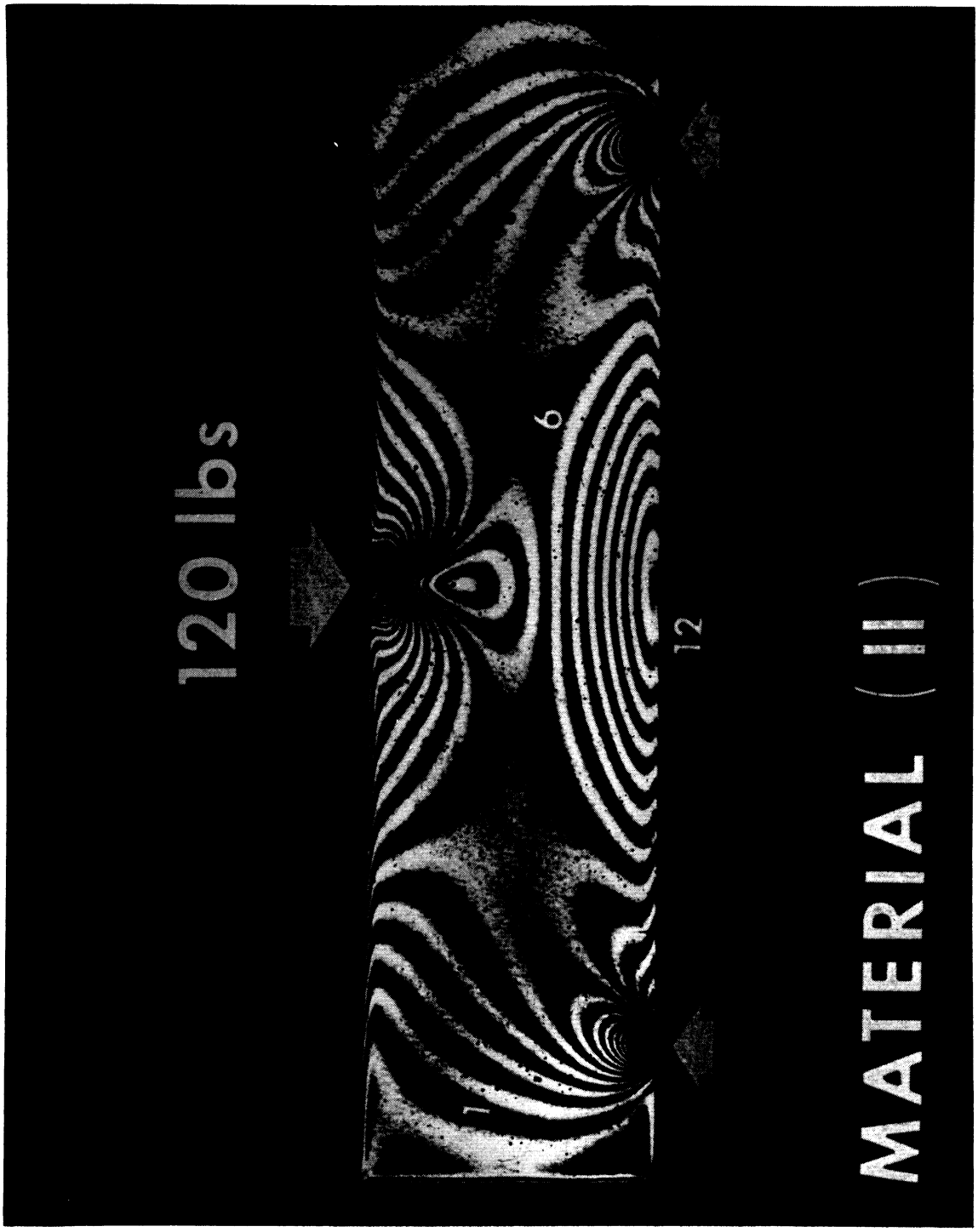

Figure 11. Isochromatics in a Beam Made of Material (II) Subjected to 120 Pounds Concentrated Load.

For material (II) using Equation (13),

$$f_2 = \frac{6 \times 120}{12x1x1} = 60 \text{ psi/fringe/inch.}$$

For material (II) using Equation (14),

$$f_2 = \frac{12 \times 120}{24.5x\ 1x1} = 59.0 \text{ psi/fringe/inch.}$$

The same method was used for material (I), and f_1 was found to be 40.1 psi/fringe/inch. These same two values were independently obtained, by the manufacturer, using a tensile sample for calibration. The values of 40 and 60 psi/fringe/inch were used as constants for materials (I) and (II) respectively.

2. Cutting the Models.

An electric jig saw* was used for cutting the models. The saw had the advantage that it had a flat table, which had a fine metal grid, which facilitated cutting along straight lines, as shown in Figure 12. Fine blades were used, and after the models were cut, their sides were filed using fine sand paper to eliminate ledges at free boundaries, prior to cementation and stress annealing.

3. The Photoelastic Models.

Composite photoelastic models were constructed to study the different design factors. All models were scaled according to Equation (12), and all were luted using the

*Syncro Jig Saw Model 2400, Syncro Corporation, Oxford, Michigan.

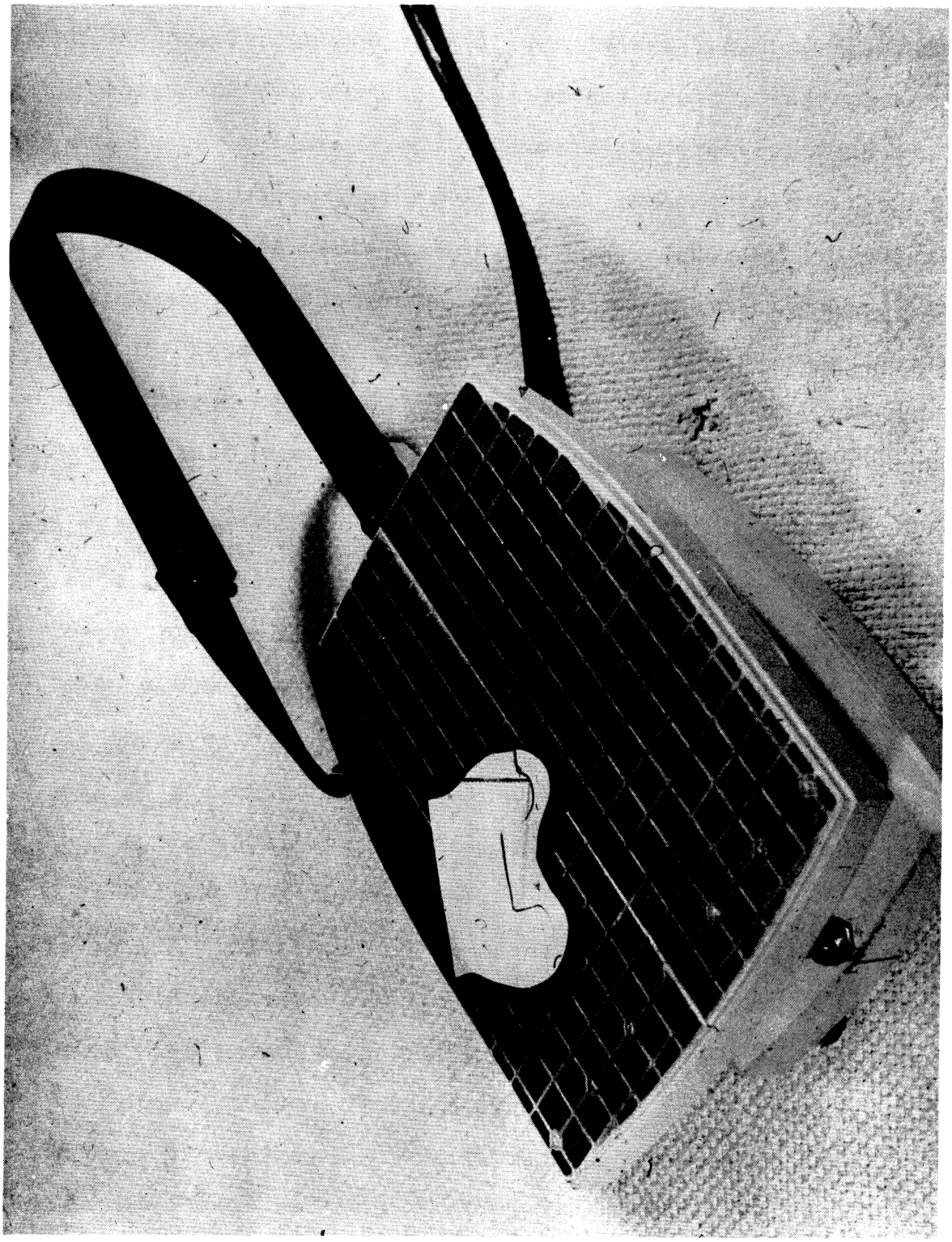

Figure 12. Electric Jig Saw Used for Cutting the Models.

same dental stone. Models were constructed to study the geometry of proximal margins (shoulder geometry), the extent of convergence of the axial wall (axial walls parallelism), the occlusal reduction, the effect of pins on design, and the proximal design in compound restorations. Three two-dimensional models of dental bridges were also constructed to study the combined effects of several factors. It is important to mention that the bridge models were fabricated after all other experiments were conducted, in order to incorporate certain features in some, and omit certain features from the others. Since the construction of models is cited in Materials and Methods, it is proper to describe the models built for each design factor.

a. Shoulder Geometry (proximal margins) Models. Since the proximal margin is one of the most important parts of a dental restoration, seven variations were included in these models. The peripheral dimensions of all seven models were constant and the models represent a mesio-distal section of lower posterior molar. The constant characteristics of all models included vertical walls, flat pulpal floor and a rounded axiopulpal line angle. All restorations represented an occlusomesial restoration, as shown in Figure 13. All models were scaled to be larger than the natural corresponding teeth by a factor of seven and they are shown in Figure 14. Model No. 1 represents the chisel edge margin (shoulderless), Model No. 2 represents the chamfer, No. 3 represents a rounded shoulder, No. 4 represents a flat shoulder (axial wall

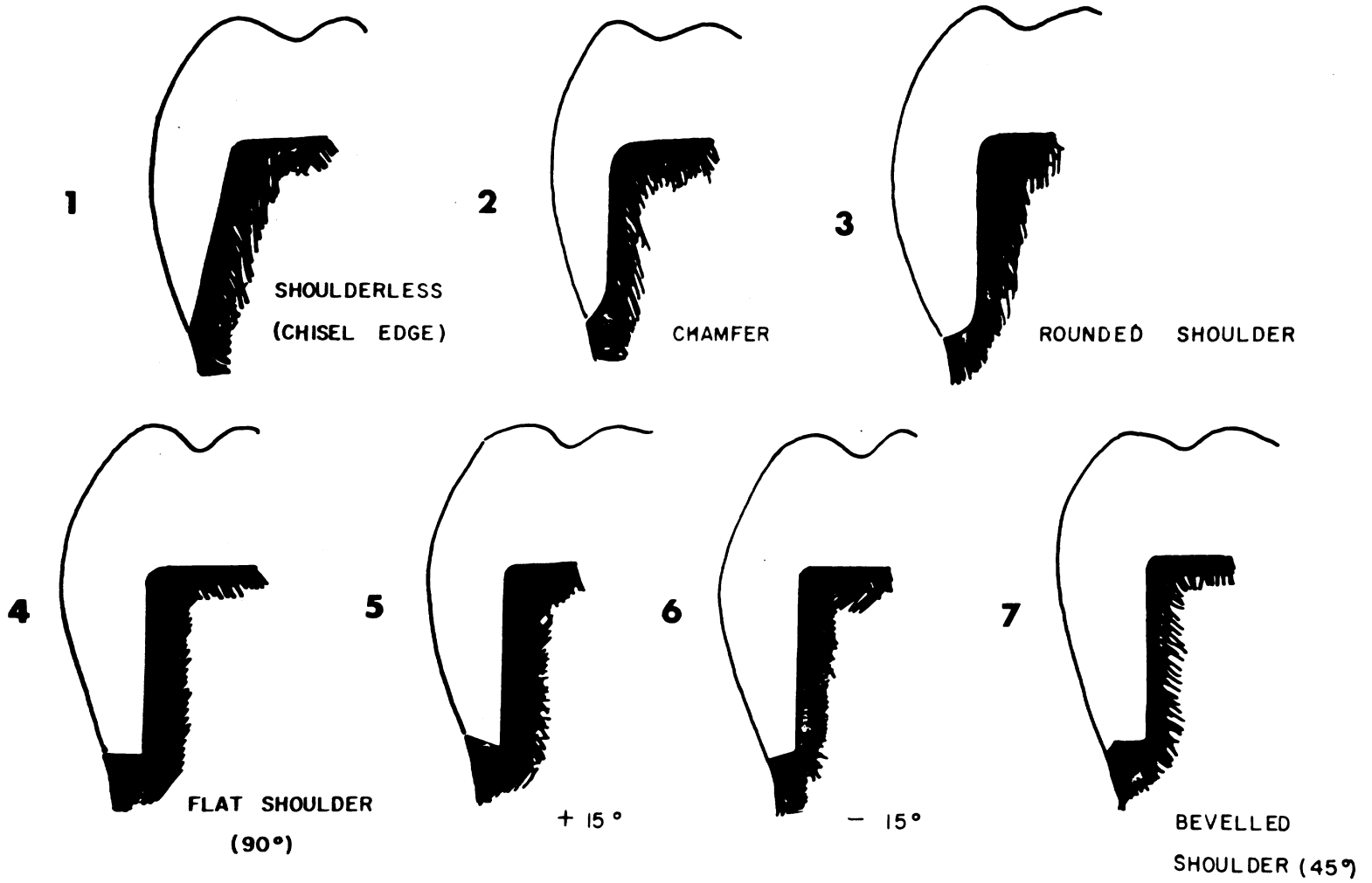

Figure 13. Shoulder Geometry Models.

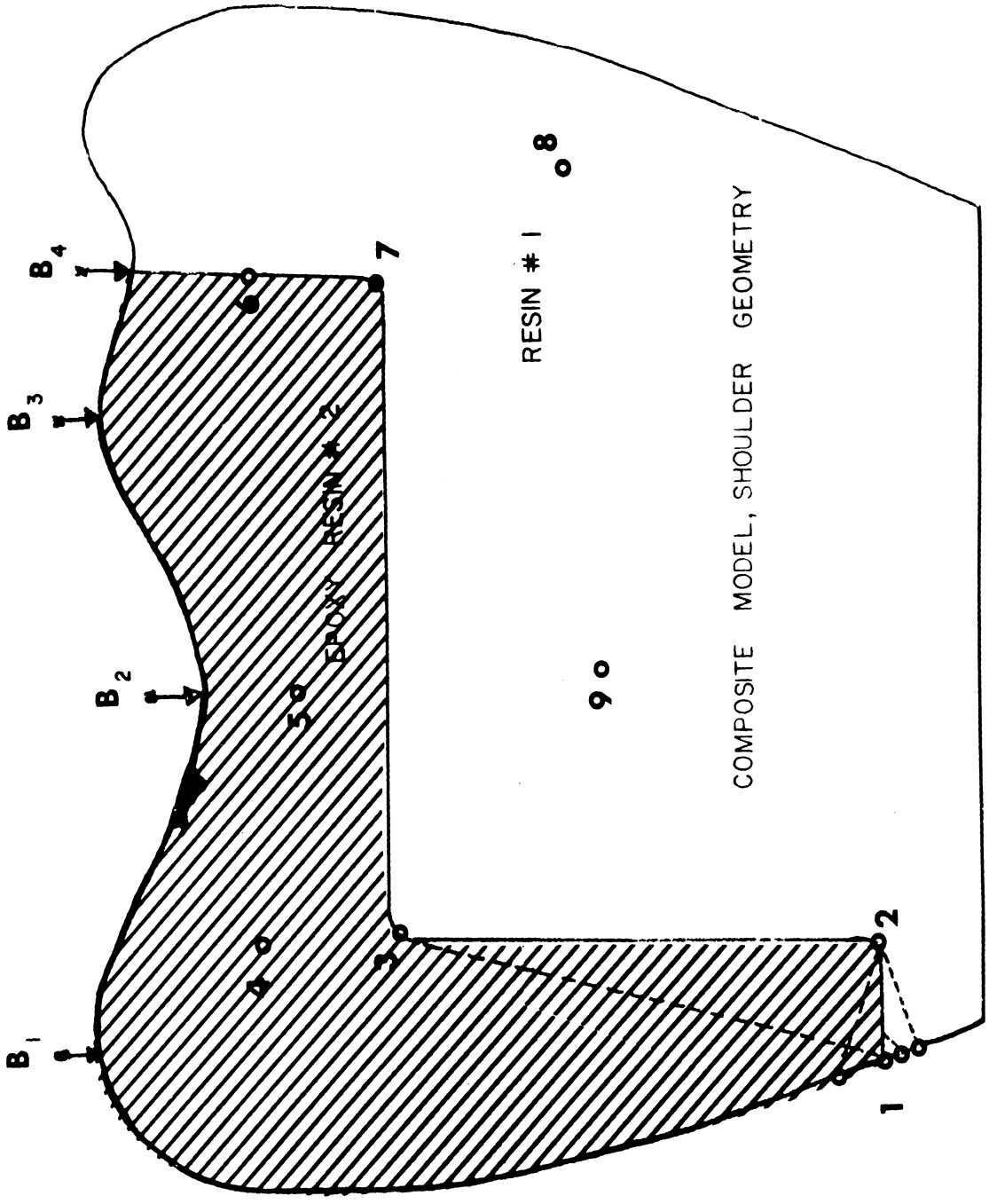

Figure 14. Different Loading Sites of Shoulder Geometry Models. Points 1 to 9 are of Interest in Final Stress Analysis.

is at a right angle to the gingival wall), model No. 5 represents + 15° angulation, Model No. 6 has a -15° angulation, and Model No. 7 is the same as No. 4 except it has a 45° bevel. The models were loaded at four different sites, B_1 to B_4 as shown in Figure 14. All seven models had their number written on the lower left corner by a waxpencil, so that the number will show in the photograph, hence the resins are transparent.

b. Axial Wall Convergence Models. Models were constructed to investigate the effect of parallelism or near parallelism on the stress distribution. Geometrical idealized models were used to study the variations of convergence of axial walls. Five models were built, as shown in Figure 15. The angle of convergence on one proximal side was considered α , and the convergence angle of both sides in relation with the axial wall was 2α . The models were cut so 2α increased from 0° to 20° (model 5). The three loading sites are also shown in Figure 15, as arrows at the top of the model.

c. Occlusal Reduction Models. Models investigating the extent of occlusal reduction, are shown in buccolingual sections in Figure 16 and 17. All models represent the geometry of a lower second molar scaled seven times larger. Model No. 1 has a cavity depth of 15 mm x 26 mm and has a cavosurface bevel. An inlay-onlay was represented by Model 2, where gold covered the tip of the cusps. The thickness of occlusal material was

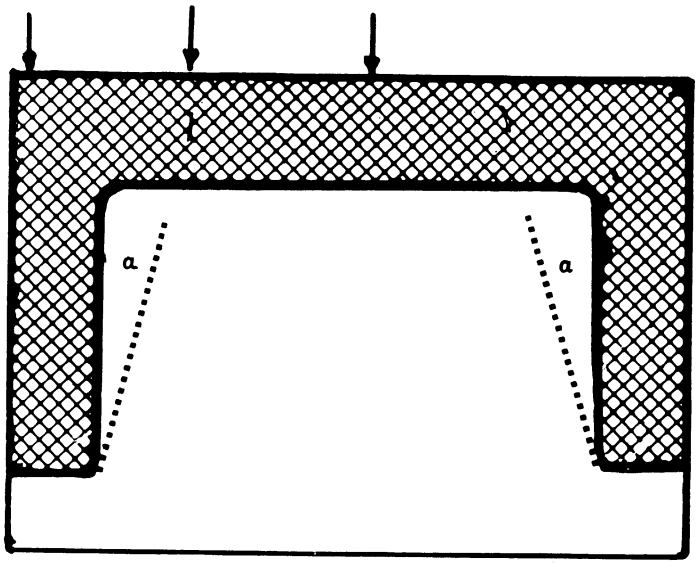

Model # 1	Parallel Axial Walls
Model # 2	$2\alpha = 5°$
Model # 3	$2\alpha = 10°$
Model # 4	$2\alpha = 15°$
Model # 5	$2\alpha = 20°$

Figure 15. Axial Wall Convergence Models.

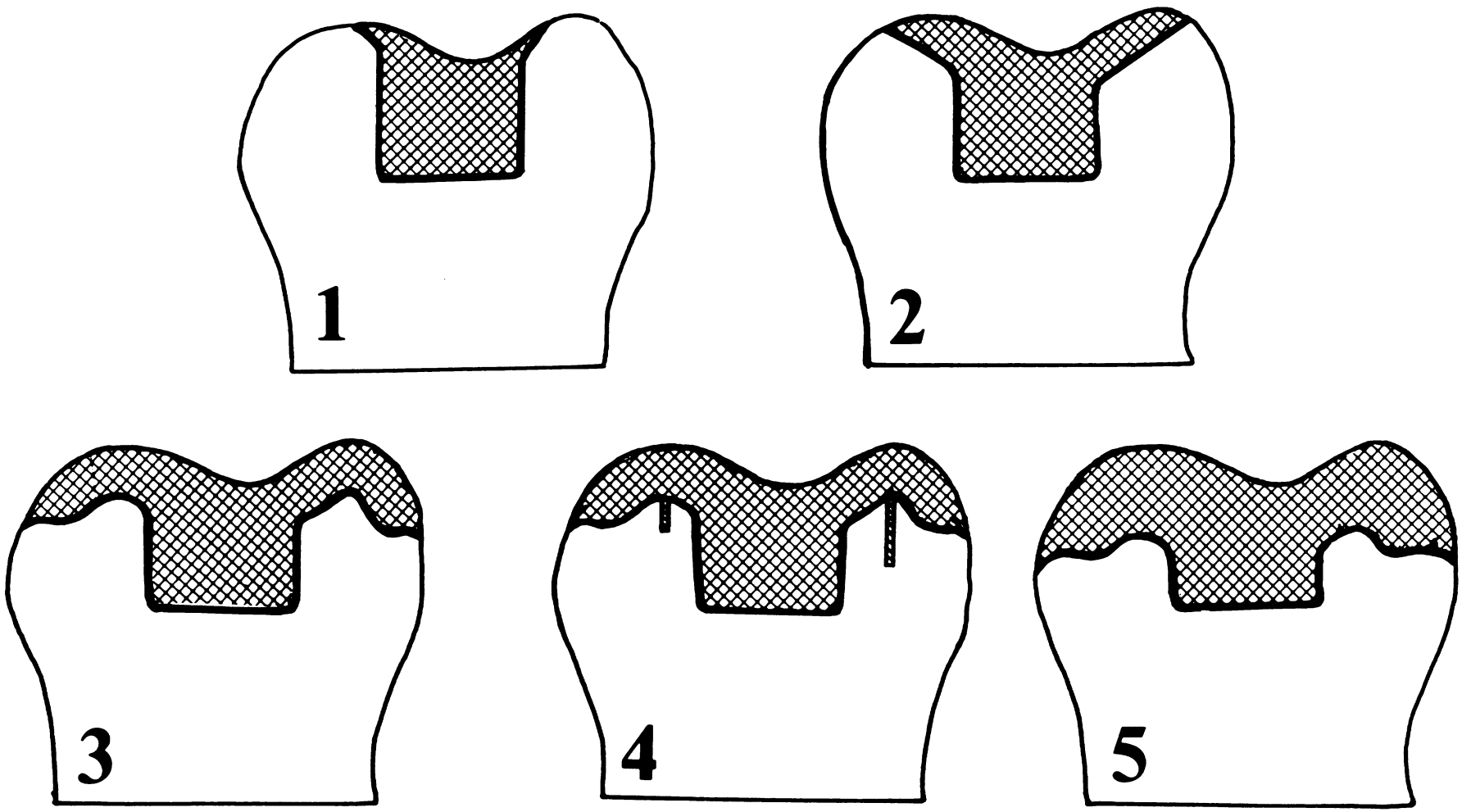

Figure 16. Occlusal Reduction Models 1 to 5.

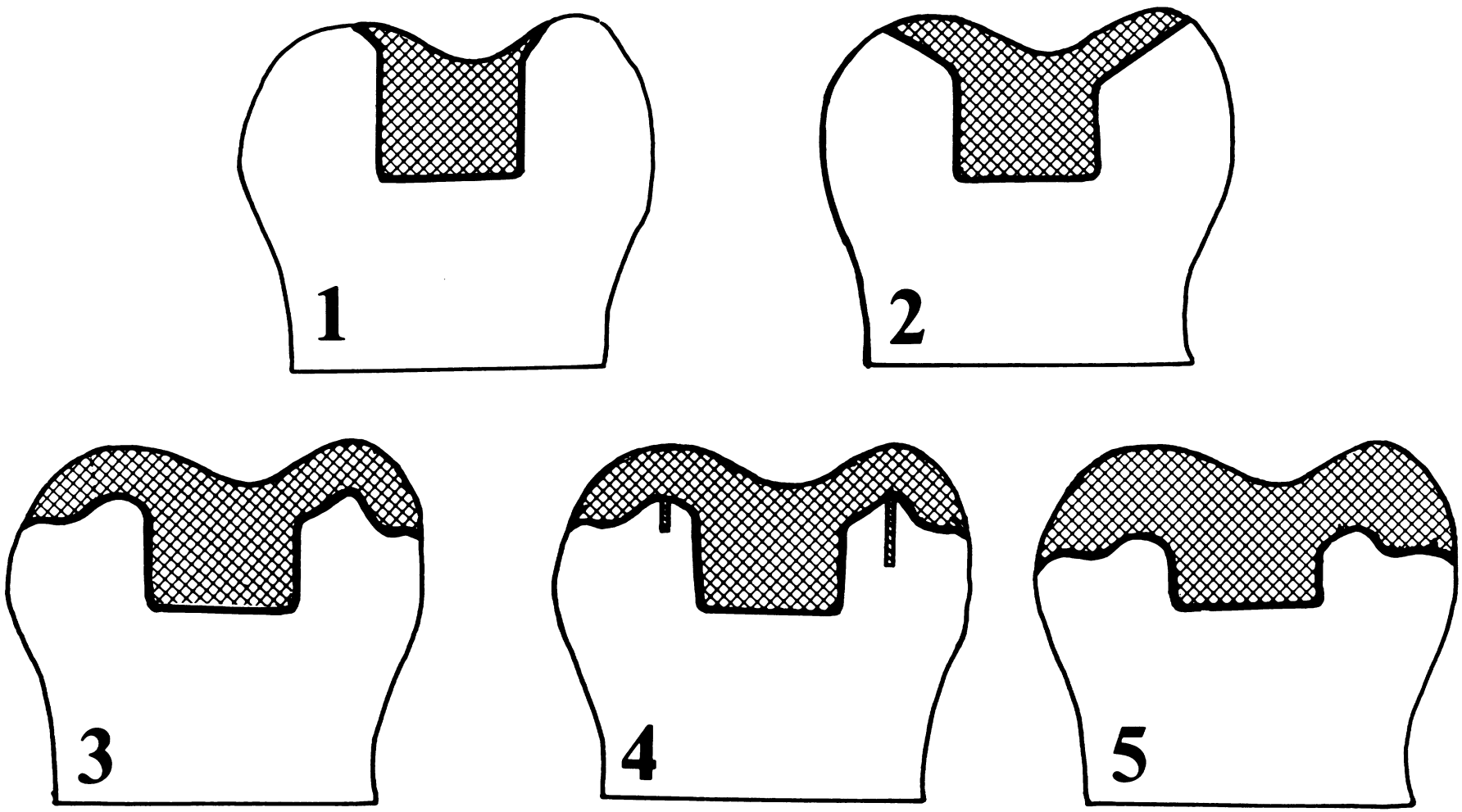

Figure 16. Occlusal Reduction Models 1 to 5.

7 mm buccally, and 5 mm lingually, which in the restoration corresponds to 1 mm and 0.715 mm of gold buccally and lingually. Model No. 3 had 7 mm of occlusal coverage both buccally and lingually. Model No. 4 was the same as 3, except that it had two pins, 3.5 mm long (0.5 mm in the restoration) buccally and 7 mm long (1 mm in the restoration) lingually. Model No. 5 was the same as Model No. 3, except the occlusal coverage was doubled from 7 to 14 mm (1 to 2 mm gold). Model 6 was the same as Model 5, except it had two pins similar in geometry to those of Model 4. Model 7 had 21 mm occlusal reduction, with 11 mm flat cuspal reduction. Model 8 was the same as 7, except that it had pins. Model 9 was a theoretical model, not used in the mouth, which had a 7 mm thick membrane around the whole crown, representing an unrealistic restoration, i.e., a gold crown with an undercut.

All models were cut and luted according to the previously cited procedure. These nine models were used in a three factor experimental design (9 x 3 x 3), as will be shown in Chapter 5.

d. Vertical Pins Models. Six models were selected from the previous nine models. Each design was assigned a letter and subscript, i.e., a_4 represents Model 4. A four-factorial design was planned for the chosen six models, as shown in Table II. Models 4, 6, and 8 were used as those having pins, while 3, 5, and 7 were their counterparts but without pins. The letter d was used to denote the levels

of the design (d_1 means 1 mm gold (7 mm in the model, etc.). This separation of the models would facilitate the separation of the effect of pins from the effect of gold thickness.

e. Proximal Reduction Models. Models investigating proximal reduction in compound restorations, are shown in Figure 18. Model No. 1 represents the slice concept, where AB is 180° to CD , Model No. 2 uses the concept with parallel walls, and Model No. 3 is a box where AB is perpendicular to CD . All three basic designs were constructed in models to represent compound restorations in the mandibular right first molar.

f. Fixed Bridge Models. Sketches of these models are shown in Figure 19, where the shoulderless margins and anatomical occlusal reduction are incorporated in Bridge No. 1. Rounded shoulders and flat occlusal reduction are incorporated in Bridge No 2, while Bridge No. 3 is a cantilever bridge. All r/d ratios were the same for the bridges, as shown in Figure 19. Other similar bridges were constructed, with V or U notches, deliberately included, for comparison purposes.

As a general rule, all drawings were traced on quadrille paper, with five squares to the inch. Then the tracings were cut by a scissor and were luted to the coating paper on the plastic sheet by a double adhesive Scotch tape. Then the models were cut, margins filed and cemented to the substructure. Then models were stress annealed and inspected visually,

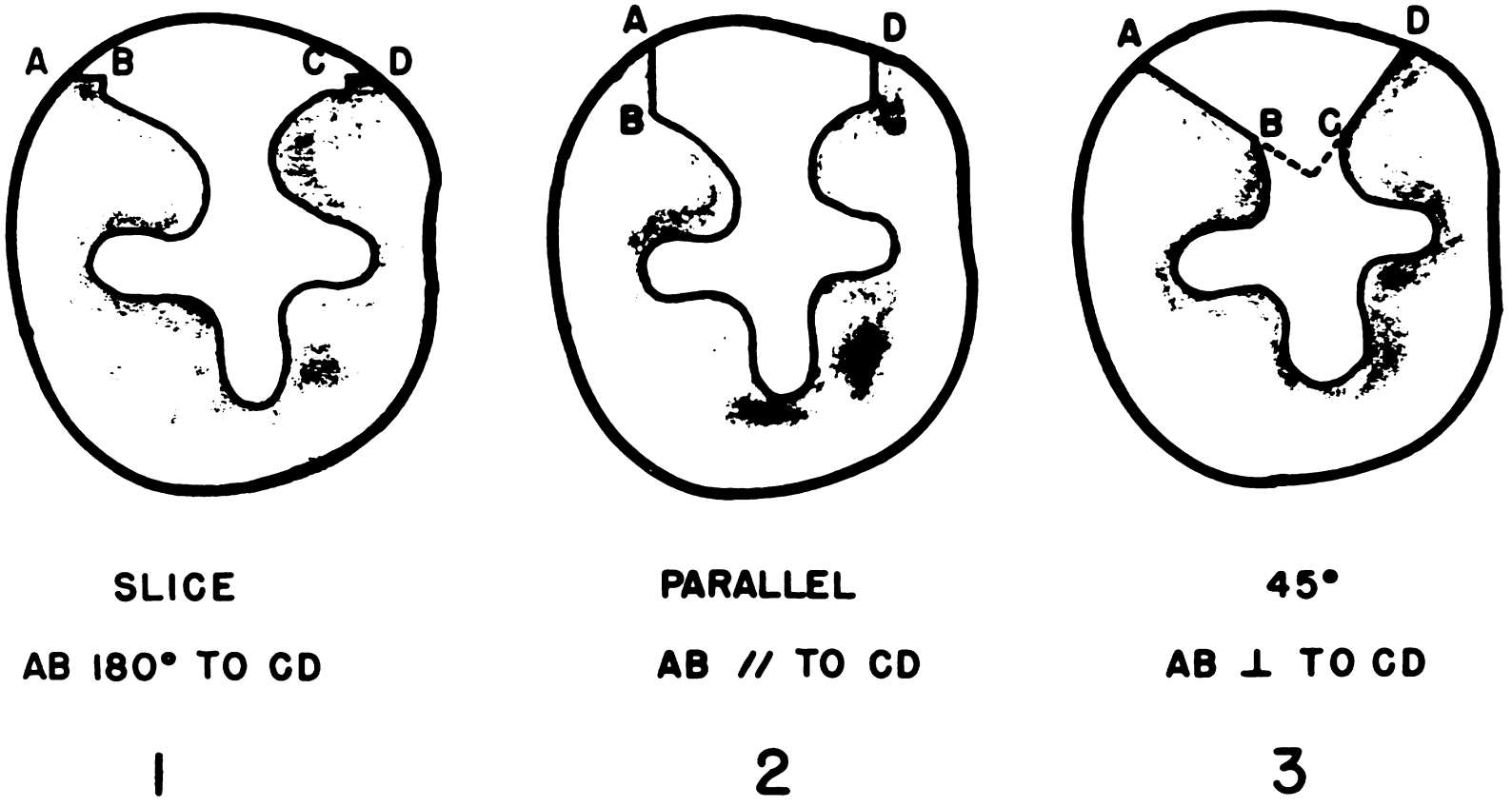

Figure 18. Proximal Reduction Models.

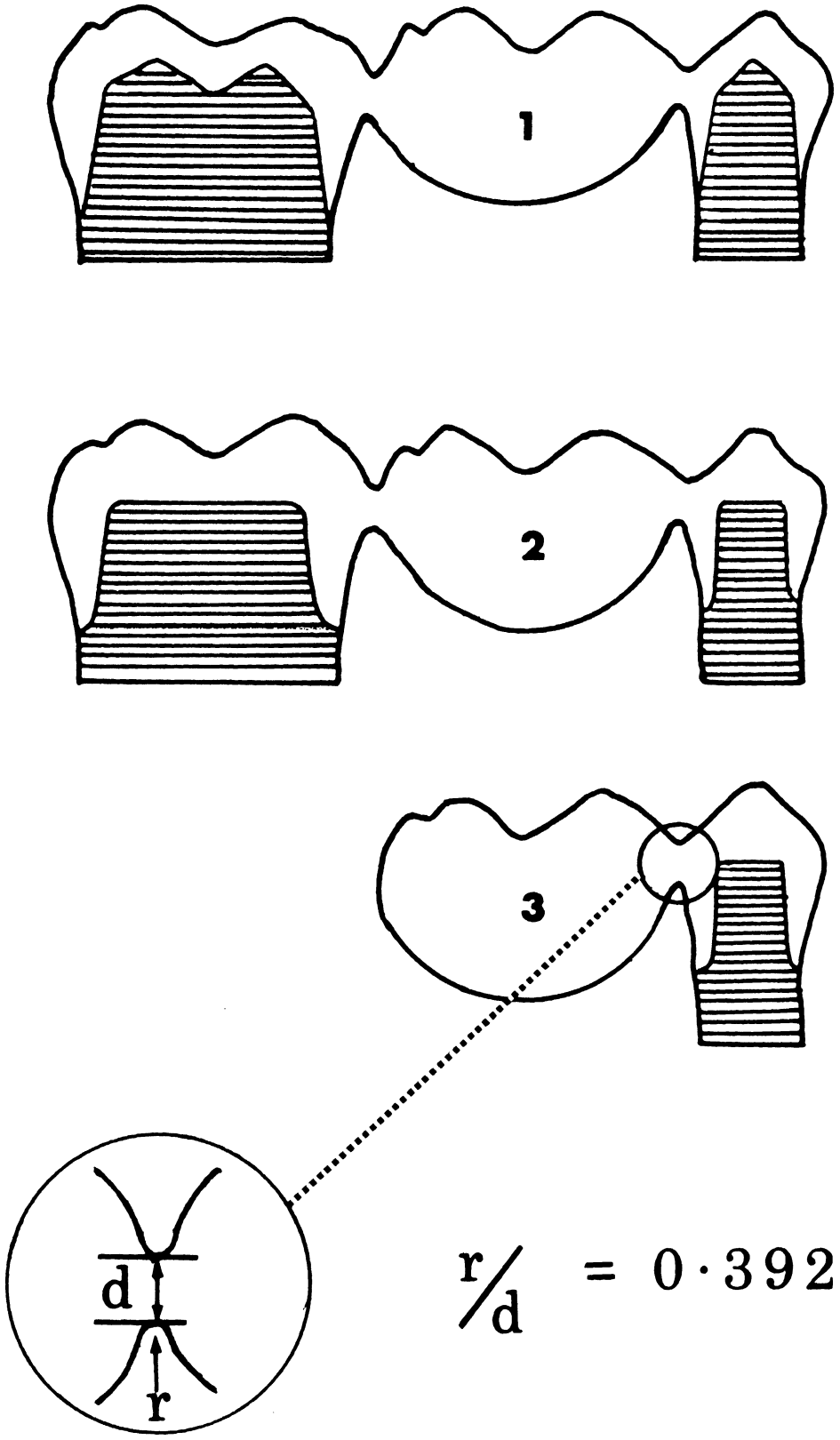

Figure 19. Fixed Bridges Models.

by stacking them. It is estimated that discrepancies in sizes would not exceed one percent by any means.

D. Determination of Stress Concentration Factors.

Stress concentration factor (K) is a dimensionless quantity, which can be expressed by Equation (15).

$$K = \frac{\sigma_{max}}{\sigma_{nom}} \tag{15}$$

where σ_{max} is the maximum stress in a component, and σ_{nom} is the nominal stress. In a situation of uniaxial stress distribution, the nominal stress is the average (P/A) in the net section, e.g., containing a discontinuity. In a situation involving bending, the nominal stress is obtained from the linear distribution (Mc/I) across the height of the beam. Similar basic formulas are used for other cases. Photoelasticity is the most important method for the computation of K , as expressed by Equation (16),

$$K = \frac{\sigma_{max}}{\sigma_{nom}} = \frac{2\,N_{max} \cdot f}{2\,N_{nom} \cdot f} = \frac{N_{max}}{N_{nom}} \tag{16}$$

where N_{max} is determined near the investigated stress raiser and N_{nom} is determined by using a grid over the photoelastic recording.

Stress concentration factor K , is usually referred to as the geometrical or theoretical K , which should be differentiated from fatigue stress concentration factor.

The latter is expressed by Juvinall[118] in Equation (17).

$$K_f = \frac{S_n \text{ for unnotched sample (torsion)}}{S_n \text{ for notched sample (torsion)}} \qquad (17)$$

where K_f is the fatigue stress concentration factor, and S_n is the endurance limit or endurance strength at an arbitrary large number of cycles, such as 5×10^8.

In the present investigation K will be computed according to Equation (16) for different dental structural designs.

It is important to point out that stress concentration factors, determined by two-dimensional photoelasticity are higher numerically than those determined by three-dimensional photoelasticity. The reason is the lack of the reinforcing effect of a three-dimensional structure. The computed K should show a trend, however, as the variations of design in dentistry are irregular and ambiguous.

E. Dimensional Analysis.

One of the most valuable tools available for the interpretation of experimental data is that branch of applied mathematics known as dimensional analysis. In 1915, Buckingham[19] published his now well-known pi-theorem. Since then dimensional analysis has been invaluable to scientific research in applying the results obtained from tests on models in the prediction of the behavior of the prototype and also in generalizing the results from specific tests.

The present method of analysis is limited, however, to the derivation of functional relationships between the variables involved in geometrically similar systems or structures. The dimensional system of mass length and time, denoted respectively by M , L , and T , is more easily applied to the problems in mechanical systems, especially experimental stress analysis. Dimensional analysis is quite general; no previous knowledge of the behavior of the structure or its component parts is necessary. Dimensional analysis is limited to the application of results to geometrically similar structures.

In experimental stress analysis, it is often impracticable to perform tests on the real structure or prototype. Experiments are performed on models, and the stresses or strains in the model are determined. The stresses and strains can then be obtained if the relations between the stresses and strains in the model are known. If subscript m is used for the model, and subscript p for the prototype, σ_p and σ_m will denote stresses in the prototype and model respectively. The transition from model to prototype relationship is shown in Figure 20 (Equation 18). The assumptions are that the phenomena investigated occur entirely within the elastic range. Isotropy and homogeneity, are of course, also assumed, along with geometric similarity.

Another example showing the value of dimensional analysis, is loading of beams. A cantilever beam under concentrated load could be studied. If the beam length is l, load is F , and maximum deflection is Y max , then

TRANSITION FROM MODEL TO PROTOTYPE

$$\sigma_p = \frac{F_p L_m^2}{F_m L^2} \sigma_m \qquad (18)$$

σ_p = Stress in the prototype.

σ_m = Stress in the model.

F_p = A force applied to the prototype.

L = A linear dimension in the prototype.

m = A subscript denoting corresponding values for the model.

Figure 20. Dimensional Analysis Equation for Interpretation of Experimental Data.

$$Y \text{ max} = \frac{Fl^3}{3EI} \tag{19}$$

If the models were constructed geometrically similar to the prototype, its length would be given as $l_m = \lambda l_p$, and the moment of inertia I_m would be given as $I_m = \lambda^4 I_p$. As is easily observed the equations for maximum deflection in the prototype are given respectively

$$Y_p \text{ max} = \frac{F_p \; l^3_p}{3E_p \; I_p} \tag{20}$$

$$Y_m \text{ max} = \frac{F_m \; l^3_m}{3E_m \; I_m} \tag{21}$$

By substituting the geometrical dimensions of the model in terms of those of the prototype, we obtain scale factor law for the maximum deflections

$$Y_m \text{ max} = \frac{F_m \; E_p \; (Y_p \text{ max})}{F_p \; E_m \; \lambda} \tag{22}$$

From this equation it can be seen that one way to have Y_m max = Y_p max is to make $E_p = E_m$ and $F_m = F_p$, where λ is the scale factor.

CHAPTER V

RESULTS

The interpretation was performed based on cause and effect as well as detailed statistical inference. The results will be cited for each design factor separately under four separate titles, namely: (1) Photoelastic interpretation, (2) Statistical inference, (3) Computation of stress concentration factors, and (4) Stress analysis of the optimum restoration. Some of the design factors will be combined together, and discussed later under the preliminary investigation of dental bridges.

A. Shoulder Geometry Experiments

1. Photoelastic Interpretation.

Seven different margins were investigated, which were shown in Figure 14. All models were loaded at four different sites, using two different concentrated loads (50 and 100 pounds) at each site for each model. Complete factorial design was used in the experiments, as shown in Table I. In the present experiments the third row for b_2 was dropped (which begins with $a_1b_1c_3$ and ends with $a_7b_2c_3$). All cells were completely investigated, which would help increase the precision of the experiments. Since hundreds of pictures were recorded, only examples will be supplied in the present study, taking into consideration that the same site and the same load will be shown in the same figure. This procedure will help in the comparative description of the corresponding models.

Examples of the present experiments are shown in Figures 21 and 22. Figure 21 shows models having two different margins (rounded shoulder and knife edges shoulder) under 100 pounds load. The concentrated normal load was applied occlusally on the proximal side which was being restored. Both photographs were taken when the polarizer and analyzer were parallel, i.e., light field. The upper photograph shows 10 fringes near the margin investigated, while the lower picture shows 17 fringes, which is quite high. The letter p in the lower picture, indicates parasitic birefringence which was not removed after stress annealing.

Figure 22 shows two different model designs, with 100 pounds load applied to both. The upper picture shows Model 6 (-15°), using dark field photography, (full-order isochromatics). The maximum fringes which could be counted near the site of load application was 16. The arrow at lower right corner, indicates an area of high stress concentration. All the important fringes (high order) appeared in the tooth structure, and no significant isochromatics were found in the restoration. The lower photograph in Figure 22, shows Model 4 (flat shoulder with axial wall perpendicular to the gingival floor) employing light field photography, (half-order isochromatics). The maximum fringes near the site of load application was found to be 16.5. The arrow at the lower right corner indicates an identical area of high stress concentration to that in the upper picture of Figure 22. For all practical purposes, it could be assumed that Models 4 and 6 functioned identically under the same load.

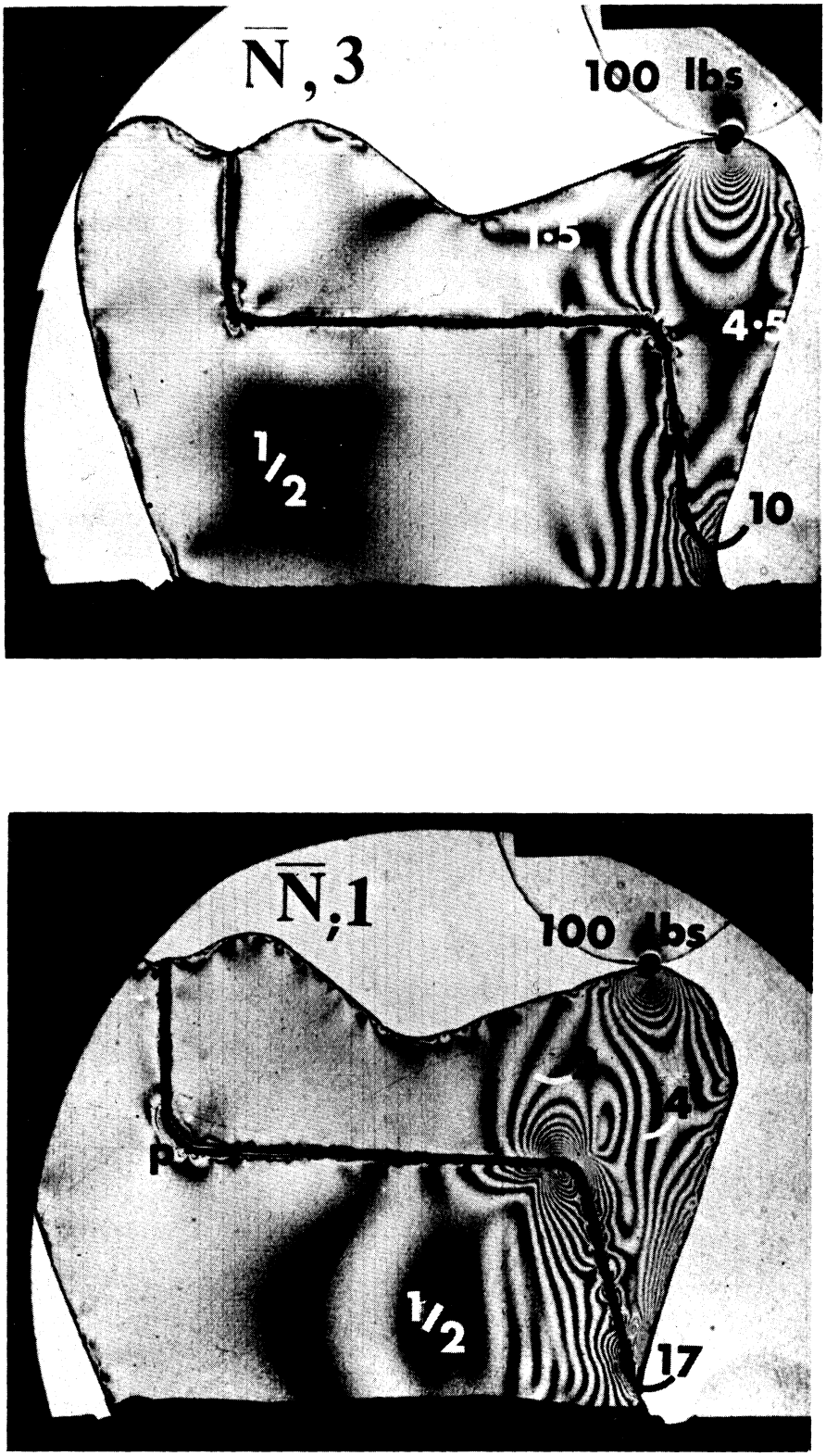

Figure 21. Light Field Isochromatics for Shoulder Model 3 (Rounded), Are Shown in Upper Photograph, and for Shoulder Model 1 (Knife-Edge) Are Shown in Lower Photograph. 100 Pounds Concentrated Load Was Used.

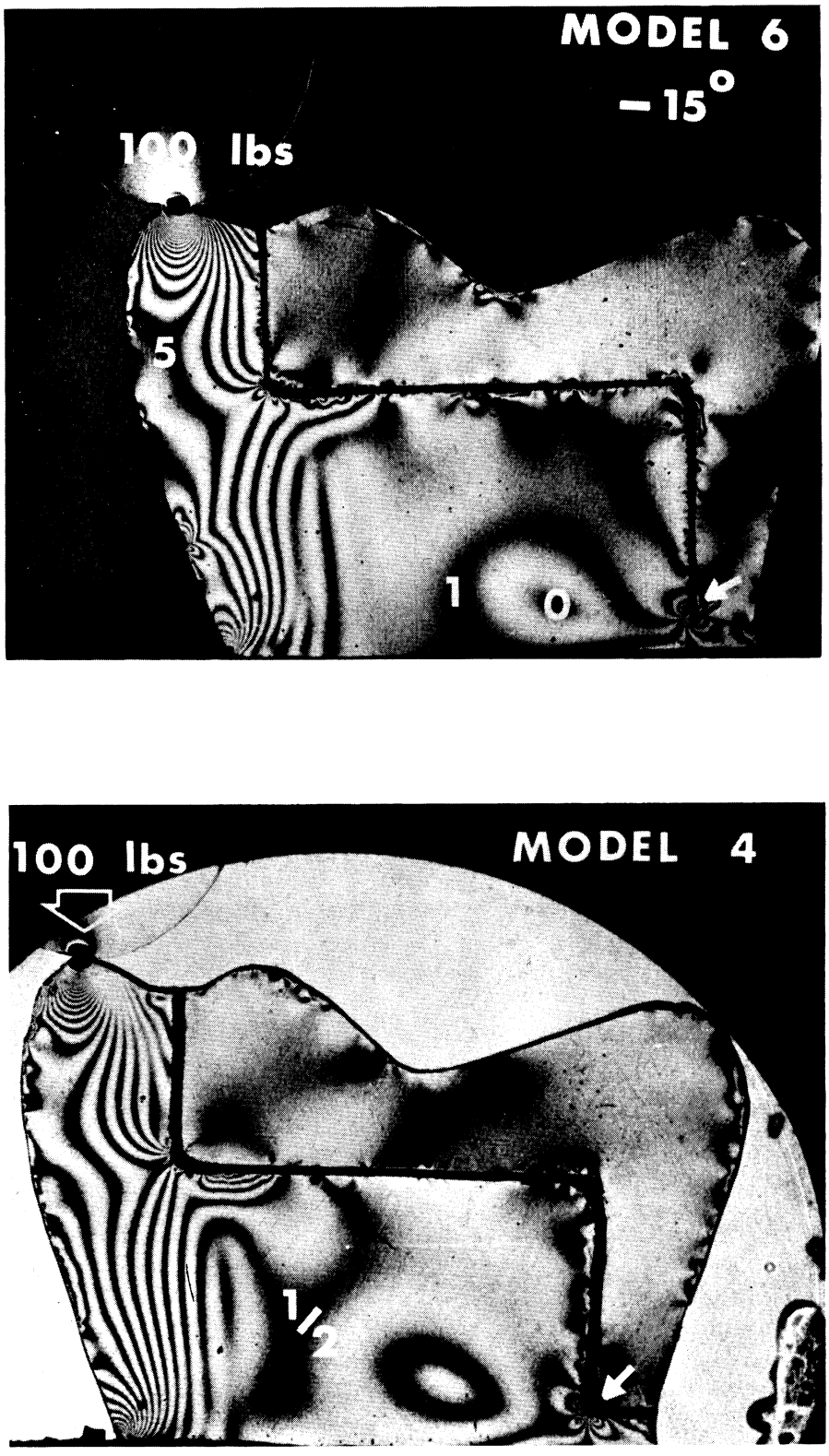

Figure 22. Dark Field Isochromatics in Shoulder Model 6 are Shown in Upper Photograph, and Light Field Isochromatics in Shoulder Model 4 are Shown in Lower Photograph. 100 Pounds Concentrated Load was Used.

2. Statistical Inference.

The results obtained photoelastically, were recorded to the nearest eighth of a fringe. All the results were tabulated, after multiplying each reading with a factor 8. This statistical transformation resulted in the sums of squares being larger by a factor of 8^2, but did not affect the accuracy of the F statistic.[13]

An analysis of variance test was made to determine the signifiance of the treatment difference with respect to the error variance. The results of this analysis are given in Table III. Factor A represents the seven shoulders, factor B the four loading sites, and factor C the two different loads. Since the F values obtained for factor A exceeded the critical $F_{(6,\infty)}$ value of 3.09 at the 0.005 level, the shoulders produced a significant difference in stress distribution. Stress distribution at the four different sites was significantly different ($7.317 > 4.28$)*** It can be deduced that there are real differences between the seven tested designs, and there are real differences between the four different sites of load application. Apparently the magnitude of loads is not highly significant, since the F ratio for factor C was significant only at 90 percent confidence level. Only one first order interaction was significant, BC, which indicated that factors B and C are not independent.

The standard error of the mean ($S_{\bar{x}}$) was computed as shown in Equation (1), and was found to be 0.78 percent.

TABLE III

ANALYSIS OF VARIANCE FOR SEVEN SHOULDERS LOADED
AT FOUR DIFFERENT SITES WITH TWO DIFFERENT LOADS

SOURCE OF VARIATION	D·F·	SUMS OF SQUARES	MEAN SQ	F
A	6	6512·30	1085·38	3·105 ***
B	3	7674·36	2558·12	7·317 ***
C	1	1005·84	1005·84	2·877 *
AB	18	2037·45	113·19	0·324 NS
AC	6	1252·02	208·67	0·597 NS
BC	3	6301·98	2100·66	6·009 ***
ABC	18	3218·93	178·83	0·512 NS
ERROR	448	15,661·45	349·58	—
TOTAL	503	184·613·33	—	—

*** = 99·5% * = 90% NS = NOT SIGNIFICANT

This estimates the variation that would arise if repeated models were constructed, the seven different designs tested, and the mean of each design computed.

In order to rank the different designs, Duncan's new multiple range test, and orthogonal contrasts were employed. The problem was to determine which of the differences among the seven means were statistically significant. The ranking of designs is shown in Figure 23. Designs 2 and 3 were the same, and all others were significantly different, ($p < 0.01$).**

The coefficient of variability (C.V.) of all the experiments was computed as shown in Equation (23),

$$C.V. = \frac{100\ S_{\bar{x}}}{\bar{\bar{x}}} \tag{23}$$

where C.V., is the coefficient of variability, $S_{\bar{x}}$ is the standard error, and $\bar{\bar{x}}$ is the mean of all the means. The coefficient of variability was found to be 5.82. This coefficient is independent of the unit of measurement used, since it is the ratio of two averages. The (C.V.) is a relative measure of variation, throughout the experiments.

3. Computation of Stress Concentration Factors.

Stress concentration factors were computed using Equations (15) and (16). The knife-edged shoulder (Model 1) had the highest value, $K = 5.1$, while the rounded margin (Model 3) had the lowest value, $K = 2.39$. Geometrically and structurally, the results were rather logical. Model 2 was the second best ($K = 2.48$) while (Model 7) was the second highest

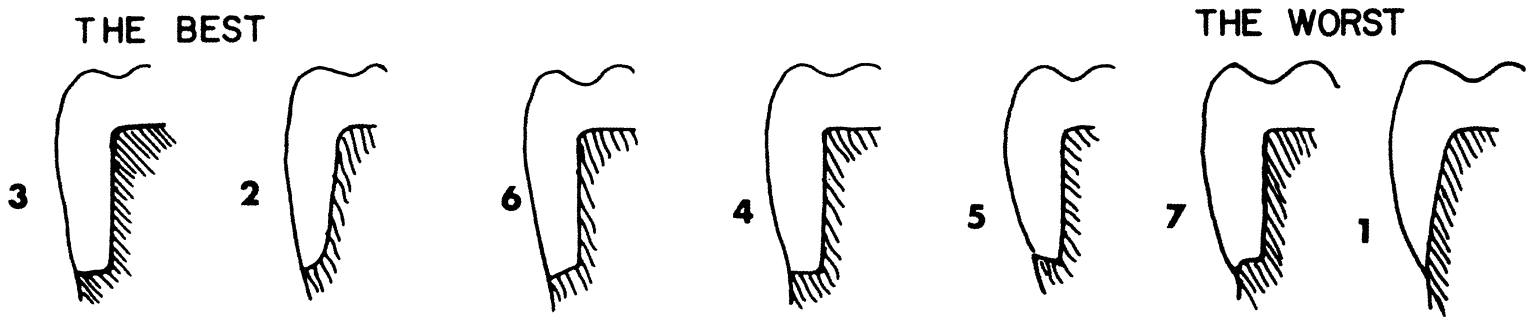

° Duncan's New Multiple Range Test.

°° Orthogonal Contrasts.

Figure 23. Results of Duncan's New Multiple Range Test and Orthogonal Contrasts for Shoulder Differences.

(K = 3.6). Stress concentration factors for Models 4, 5, and 6 were found to be 3.2, 3.8, and 2.9 respectively, as shown in Figure 24. The dotted line represents the mean K. It is assumed that all designs below the dotted line would be acceptable, if the dotted line is considered to represent 100 percent stress concentration. These results are in concordance with the statistical interpretation.

4. Stress Analysis of Shoulder Geometry Model 3.

The classical approach to any stress analysis problem would be to determine the principal stresses at each point in the structure, from which the maximum principal stresses and the planes upon which these stresses act could be determined. Since failure in proximal restorations occurs at the proximal margin, which result in macroscopic or microscopic separation of the gold restoration from the tooth structure, this area was selected for detailed analysis.

Model 3 was chosen for the complete stress analysis, since it had the lowest stress concentration factor. Isoclinic parameters are shown in the upper half of Figure 25. In general, isoclinics of different parameters do not intersect, since principal directions are unique. The only exception is an isotropic point; i.e., a point under a hydrostatic state of stress. At an isotropic point, every direction is principal and therefore all isoclinics converge toward it. No isotropic points were found.

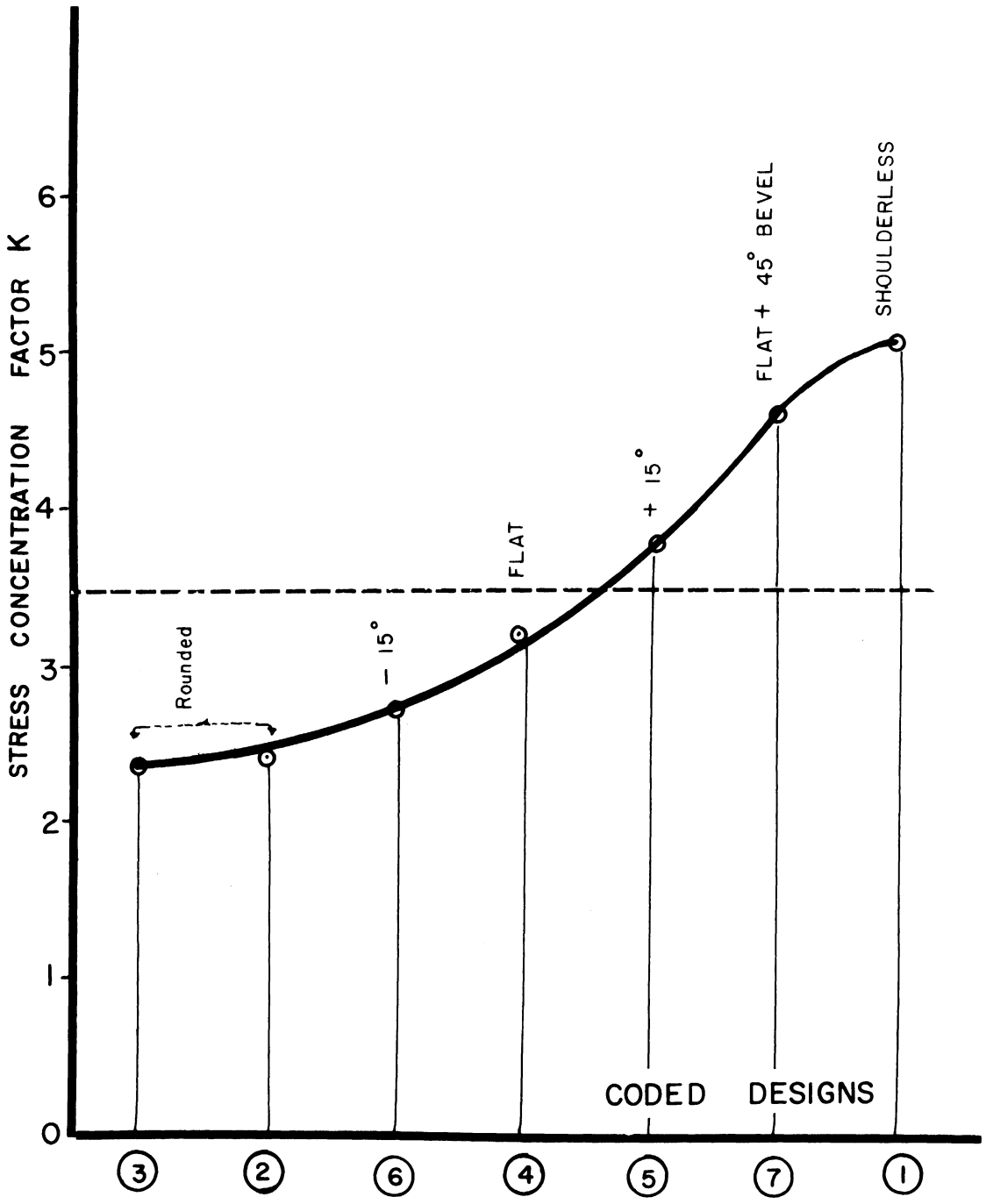

Figure 24. Stress Concentration Factors for Models with Various Shoulder Designs.

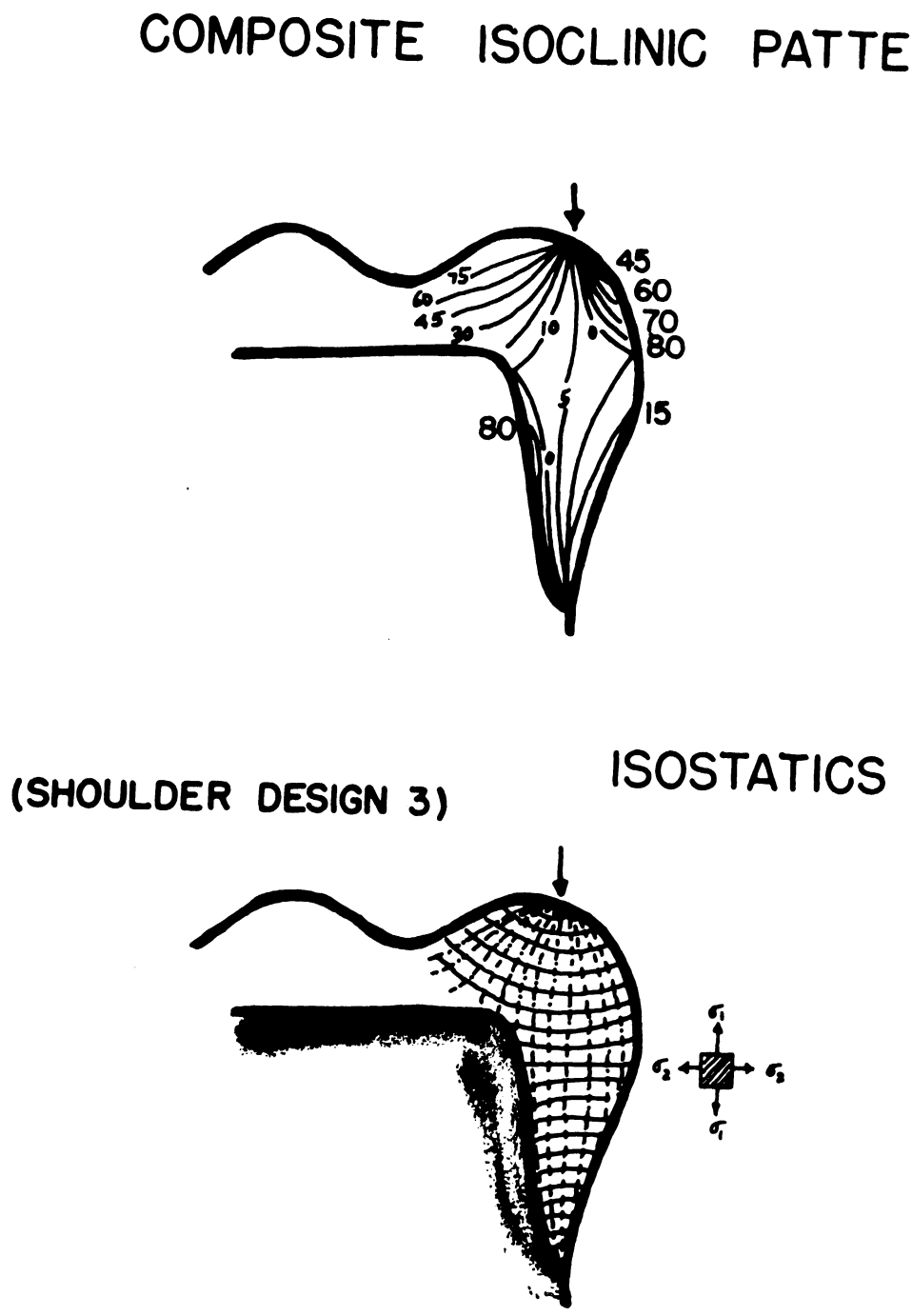

Figure 25. Isoclinics and Isostatics for Shoulder Model 3.

Lines of principal stress or stress trajectories (isostatics) were traced by use of the isoclinics. The isostatics, drawn over the whole area, give a good picture of the stress distribution with respect to directions, and from such a series the direction of principal stress at any intermediate point may be found easily by interpolation. These lines of principal stress form two sets of curves, any curve of one set intersecting any curve of the other set at right angles. Isostatics for shoulder design 3 are shown in the lower half of Figure 25. One set of curves is for σ_1, and the other is for σ_2. The principal stress difference ($\sigma_1 - \sigma_2$) at any point will then have a definite meaning in terms of the direction of σ_1 and σ_2 lines at that point. It is evident by visual inspection of isostatics that the point where a concentrated load is applied, (in this case 100 pounds), the stress system in the neighborhood of the load is principal in the σ_1 and σ_2 directions, where the point of load application is the center of this circle. This last rule applies to all isostatics in the vicinity of a concentrated normal load.

The principal stresses were separated along line AB, as shown in Figure 26. The shear-difference method was used, which was shown in Figure 5. The isochromatics were used to compute directly the difference between the principal stresses throughout the model, which is represented by the ($\sigma_1 - \sigma_2$) curve. At point 23 on the ΔX axis σ_2 approaches 100 psi, and σ_1 approaches the maximum value of 5137 psi (σ_{max});

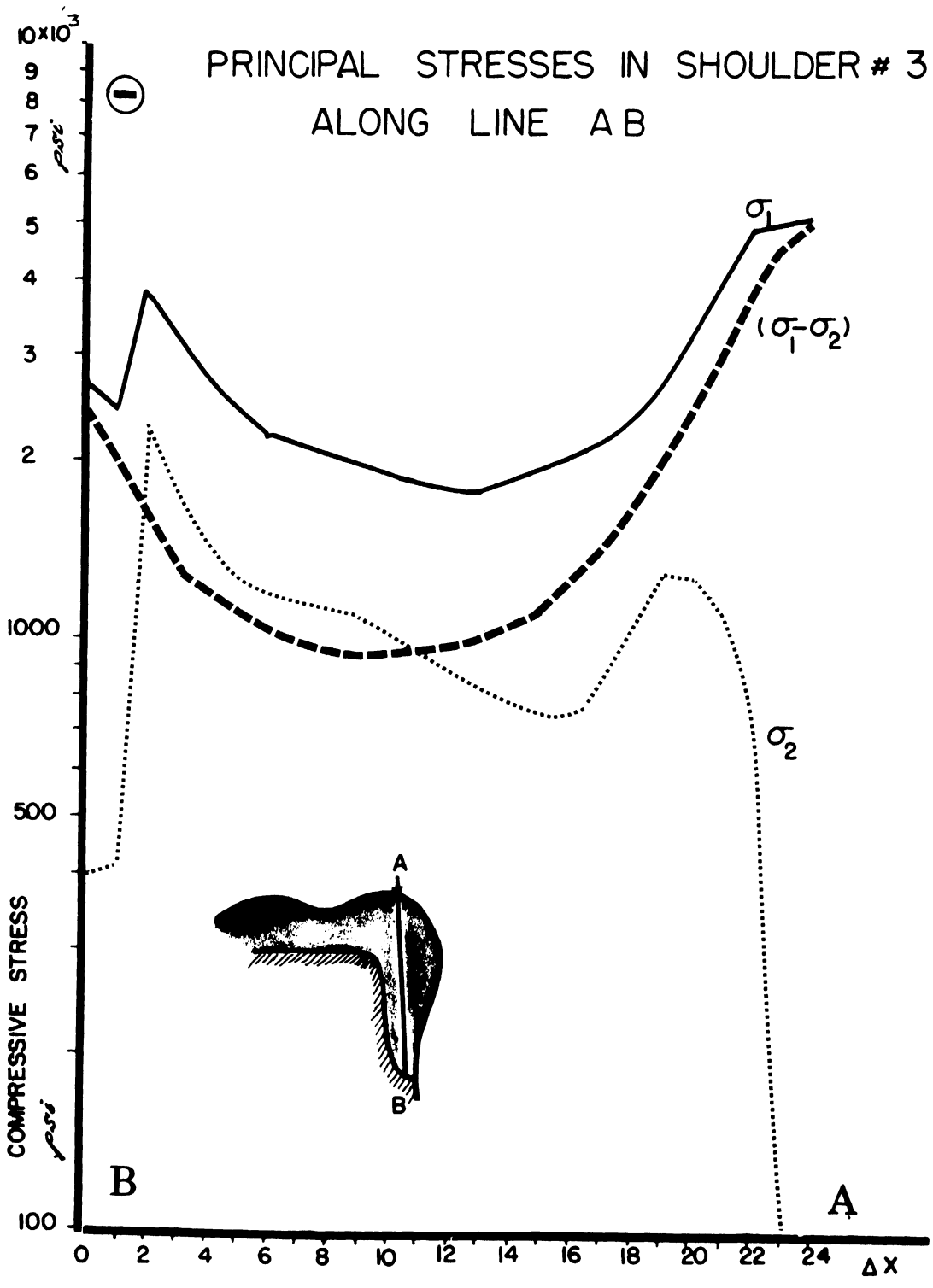

Figure 26. Separation of Principal Stresses in Shoulder Geometry Model 3 Along Line AB.

σ_1 decreases generally as B is approached, and at B has a value of 2809 psi. σ_2 becomes 403 psi at B. Both σ_1 and σ_2 at B are compressive in nature, which should be desirable from a design viewpoint. The sign of the shearing stress along AB was negative also (compression). The values of the principal stresses could be used in dimensional analysis (Equation 18), for translation from model to prototype.

B. Axial Wall Convergence Experiments

1. Photoelastic Interpretation.

In all the following photoelastic photographs the letter ϕ was stamped on the code number of the photoelastic model, in order not to confuse the order of the isochromatic fringes with the serial number of the investigated model.

Five different axial wall models were investigated, as shown in Figure 15, where 2α ranged from 0° to 20°. Three different sites of loads were selected, (1) at the center of the model, (2) midway between the center and the proximal edge, and (3) a site which was just inside the proximal edge, to avoid high bending moments. Two loads were used; 50 and 150 pounds.

Axial wall model 1 (2α = 0°) and 2 (2α = 5°) are shown in Figure 27. The upper picture shows isochromatics, using dark field photography (full order fringes), and a 150 pound load was used midway between the center and edge of the model, as indicated by the white arrow. The order of the isochromatics is shown by the white numbers, and it is evident that the fringes converge then diverge again along the restoration-tooth interface.

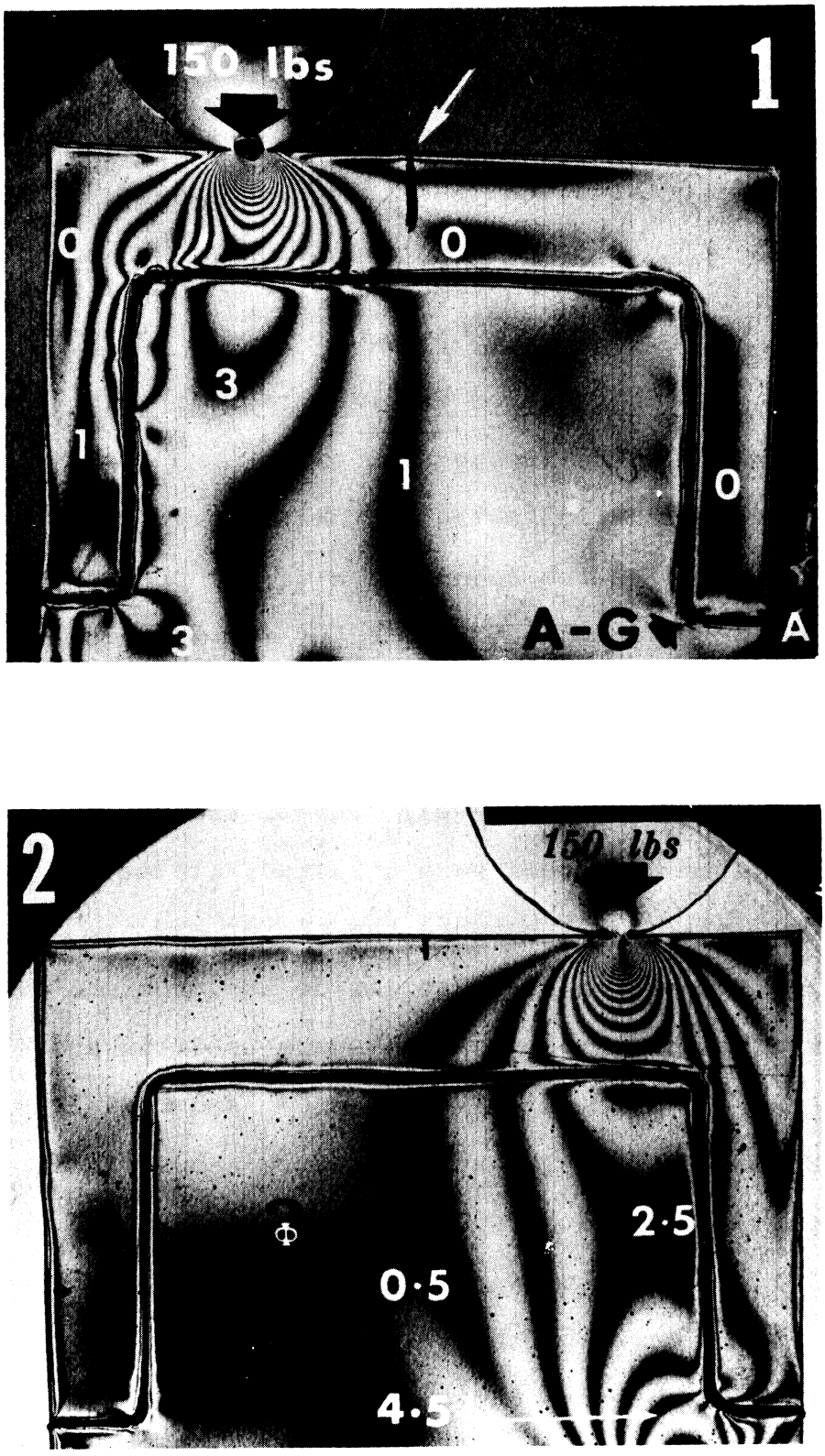

Figure 27. Axial Wall Model 1 ($2\alpha = 0°$) Is Shown in the Upper Photograph, Using Dark Field Photography. Axial Wall Model 2 ($2\alpha = 5°$) Is Shown in the Lower Photograph, Using Light Field Photography.

N_{max} , was located just under the concentrated load and was found to be about 16 fringes, i.e., about 960 psi shear stress. The white letter A at the lower right corner of the upper photograph denotes an artifact. The lower photograph shows axial wall Model 2, which was loaded at the same site, but on the other side, since there was a geometrical symmetry along the vertical axis in the convergence models. All the half-order isochromatic fringes were compressive in nature. It is interesting to note that the order of the fringe at the axio-gingival line angle (A-G) was 4.5 compared to 3 in Model 1. N_{max} was 18.5, or a shear stress of about 1100 psi.

Isochromatic fringes in axial wall Models 4 and 5 are shown in Figure 28. The upper picture represents Model 4, under 150 pounds loaded at the center. The heavy black arrow at the top, indicates the midway loading position. The two small black arrows are pointing to the axio-gingival line angles, where no crowding of fringes was observed. N_{max} in Model 4 was 18.5 fringes. The lower picture in Figure 28 shows Model 5 subjected to a load of 100 pounds and again complete symmetry was observed. The letter P at the lower right corner indicates parasitic birefringency. The fringe order in Model 5 (100 pounds) at the axio-gingival line angle was 2.5, versus 0.5 in Model 4 (150 pounds). N_{max} in axial wall Model 5 was 12 fringes. These results are only examples of the overall results, and they will be discussed in detail in the next chapter.

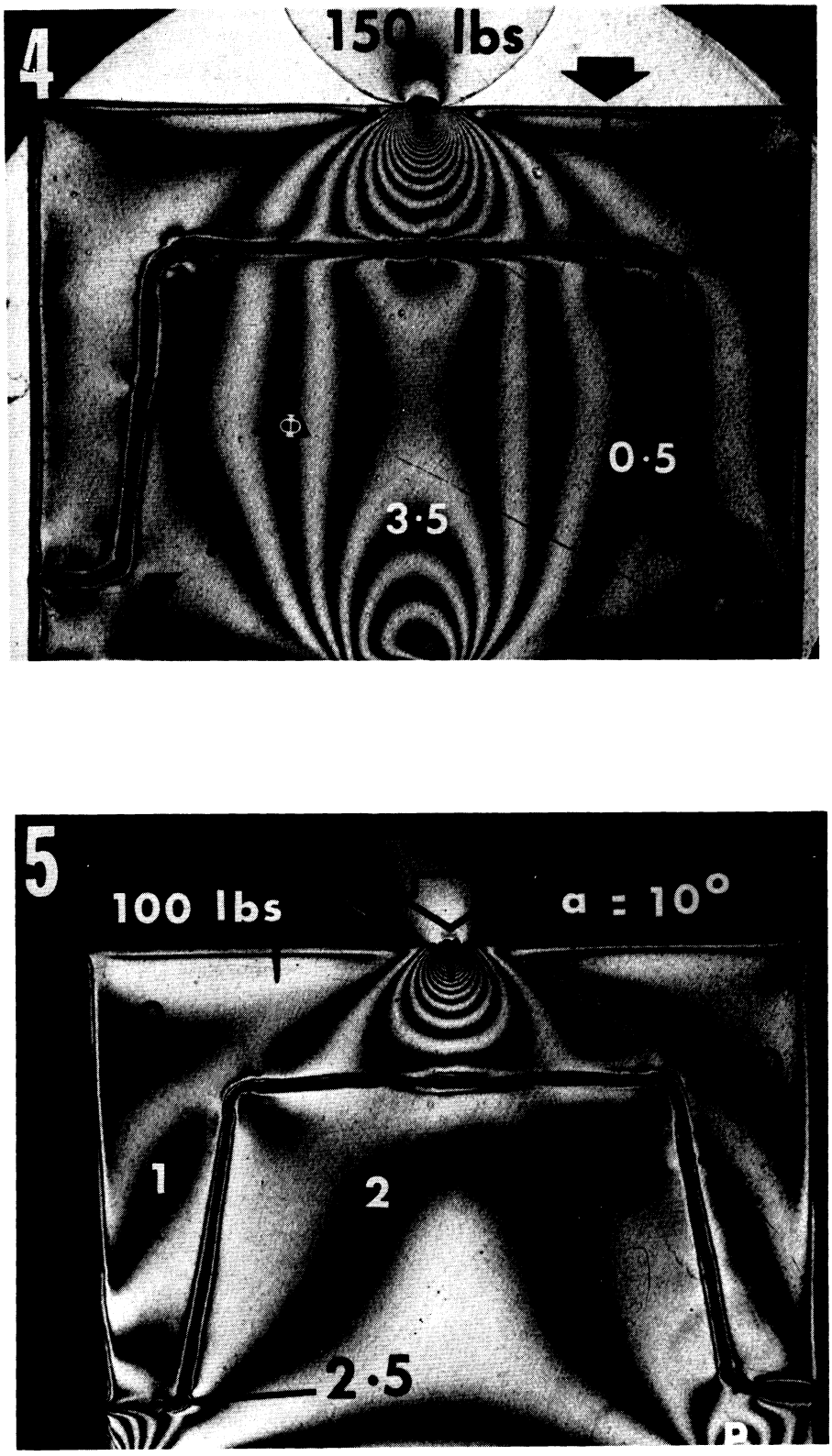

Figure 28. Isochromatic Fringes in Axial Wall Models 4 ($2\alpha = 15°$) and 5 ($2\alpha = 20°$). Upper Photograph Represents Light Field Photography and Lower Photograph Represents Dark Field Photography.

2. Statistical Inference.

The photoelastic results for all models, and all loads at different sites were tabulated to the nearest eighth of an isochromatic fringe using the grid method. The original recordings were mutliplied by a factor of 8 as in previous experiments.

The results of the analysis of variance were obtained from 7090 IBM computer, and are given in Table IV. Factor A represents the five different designs of the convergence of axial walls, factor B represents the three loading sites, while factor C denotes the two loads (50 and 150 pounds).

Since the F value obtained for factor A exceeded the critical $F_{(4,\infty)}$ value of 3.72 at the 0.005 level, it was deduced that the designs produced a significant difference in stress distribution. No significant statistical difference was detected for factor B, while factor C was significant at the 0.05 level. The first-order interaction BC was highly significant at the 0.005 level, which indicated some relationship between the magnitude of the load and the site of application due to an additional effect of the combined influence of the two factors. The same type of interaction, BC, was found significant in the Table III.

The standard error of the experiments was 0.41 percent, and the coefficient of variability was 5.54. Using Duncan's test, it was found that Model 1 was different from all other models except Model 2. By writing linear orthogonal contrasts, Models 3 and 4, and 1 and 2 did not show any significant statistical difference, $(p < 0.005)$.***

TABLE IV

ANALYSIS OF VARIANCE FOR FIVE AXIAL WALL CONVERGENCE MODELS LOADED AT THREE DIFFERENT SITES WITH TWO DIFFERENT LOADS

SOURCE OF VARIATION	D.F.	SUMS OF SQUARES	M.SQ.	F
A	4	1,363.94	340.94	3.831***
B	2	399.76	199.89	2.25 NS
C	1	516.27	516.27	5.80**
A B	8	243.81	30.48	0.343 NS
A C	4	264.57	66.14	0.743 NS
B C	2	1,473.11	736.55	8.28***
A B C	8	475.31	59.41	0.680 NS
ERROR	210	18,688.00	88.99	—
TOTAL	239	23,424.60	—	—

*** = 99.5 % ** = 95 % N S = NOT SIGNIFICANT

3. Computation of the Stress Concentration Factors.

Stress concentration factors (K) were computed and the effect of convergence angle on K is shown in Figure 29. The mean K was computed as 3.01, as indicated by the dotted horizontal line, parallel to the x-axis. The highest K was for Model 5, of 4.79, while the lowest K of 2.41 was for Model 2. Stress concentration factors for Models 1, 3, and 4 were found to be 2.5, 2.67, and 3.2, respectively. Axial wall designs 1, 2 and 3 were below the mean K, and could be considered acceptable, if the mean was to represent 100 percent stress concentration.

4. Stress Analysis of Axial Wall Model 4.

Model 4 was chosen for the complete stress analysis, because it is the most popular in dentistry. The shear stresses are shown in Figure 30, along AB (dotted line) and CD (solid line). Both AB and CD pass from the mesial to the distal sides of the model. The shear stress along AB was higher than the corresponding shear stress along CD. τ_{xy} was about 550 psi (negative sign), at $\Delta X = 9$ along AB.

The principal stresses were separated along line OP, which passed between the planes AB and CD, as shown in Figure 31. The maximum compressive stress was about 1400 psi, while the maximum tensile stress was about 55 psi.

Point 12 was chosen for further analysis, since in occlusion, load is applied in this vicinity. σ_x was 680 psi,

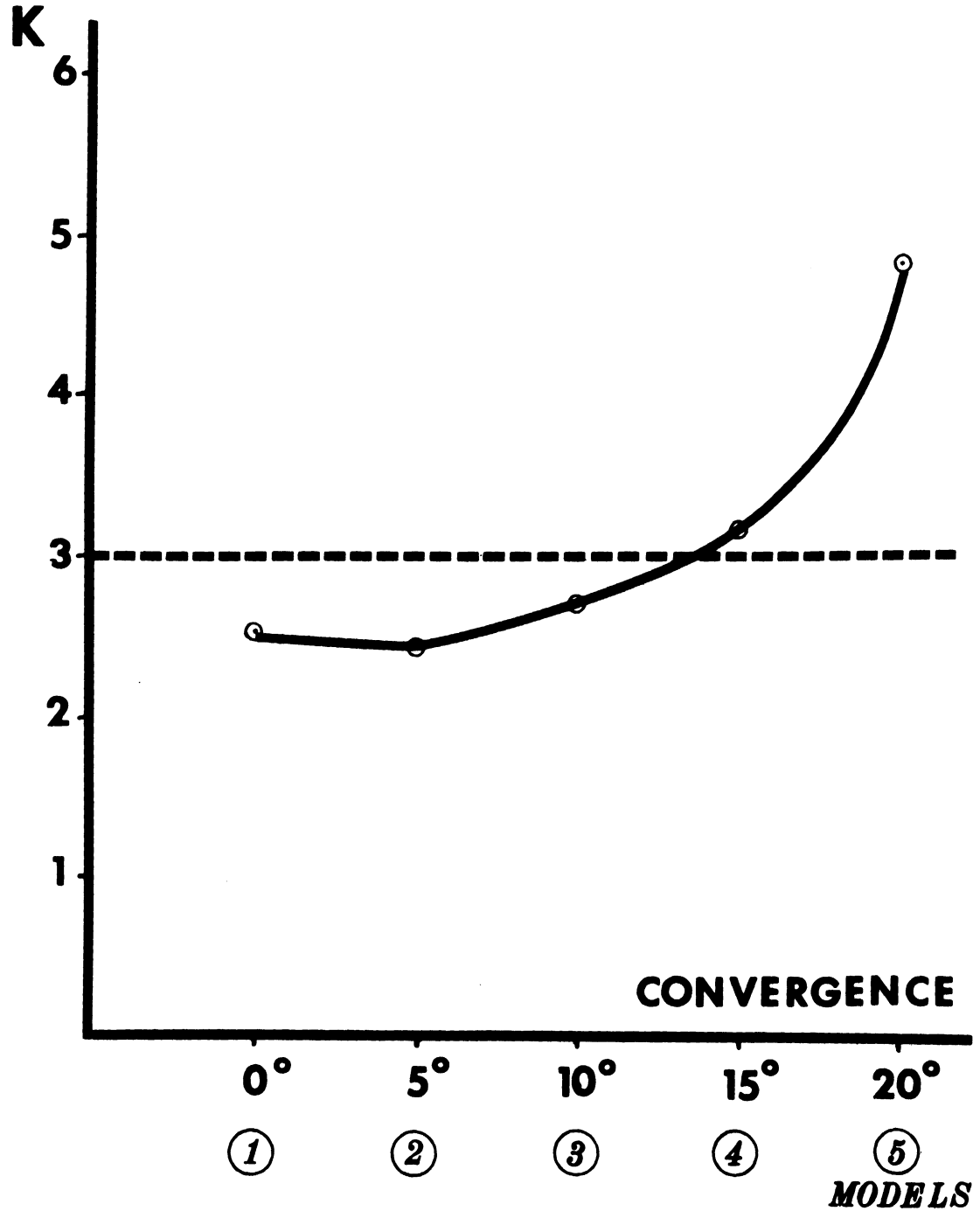

Figure 29. Stress Concentration Factors for Models with Various Axial Wall Convergence Angles.

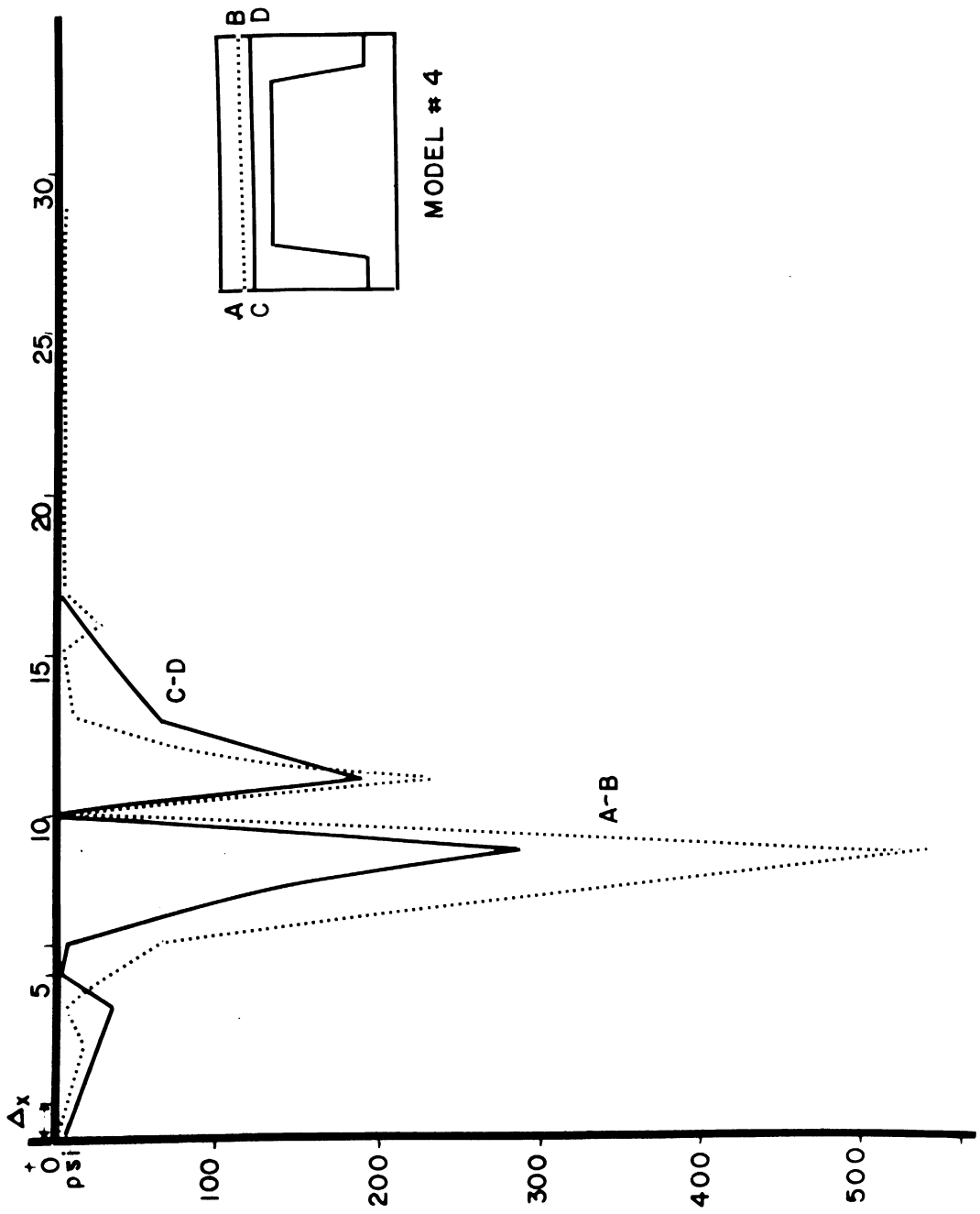

Figure 30. τ_{xy} Computed Along Lines AB and CD, for Axial Wall Model 4.

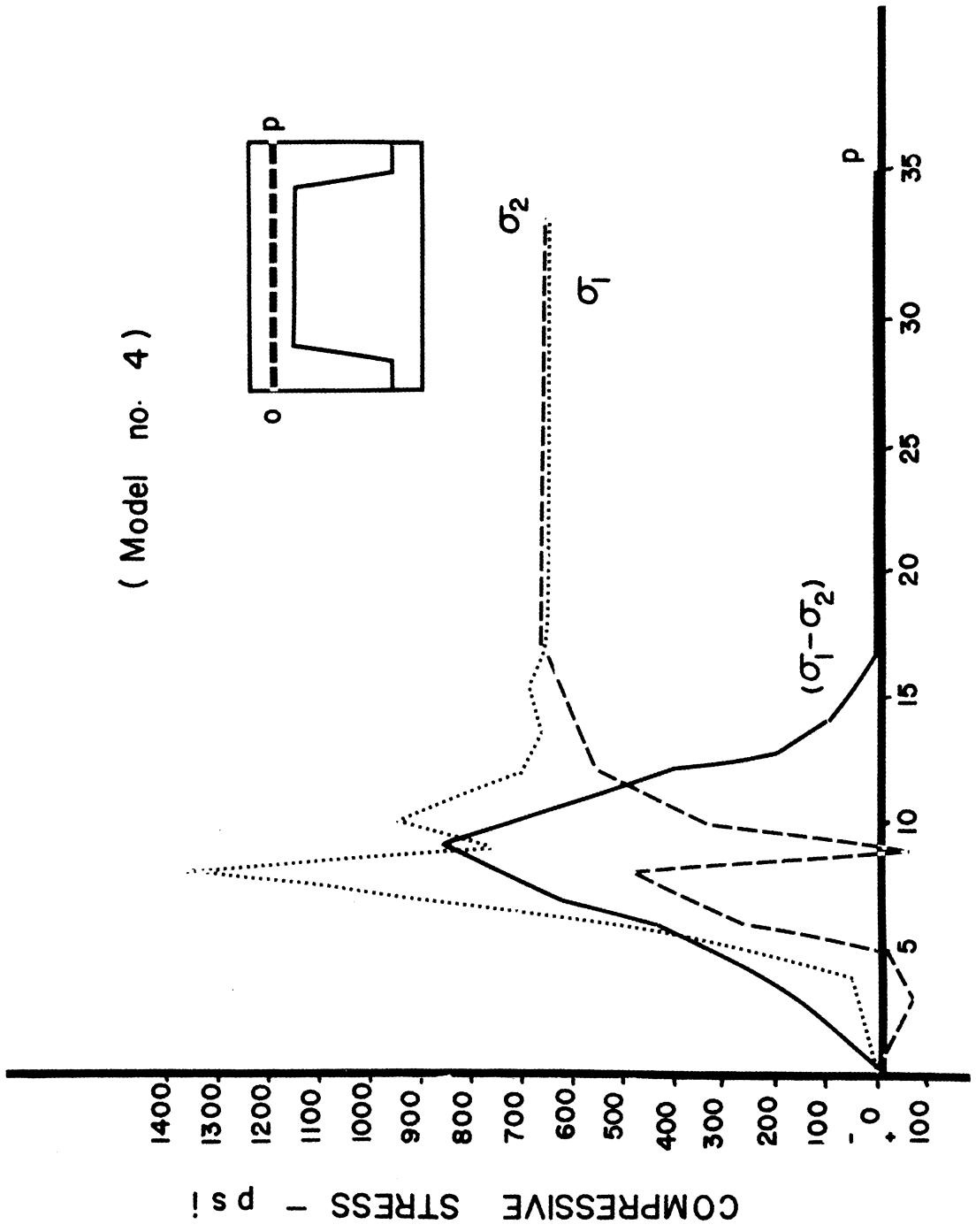

Figure 31. Separation of Principal Stresses (σ_1 and σ_2) Along Line OP in Axial Wall Model 4.

and σ_y was 576 psi, and θ, the angle between the x-axis and σ_2 was 22°. τ_{max}, at point 12 was 702 psi, while σ_2 was 1160 psi. τ_{xy} was estimated to be -247 psi, and σ_n was 628 psi

C. Occlusal Reduction Experiments

1. Photoelastic Interpretation.

Nine different designs were investigated, which were shown in Figures 16 and 17. All models were loaded at the buccal cusp, at the lingual cusp, and at the center. All models were loaded at the three preplanned sites, using three different concentrated loads of 50, 100, and 150 pounds. Complete factorial design was used in these experiments.

Examples of the present experiments are shown in Figures 32, 33, and 34. Figure 32 shows occlusal reduction Models 1 and 2, loaded on the lingual cusp, with a 150 pound concentrated load. Both photographs are light field photography of isochromatics (half-order). The upper photograph of Model 1, shows some parasitic birefringence at the buccal surface, as indicated by the letter P. The load was applied on the lingual cusp, without touching the bevel of the restoration. The order of the isochromatics ranged from one-half to about 19.5 fringes, which would be counted using a magnifying lens. No isochromatics were found in the restoration. The lower half of Figure 32, shows occlusal reduction Model 2 under the same load, at the same site. The 6.5 order fringe moved upward (occlusally) compared to the 6.5 order fringe in occlusal

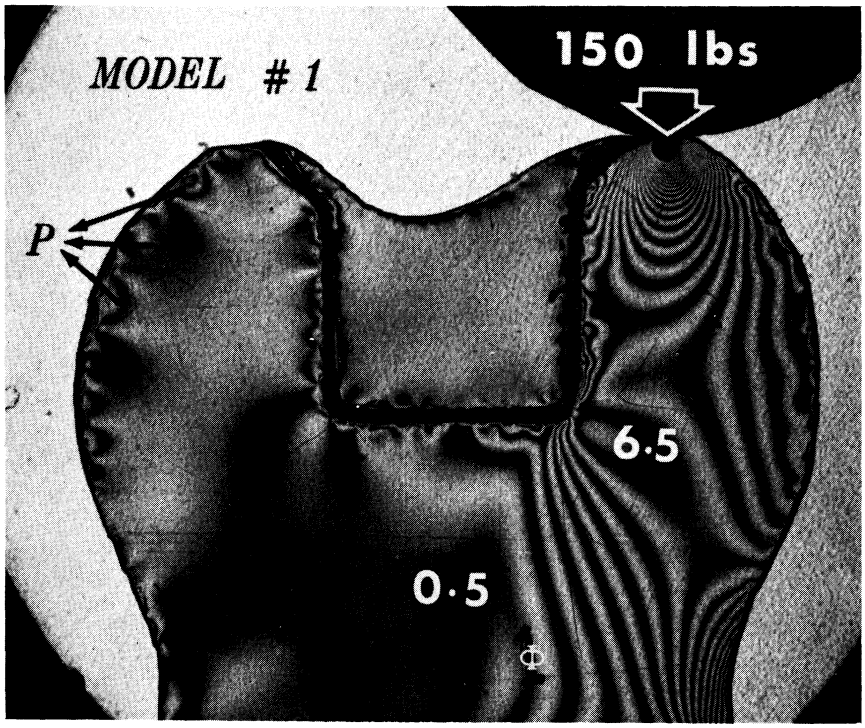

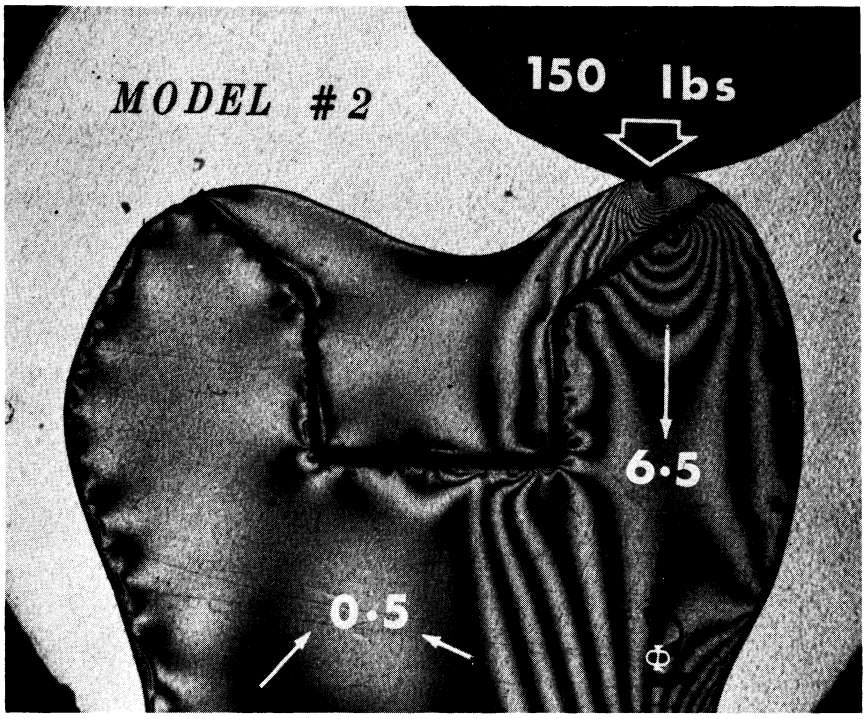

Figure 32. Occlusal Reduction Models 1 and 2, Loaded on the Lingual Cusp with 150 Pounds Concentrated Load. Both Photographs are Light Field Photographs.

reduction Model 1. The order of the fringe near the central fossa was 0.5, and still compressive in nature. The fringes in the restoration were not continuous with the fringes in the tooth structure material, which indicated a different elastic behavior. The N_{max} near the load was found to be 18.5.

Occlusal reduction Models 3 and 9 are shown in Figure 33. The same load was applied to the lingual cusp of both models as used in Figure 32. There was a high stress gradient, however, as indicated by the letter H in Model 3, due to the angle around the reduced cusp, as shown in the upper photograph of Figure 33. In Model 9, there was also an area of high stress concentration, indicated by the fringe order of 16.5, which is due to the induced undercut in the theoretical restoration. The highest compressive stresses exhibited in all designs, are shown directly under the applied concentration load in both the restoration and tooth structure.

Occlusal reduction Model 7 is shown in Figure 34, where the upper picture shows the isoclinic fringes superimposed upon the isochromatics. The parameter, θ, is 30° and the isoclinics are indicated by the letter I. There is an area of tensile stress, indicated by the letter T, near the central fossa, due to the resolution of the components of applied force. In the lower picture, half-order isochromatics are shown, when the same model was loaded on the buccal cusp, using 100 pounds concentrated load. There was a considerable reduction in the order of isochromatics in tooth structure, with a high value of 3.5

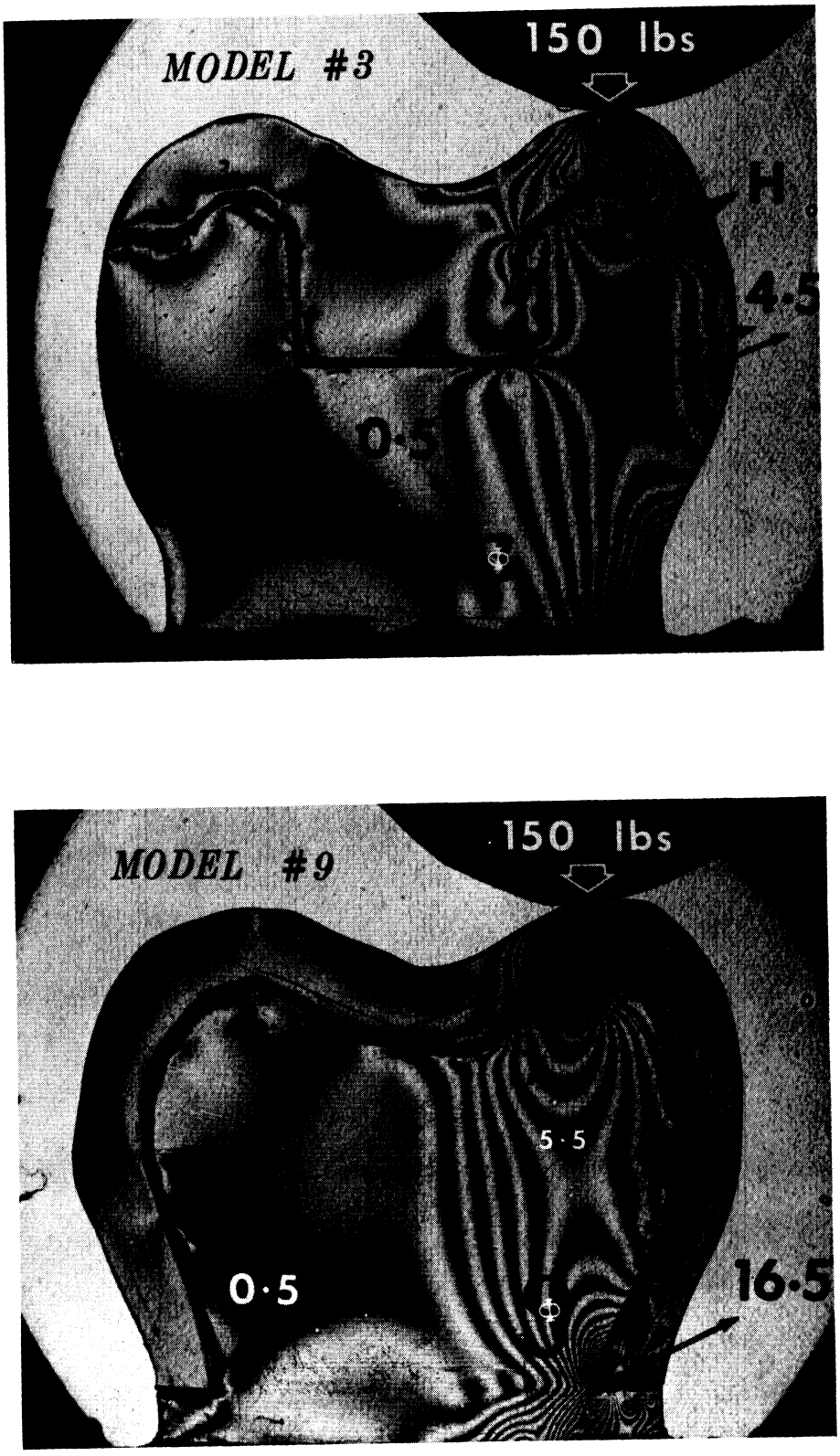

Figure 33. Occlusal Reduction Models 3 and 9, Loaded on the Lingual Cusp with 150 Pounds Load. Both Photographs are Light Field Photographs.

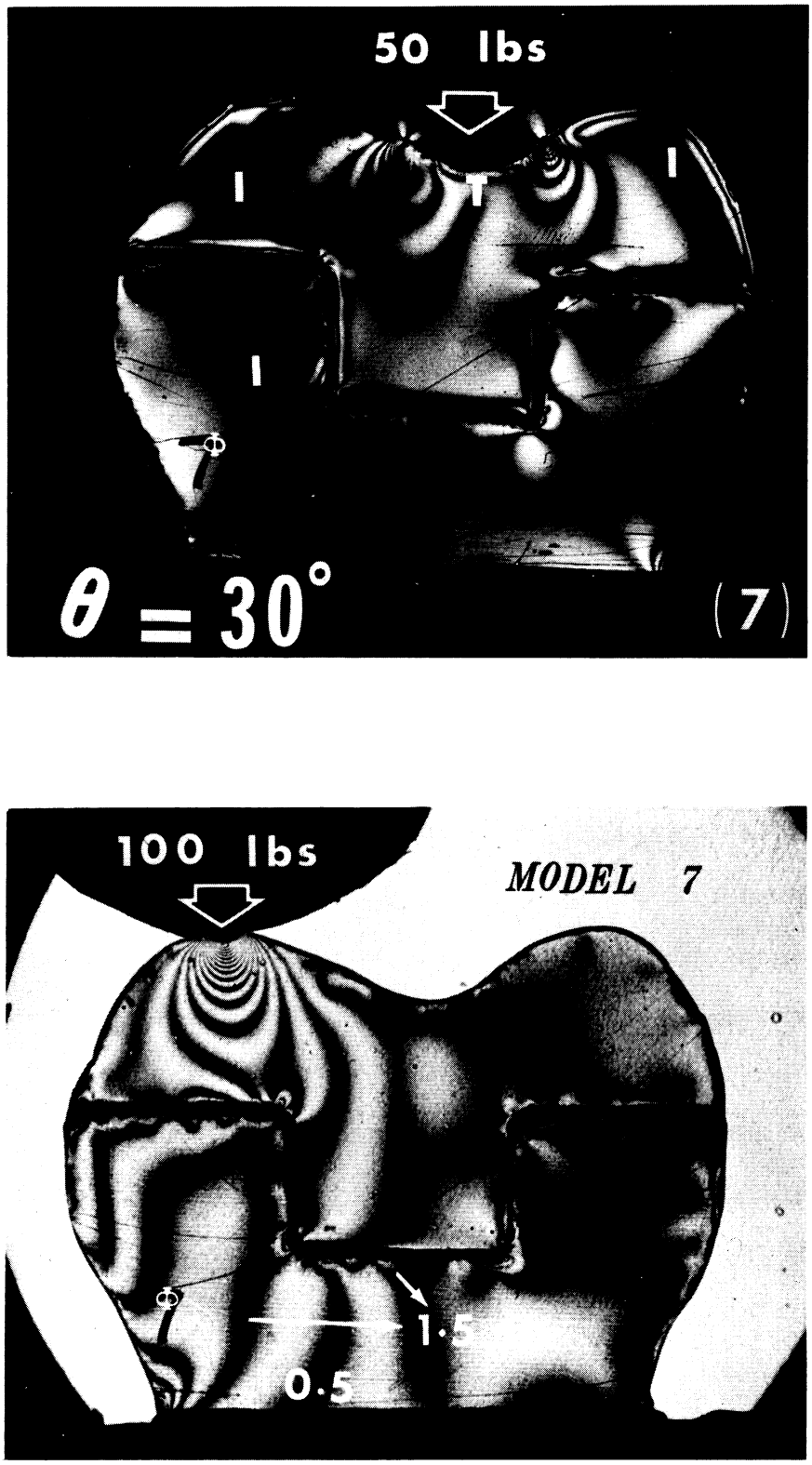

Figure 34. Occlusal Reduction Model 7. Upper Photograph Shows the Superimposition of Isoclinics ($\theta = 30°$) on the Isochromatics. The Lower Photograph Shows Half-Order Isochromatics, When the Buccal Cusp was Loaded with 100 Pounds.

compared to 7.5 in Model 3 (Figure 33). There was also a considerable reduction of shear stress directly under the load, with an N_{max} of 11.5, due to the increased thickness of the restoration from 7 mm in Model 3, to 21 mm in Model 7.

2. Statistical Inference.

All the results were tabulated, after multiplying each reading with a factor of 8; as in previous experiments.

An analysis of variance test was made to determine the significance of the treatment differences with respect to the error variance. The results of the analysis of variance are given in Table V. Factor A represents the nine designs of the extent of occlusal reduction, factor B represents the three loading sites, and factor C represents the three different concentrated loads. Since the F value obtained for factor A exceeded the critical $F_{(8,\infty)}$ of 3.27 at the 0.001 level, the designs produced a significant difference in stress distribution. The same conclusion could be reached for factors B and C. The three main factors are independent, since there is no significant first or second-order interactions.

The standard error of the experiments was 0.326 percent, and coefficient of variability was 3.5. Using the Duncan's test, however, it was not possible to rank the means. Linear orthogonal contrasts were written for the different designs. Occlusal reduction Model 7, which showed the lowest mean stress, was significantly different from any other model $(p < 0.0005)$,***

TABLE V

ANALYSIS OF VARIANCE FOR NINE OCCLUSAL REDUCTION MODELS LOADED AT THREE DIFFERENT SITES WITH THREE DIFFERENT LOADS

SOURCE OF VARIATION	D·F·	SUMS OF SQUARES	M· SQUARE	F
A	8	4731·29	591·41	4·39 ****
B	2	23,196·34	11,598·17	86·00 ****
C	2	6,359·30	3,179·61	23·51 ****
AB	16	848·59	53·04	0·39 NS
AC	16	1,538·90	96·18	0·711 NS
BC	4	832·34	208·08	1·53 NS
ABC	32	816·36	25·51	0·188 NS
ERROR	1539	209,103·05	135·87	——
TOTAL	1619	247,426·17	——	——

**** 99·95 { p < 0·0005 } NS = NOT SIGNIFICANT

and both Models 7 and 5 were significantly different from all other models, excluding Model 9 ($p < 0.0005$) .*** No significant differences were detected between Models 3 and 4, or between Models 5 and 6.

3. Computation of Stress Concentration Factors.

Stress concentration factors (K) were computed and are shown in Figure 35. The theoretical design Model 9 showed the highest K of 7.8, while Model 7 showed the lowest K of 3.25. The mean K was found to be 4.5, as shown in Figure 35, and all models falling below the mean, would be considered acceptable, if the mean was to represent 100 percent stress concentration. When the gold thickness decreased from 3 mm to 1 mm the K increased from 3.25 (Model 7) to 4.9 (Model 2). When the gold was extended to cover or protect part of the cusp, a high K of 5.9 resulted (Model 1). The computed stress concentration factors agreed with the statistical interpretation, that the difference between tested designs was statistically significant.

4. Stress Analysis of Occlusal Reduction Model 7.

Model 7 was chosen for the complete stress analysis, since it had the lowest stress concentration factor. The shear stress was found to be 440 psi midway between the buccal and lingual cusps (about 4 mm from the occlusal). The shear stress along two parallel planes passing through the

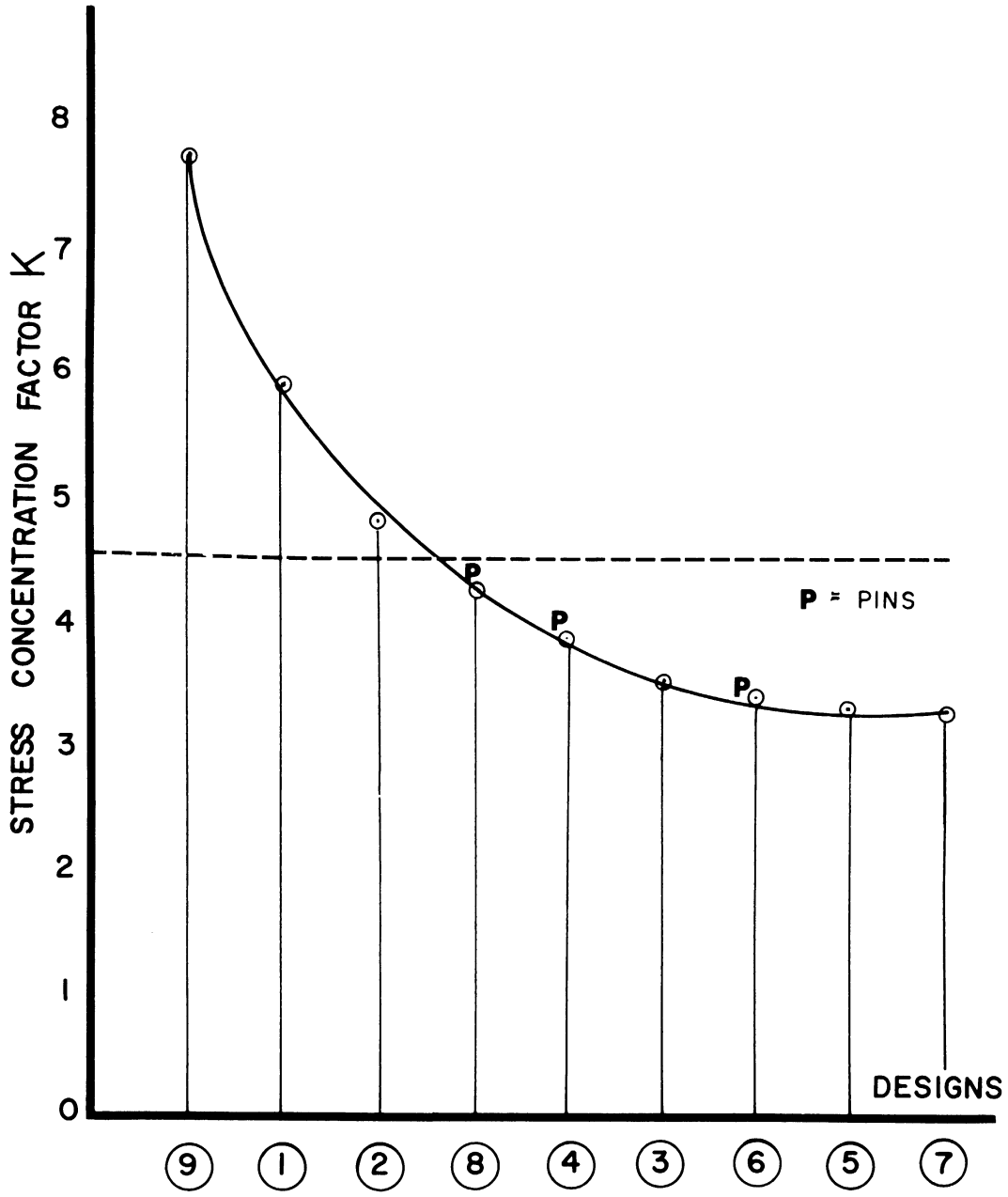

Figure 35. Stress Concentration Factors for Models with Various Modifications of Occlusal Reduction of Tooth Structure.

restoration is shown in Figure 36. The shear stress is shown along two parallel lines passing buccolingually; AB is the dotted line, and CD is the solid line.

The principal stresses were separated along line OP, as shown in Figure 37. Line OP lies between CD and AB. σ_1 had the largest algebraic sum. Point 14 along line OP was selected in the grid for application of Mohr's circle, where $\theta = 5°$, $\sigma_x = -968$ psi, $\sigma_y = -352$ psi, and $\tau_{xy} = 56$ psi. At the same point 14, σ_1 was found to be -978 psi, and $\sigma_2 = -341$. The maximum shear, τ_{max} was estimated -313 psi, and tan $2\theta = 17.5$, where θ of $\tau_{max} = 44.20'$, and σ_n was -660 psi.

D. Vertical Pin Experiments

1. Photoelastic Interpretation.

Six different models were investigated. The models selected were Models 4, 6, and 8 (models with pins), and Model 3, 5, and 7 (corresponding models without pins) which were selected from the previous experiment and were shown in Figures 16 and 17. This represents a paired approach, i.e., Models 4 and 3 are the same, except that the former has two vertical pins, a buccal pin which was 3.5 mm (0.5 mm in the prototype) and a lingual pin which was 7 mm (1 mm in the prototype). The same applied to Models 6 and 5, and to Models 8 and 7. All models were loaded at three different sites, using three different concentrated loads at each site, which was exactly the same procedure adopted for the occlusal reduction experiments.

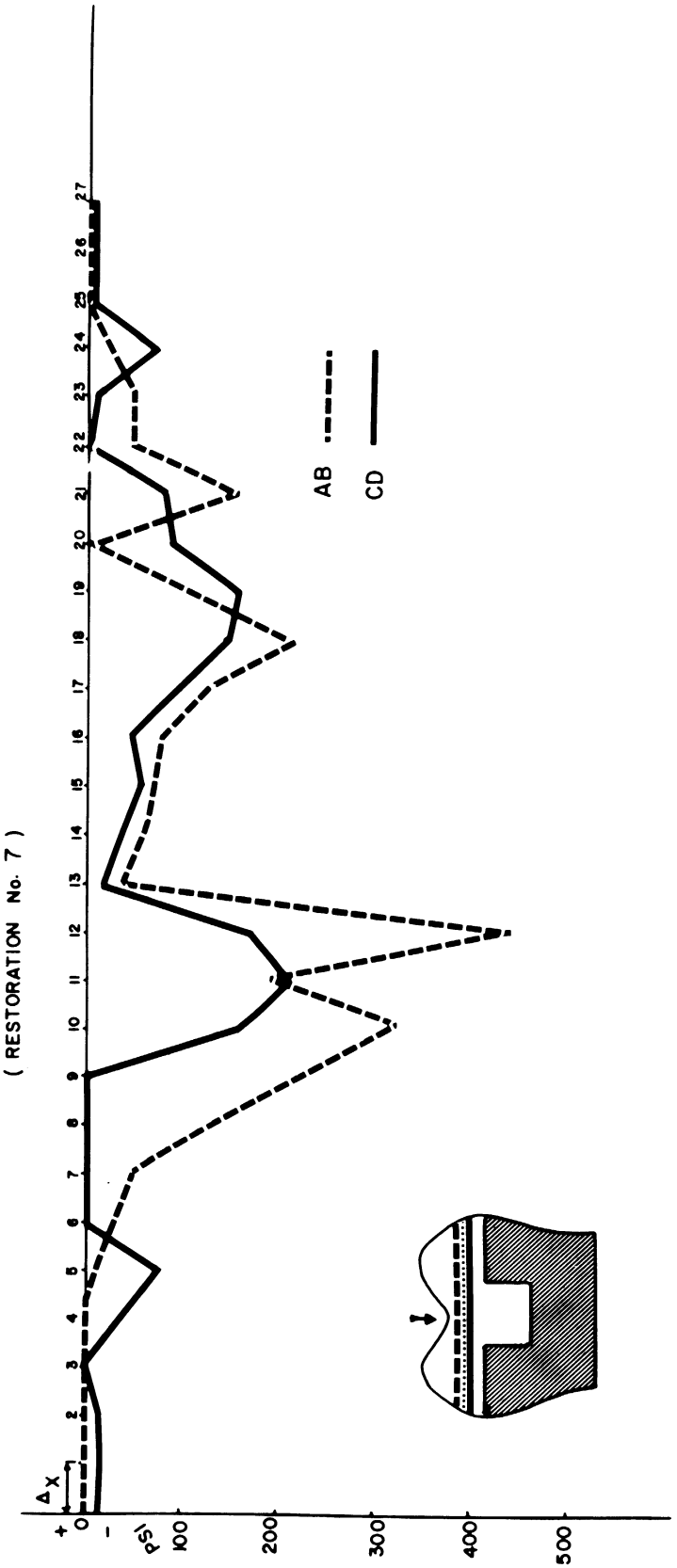

Figure 36. τ_{xy} Computed Along Lines AB and CD for Occlusal Reduction Model 7.

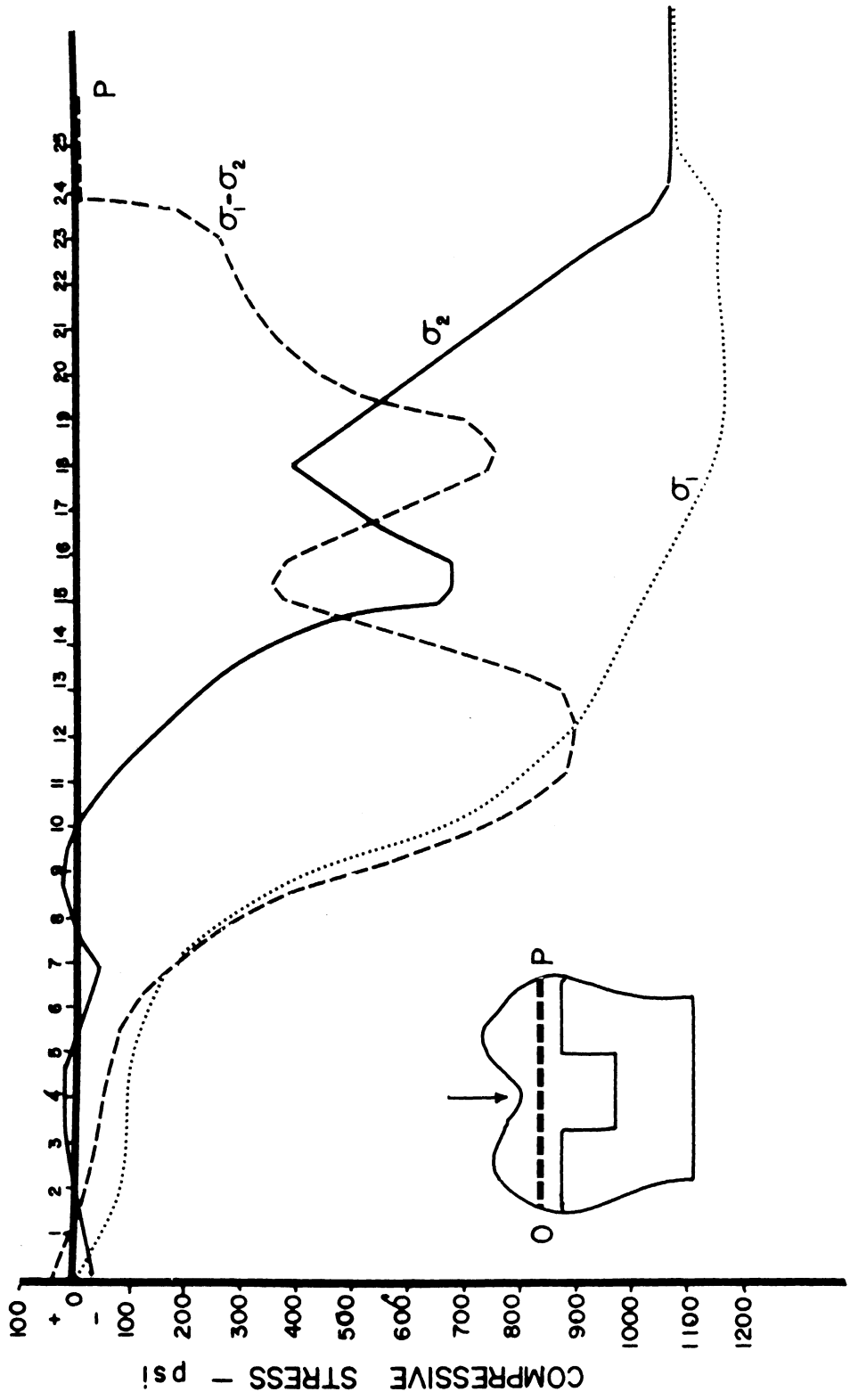

Figure 37. Principal Stresses Along Line OP in Occlusal Reduction Model 7.

Some representative photoelastic results are shown in Figures 38 and 39. Vertical pin Model 4 is shown in Figure 38. The upper picture was in dark field photography, using 100 pound load, applied on the buccal cusp. The letter T denotes the presence of tensile stress in the area of the central fossa. The isochromatic fringe around the short buccal pin had an order of 4 (i.e., 160 psi shear stress). There was considerable crowding of the isochromatic fringes in the part representing the gold restoration, and the countable N_{max} was about 16 fringes, which indicated the presence of high stress gradient. The lingual half of the model was completely in compression.

In lower picture in Figure 38, the 100 pound load was moved from the buccal cusp to center and tangential to the inclined planes. Under the two white outlined arrows at the top, there were two compressive areas, with a tensile area in between denoted by the letter T. N under each white arrow was found to be 11, or 660 psi shear stress on the surface of the restoration.

Vertical pin Models 6 and 8 are shown in Figure 39. The load used was 150 pounds, and the upper photograph showed that the isochromatic fringe order around the short pin was 1.5, while that around the long pin was 2.5. N_{max} directly under the applied load was about 14.5, or about 870 psi shear stress. In the lower picture showing Model 8, the isochromatic fringe order around the short buccal pin was 1.5, while that around the long lingual pin was 2.5. In the restoration part of the

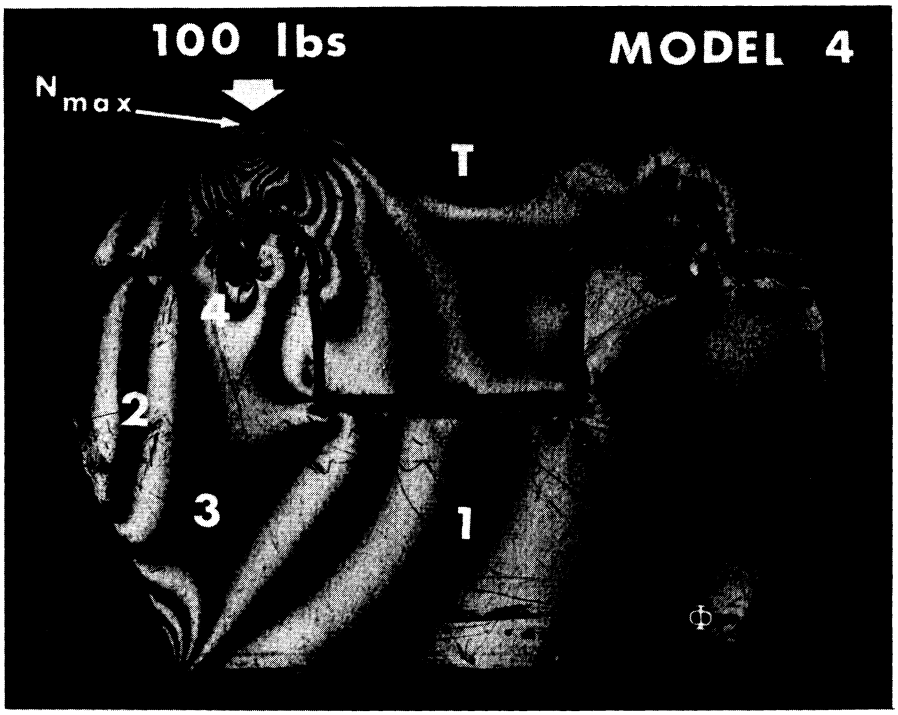

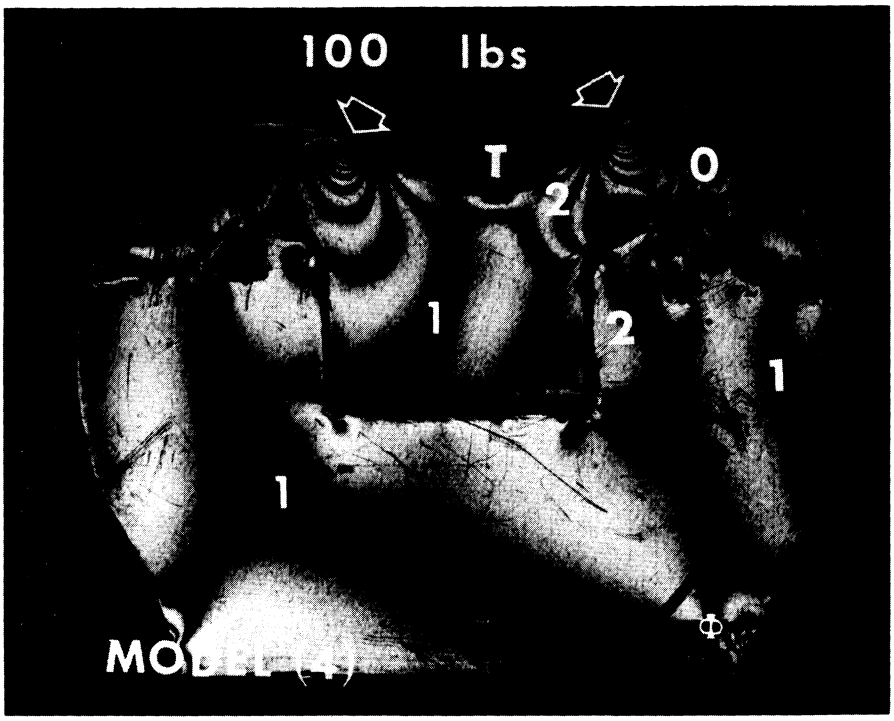

Figure 38. Vertical Pin Model 4, Loaded with 100 Pounds Load on the Buccal Cusp (Upper Photograph) and on the Inclines of Buccal and Lingual Cusps (Lower Photograph). Both Photographs Were Recorded Using Dark Field Photography.

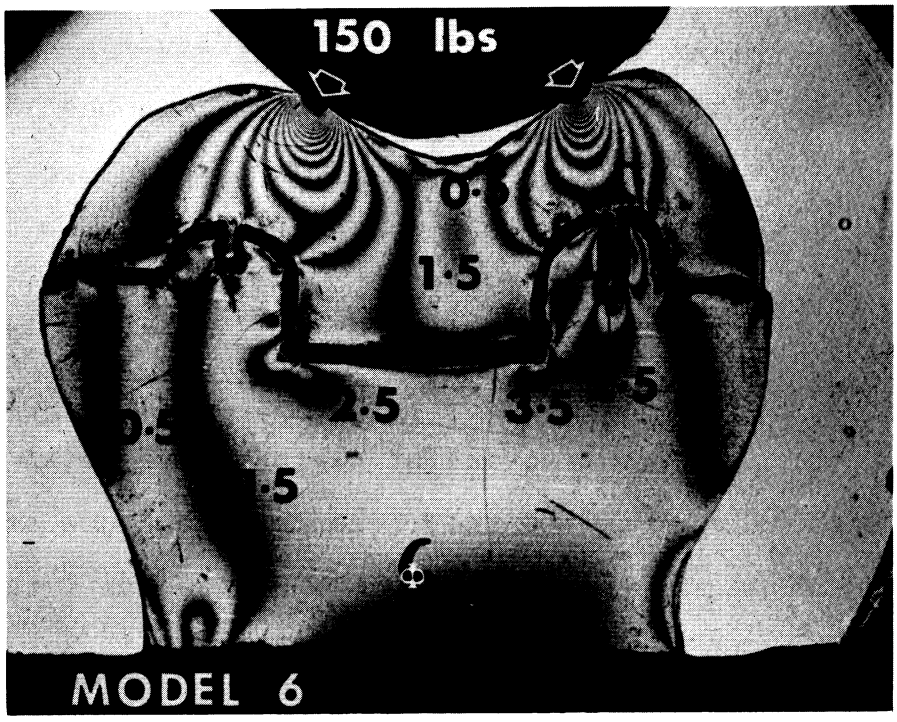

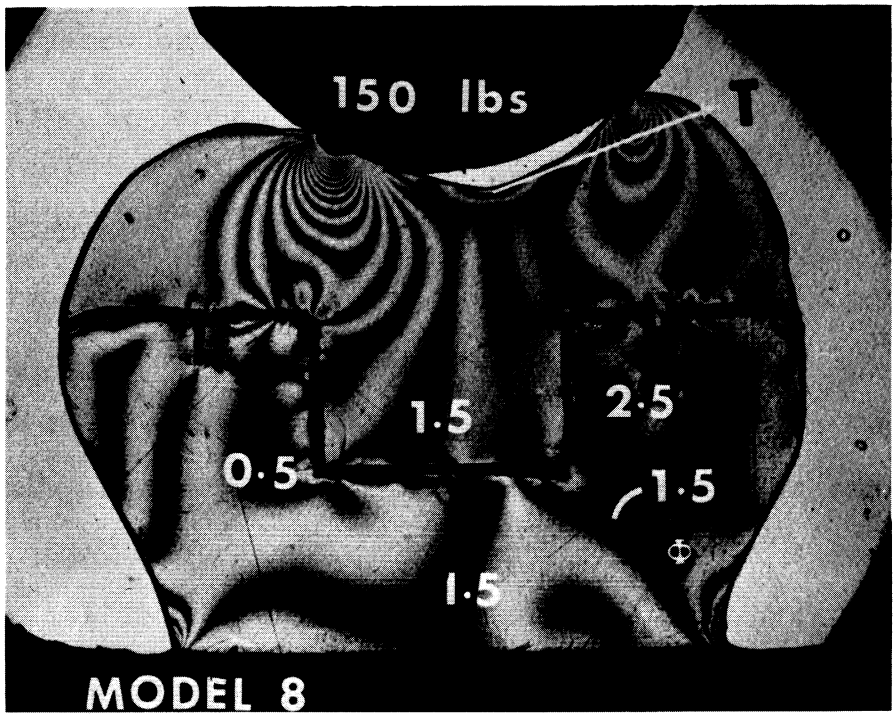

Figure 39. A Comparison of Vertical Pin Models 6 and 8, Loaded with 150 Pound Load, and Photographed Using Light Field Photography.

model, N_{max} directly under the applied load was about 13.5 fringes. These results showed the stress distribution in the tooth structure was about the same, while there was one less isochromatic fringe in Model 8 than in Model 6, or about 60 psi less shear stress. The letter T in the lower picture denotes the presence of tensile stresses in the central fossa.

2. Statistical Inference.

The results of the analysis of variance are given in Table VI. Factor A represented the presence or absence of pins, factor B represented the three sites of loads, factor C represented the three used loads, and factor D denoted the extent of occlusal reduction (7, 14, and 21 mm). The F value obtained for A was not significant, i.e., the null hypothesis was accepted that there was no difference between restorations with or without pins. The F value obtained for B was also not significant, which indicated that loading at any site is the same, as far as the stress distribution is concerned. The F value for factor C was highly significant ($p < 0.0005$)***, which showed there is a significant difference in the stress distribution of any tested design, when different loads were used. The F value obtained for factor D was highly significant ($p < 0.0005$)***, which indicated that there are significant statistical differences between the three models in each group A (see Table II). No significant interactions were detected. The most important possible interaction, was AD, which was that between pins and occlusal reduction. The F value for AD interaction was significant at the 75 percent level, which was very low.

TABLE VI

ANALYSIS OF VARIANCE FOR THREE MODELS WITH VERTICAL PINS VERSUS THREE MODELS WITHOUT PINS, LOADED AT THREE DIFFERENT SITES WITH THREE DIFFERENT CONCENTRATED LOADS

SOURCE OF VARIATION	D·F·	SUMS OF SQUARES	M SQUARE	F
A	1	32·73	32·73	0·327 NS
B	2	196·32	98·16	1·055 NS
C	2	12,816·69	6408·34	68·51****
D	2	3,251·54	1625·77	17·85****
A B	2	1·09	0·55	0·005 NS
A C	2	2·25	1·13	0·012 NS
A D	2	355·22	177·61	1·89 NS
B C	4	135·86	33·97	0·33 NS
B D	4	93·03	23·26	0·24 NS
C D	4	524·12	131·03	1·41 NS
A B C	4	35·40	8·85	0·095 NS
A B D	4	174·31	43·58	0·436 NS
A C D	4	121·98	30·5	0·325 NS
B C D	8	194·64	24·33	0·26 NS
A B C D	8	266·12	33·26	0·331 NS
ERROR	1026	96,051·50	93·62	
TOTAL	1079	114,252·80		

**** 99·95 { p < 0·0005 } / NS = NOT SIGNIFICANT

The standard error of the experiments was found to be 0.85 percent. Duncan's test failed to detect any significant differences between the estimated means.

3. Computation of the Stress Concentration Factors.

The computed K values are shown in Figure 35, showing that all six tested designs fell below the dotted line, with the design incorporating the pins slightly higher than those which did not have any pins.

4. Stress Analysis of the Optimum Restoration.

No design with pins was analysed in detail, since it was believed that the detailed analysis of restoration Model 7 was sufficient.

E. Proximal Reduction in Compound Restorations Experiments

1. Photoelastic Interpretation.

The three basic designs shown in Figure 18 were loaded in the area of proximal contact, using three different loads; 50, 100 and 150 pounds. Examples of the results of proximal reduction Models 1, 2 and 3 are shown in Figure 40, 41 and 42, respectively. All figures were photographed using dark field.

Figure 40 shows Model 1, under 50 and 150 pound load. The letter A indicates an artifact and P denotes parasitic birefringency. In the upper picture, an area of high stress concentration (H) was noticed, as shown by the white arrow which indicates five fringes. N_{max} in the area directly under

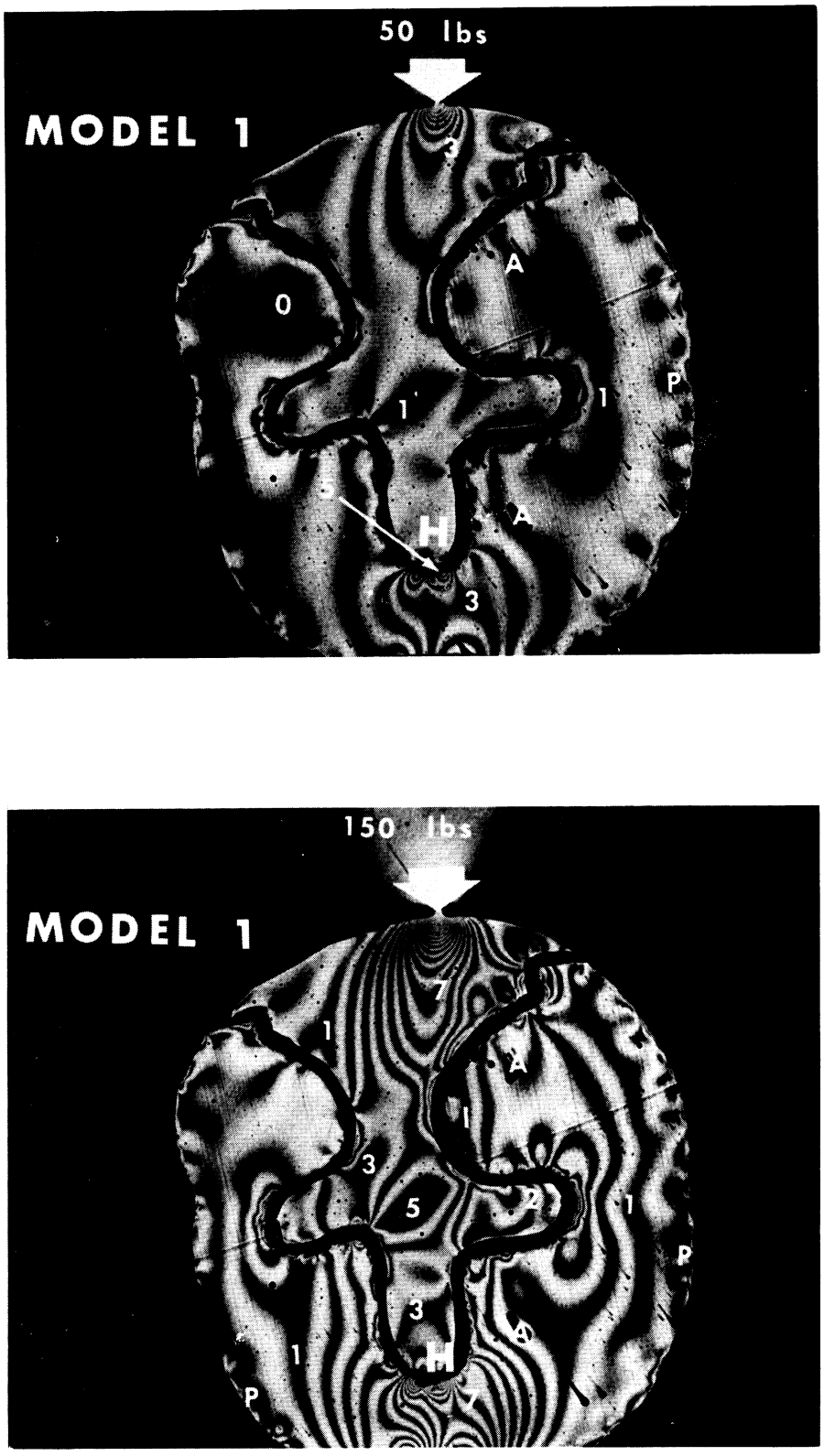

Figure 40. Proximal Reduction Model 1, Loaded with 50 and 150 Pounds Concentrated Proximal Load.

the load was 8 fringes. The lower picture shows the same model under 150 pound load. The "hot spot" (H) corresponding to the one discussed above showed 14 fringes. The stresses in the center of the restoration increased from one to five fringes. N_{max} in the area directly under the load increased to about 20 fringes. The shear stresses in the restoration increased markedly when the load was increased from 50 to 150 pounds.

Figure 41 shows some results of proximal reduction Model 2. The upper picture shows the isochromatics produced by the 50 pound load. The stresses in the "hot area" indicated by the letter H, as shown by five fringes. N_{max} directly under the load was 8 fringes. The stress distribution in the restoration in Model 2 was almost the same as in Model 1 (Figure 40), except that the fringe order in the center in Model 2 was zero, while it was one in Model 1.

The lower picture shows Model 2 under 150 pound load. There was a marked difference between the stress patterns of Models 1 and 2, as indicated by the fringe orders on the isochromatics in comparative areas. N_{max} directly under the 150 pound load was 20 fringes.

Some representative results of proximal reduction Model 3 are shown in Figure 42. The upper picture shows the area of high stress concentration at the lower tip of the restoration, (H) showing 10 fringes. N_{max} directly under the load was about 8 fringes. Generally, the stress distribution in the three models was comparable. The lower half of Figure 42 shows

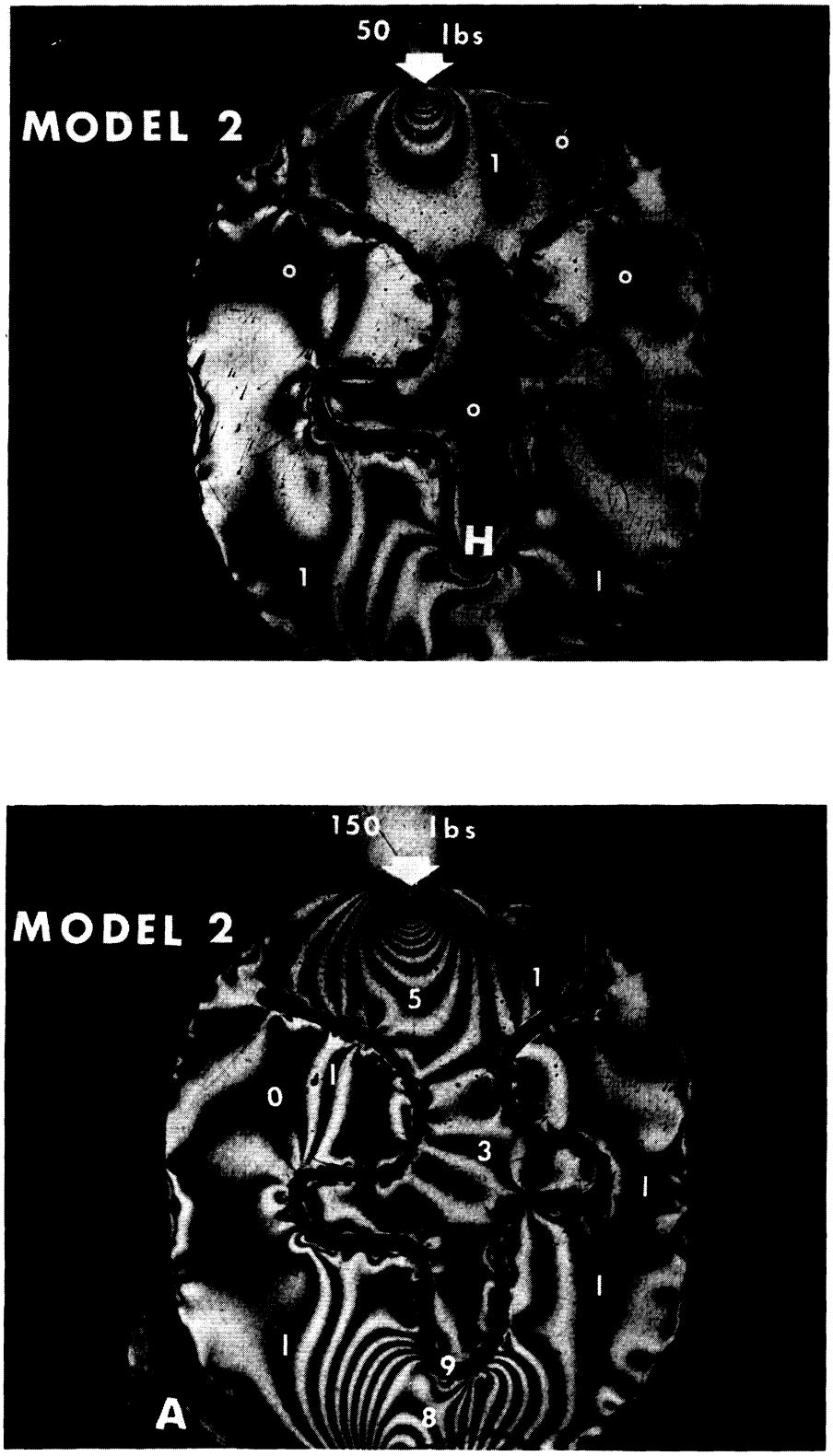

Figure 41. Proximal Reduction Model 2, Loaded with 50 and 150 Pounds Concentrated Proximal Load.

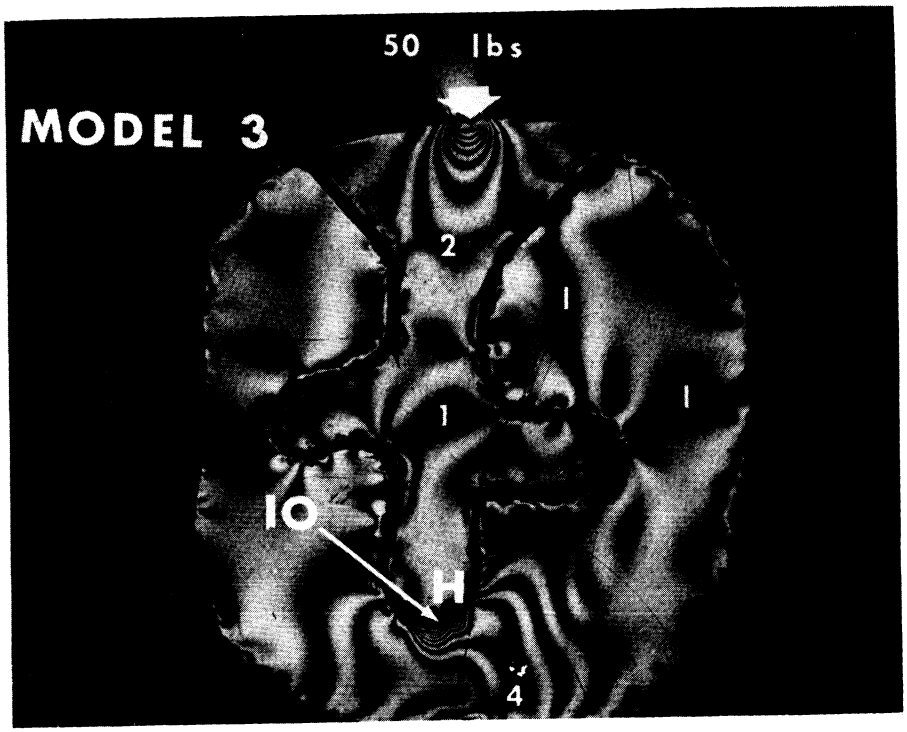

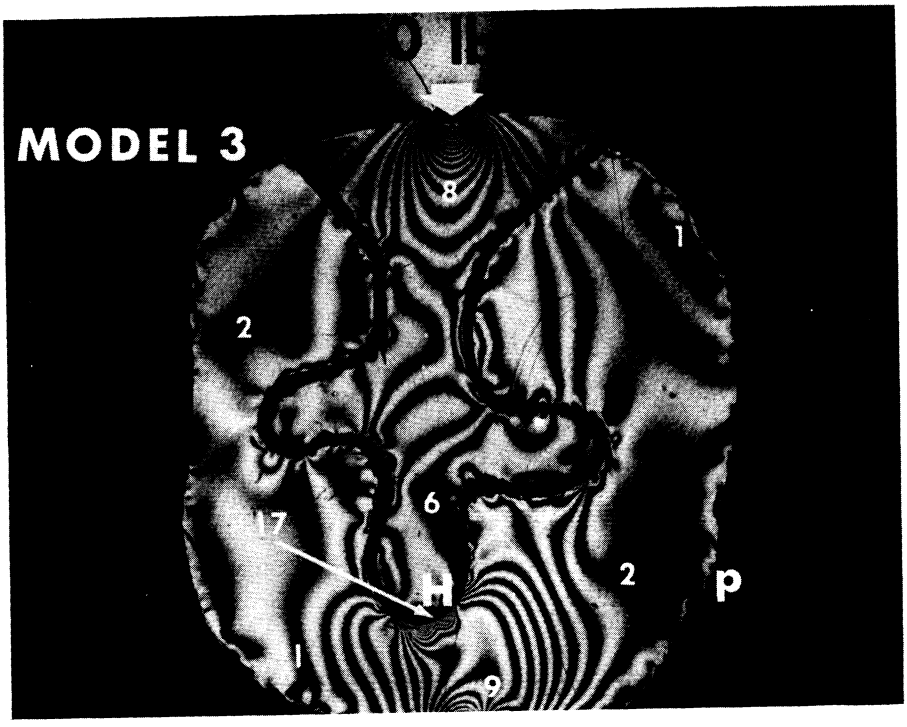

Fiugre 42. Proximal Reduction Model 3, Loaded with 50 and 150 Pounds Concentrated Proximal Load.

Model 3 under 150 pound load, with the area of high stress concentration (H) showing 17 fringes (the lower arrow).

2. Statistical Inference.

A two-way analysis of variance test was used to test the null hypothesis that the three designs are the same, i.e., they have the same stress distribution. Table VII shows the final computations, where factor A refers to the three tested designs, and factor B refers to the three loads used. The F value obtained for factor A was smaller than the critical value of $F_{(2,288)}$= 4.75, and the null hypothesis was thus accepted. The F value for factor B was much larger than the critical value (30.71 > 6.91) at the 0.001 level, which indicated that the stress distribution did change with the change of the magnitudes of loads. The AB interaction was found non-significant. The standard error ($S_{\bar{x}}$) was estimated to be equal to 0.99 percent. Duncan's test was not used for ranking, because the null hypothesis was accepted.

3. Computation of the Stress Concentration Factors.

The stress concentration factor for Model 1 was 2.78, for Model 2 was 2.81, and for Model 3 was 2.82. This led to the conclusion that for all practical purposes the three tested designs had the same stress concentration factor.

4. Stress Analysis of Proximal Reduction Model 1.

Model 1 was chosen for the complete stress analysis because of its popularity in dentistry. Tracings of the isoclinics

TABLE VII

ANALYSIS OF VARIANCE FOR THREE PROXIMAL REDUCTION MODELS LOADED ON THE PROXIMAL AREA WITH THREE DIFFERENT CONCENTRATED LOADS

Source of Variation	D·F·	S· Sqs.	Mean Sq·	F
A	2	75·99	37·99	0·5897
B	2	8957·38	1978·69	30·710 *
A B	4	136·94	34·24	0·5314
ERROR	288	18555·27	64·43	
TOTAL	296	22725·58		

* $\{p < 0.001\}$

of the slice restoration are shown in Figure 43. The isoclinic parameters are indicated on the isoclinics, and the picture looks like a ring or a disc under diametrical compression.

τ_{xy} was computed, as shown in Figure 44 along two lines AB and CD. The AB (dotted line) passes entirely through the restoration part, while CD (solid line) passes partly in the tooth structure and partly in the restoration. The highest value obtained for τ_{xy} was 415 psi along AB (point 5). The two values for τ_{xy} for each point along the x-axis were used for the computations of $\Delta\tau_{xy}$ which was used for the computations of the principal stresses.

The separated principal stresses are shown in Figure 45. σ_2 was found to be larger than σ_1, and the two corresponding curves did not cross. σ_{max} was +1029 psi, and σ_{min} was -520 psi. The solid curve denotes $(\sigma_1 - \sigma_2)$ as obtained from the isochromatics. It was interesting to find that both σ_1 and σ_2 at or near B became tensile in nature.

The principal stresses in the investigated slice restoration (Model 1) are diagrammatically shown in Figure 46. The stresses shown, were computed along AB, which passed from one edge of the restoration to the other. The principal stresses, are shown superimposed on the model, which was composed of two photoelastic materials representing dental gold and tooth structure. σ_1, was generally compressive in nature (-) except in two specific areas, first one third of the way between A and B, where it reached 180 psi (+), and the second near the edge B,

"SLICED RESTORATION"

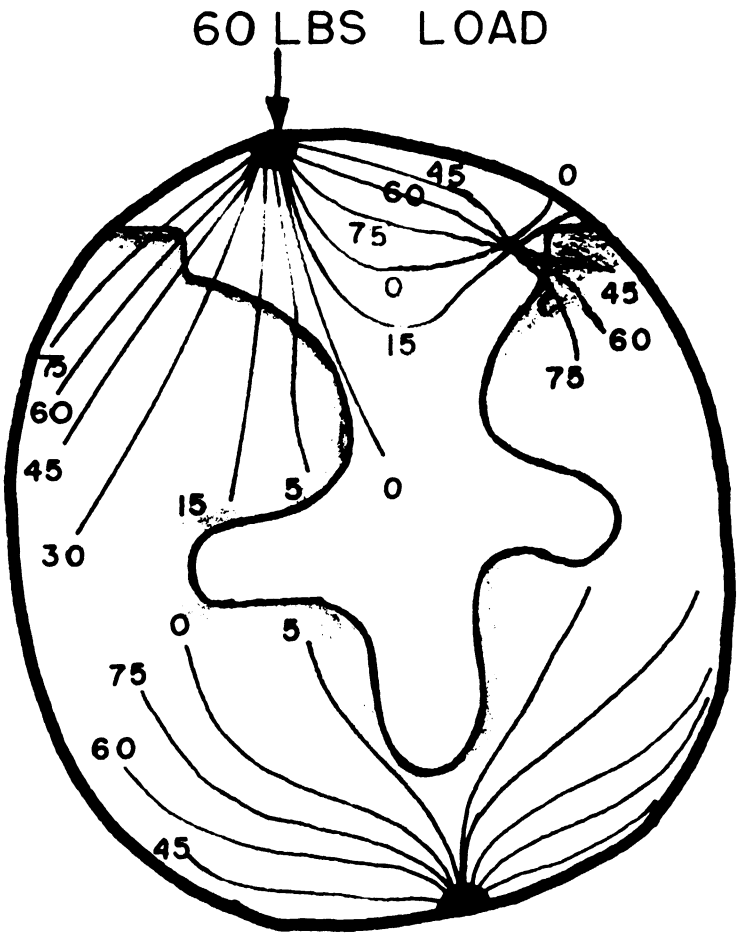

Figure 43. Isoclinic Fringes in Proximal Reduction Model 1.

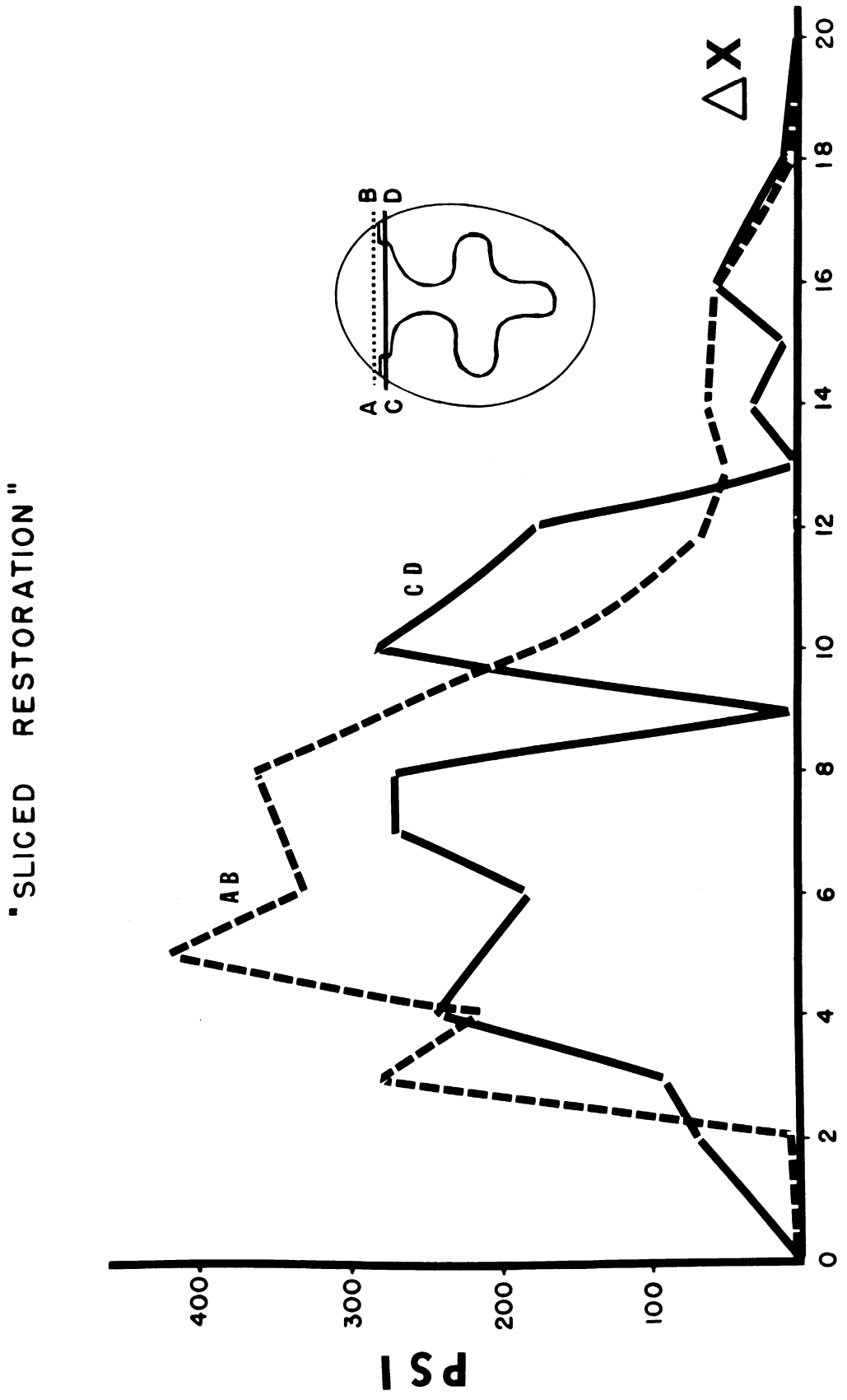

Figure 44. τ_{xy} Computed Along AB and CD Lines in Proximal Reduction Model 1.

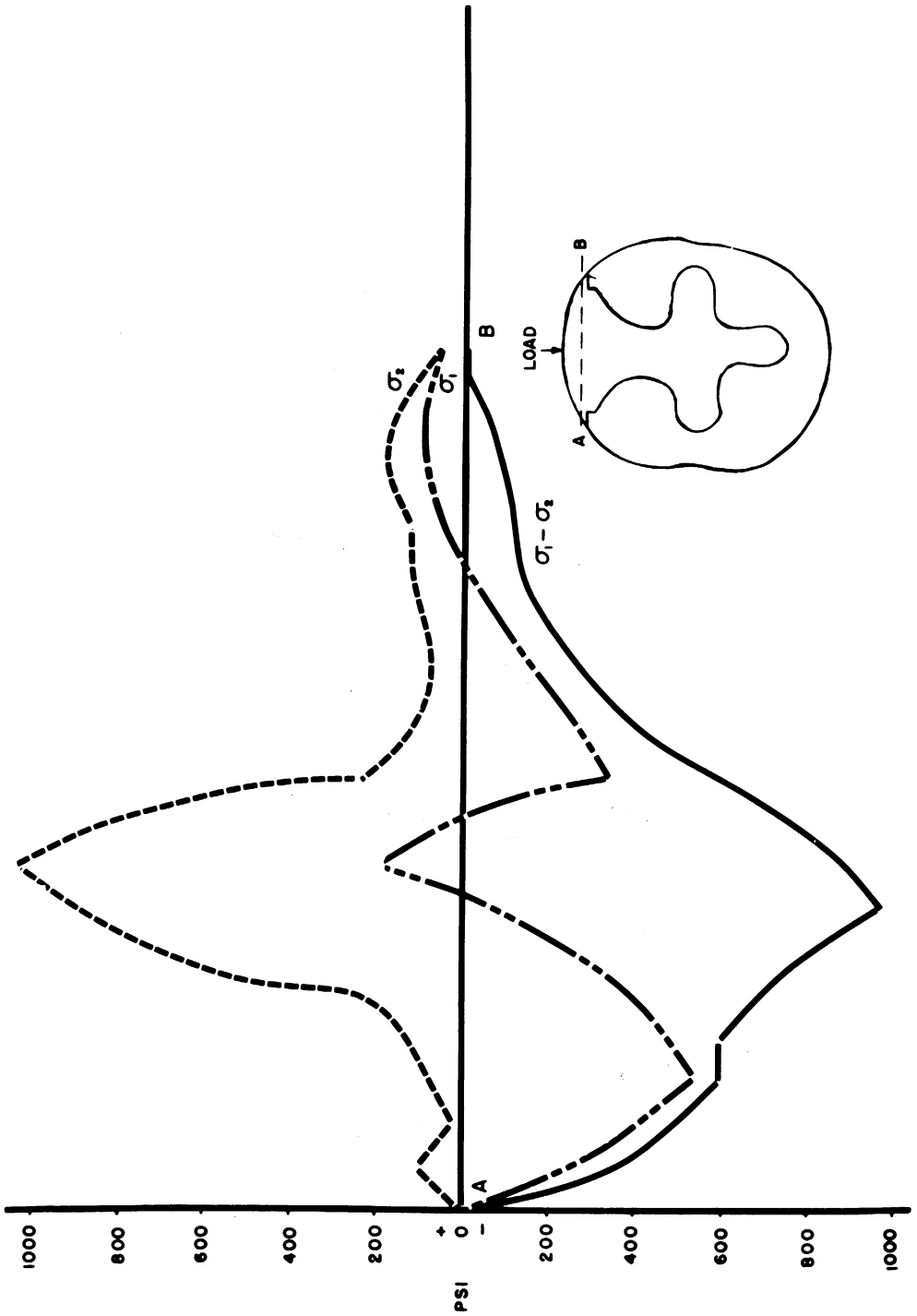

Figure 45. Computed Principal Stresses Along AB Line in Proximal Reduction Model 1.

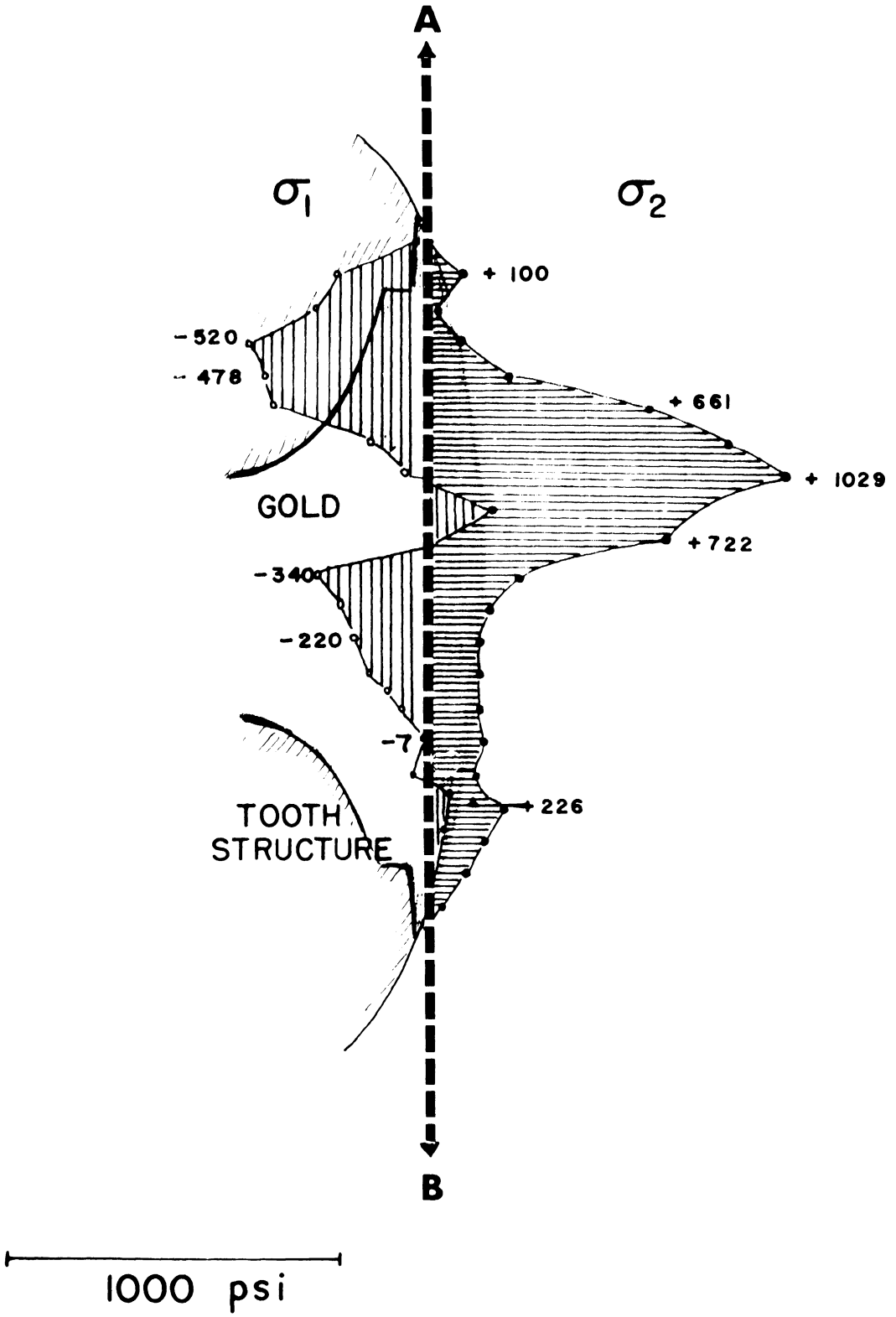

Figure 46. Principal Stresses in Proximal Reduction Model 1, in Relation to the "Gold" and "Tooth Structure" Portions of the Photoelastic Model.

where it reached 110 psi (+). σ_2 , was generally tensile in nature, with two significant "humps" near the buccal and lingual edges, i.e., A and B respectively. σ_1 and σ_2 represent principal stresses which act perpendicularly to each other. The shear stress (τ_{xy}) was shown in Figure 45, and it began from a value of zero at A to a maximum of about 990 psi (-), then to zero again near B, when $\sigma_1 = \sigma_2$.

F. Posterior Fixed Bridges Experiments

1. Photoelastic Interpretation.

Three different posterior bridges, which were shown in Figure 19, were loaded, using one concentrated load at different sites on the bridges. In some instances multiple point-contact loading was attempted to simulate upper posterior teeth occluding against a lower fixed bridge. Shoulderless margins and anatomical occlusal reduction were incorporated in bridge 1, and rounded shoulders and flat occlusal reduction were incorporated in bridge 2. Bridge 3 was a cantilever bridge, i.e., fixed at one end only. Examples of the results are shown in Figures 47 through 57.

Figure 47 shows both bridges 1 and 2, without loading, in order to detect parasitic birefringency, induced in the models due to fabrication and filing operations. In the upper photograph, bridge 1 had two significant areas of parasitic birefringency, as indicated by the two white arrows in the upper left occlusal area. The letters F, P, and A denote

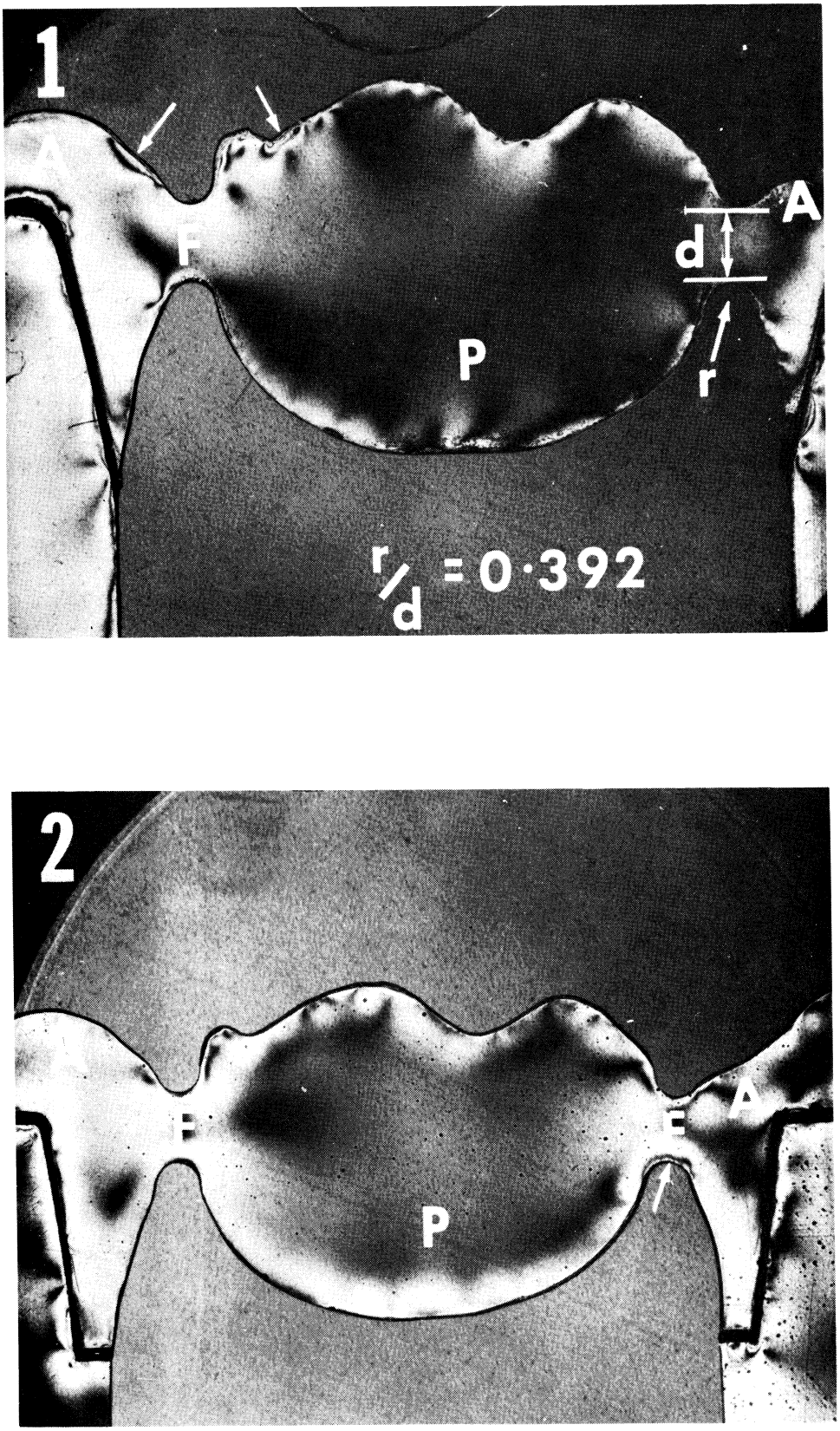

Figure 47. Fixed Bridge Models 1 and 2, Showing Some Evidence of Parasitic Birefringency. For Both Bridges r/d was 0.392. (Dark Field Photographs).

fixed joint, pontic or the suspended member of the bridge, and abutment, respectively. An abutment is defined in dentistry as a tooth used for the support or anchorage of a fixed prosthesis, which is united to the bridge proper by means of the retainer. The lower picture in Figure 47 shows bridge 2, with one parasitic fringe at the junction of the pontic and the mesial abutment, indicated by a white arrow. For both bridges, r/d was 0.392.

The two bridges (1 and 2) were loaded on the pontic, using 50 pound concentrated load, as shown in Figure 48. The fringes were photographed using a dark field arrangement. The loading site was more to the mesial side of the pontic, which explains the presence of more fringes at the mesial joint compared to those at the distal fixed joint. In bridge 1 (upper photograph), five fringes are shown at the mesial area (300 psi shear stress), while three fringes (180 psi shear stress) appeared at the distal area. Only a part of the bridge is shown in Figure 48, but the photoelastic stress distribution for the entire bridge is shown in Figure 49, by the use of composite photographs. Both bridges showed that even at a low load of 50 pounds, two areas of stress-concentration appeared at the fixed joints, and both areas were tensile in nature. Comparing the distal fixed joint (D) in both bridges, bridge 2 had two isochromatic fringes at the center of the joint, while bridge 1 had three isochromatic fringes. The letter P denotes some parasitic birefringency due to the luting process

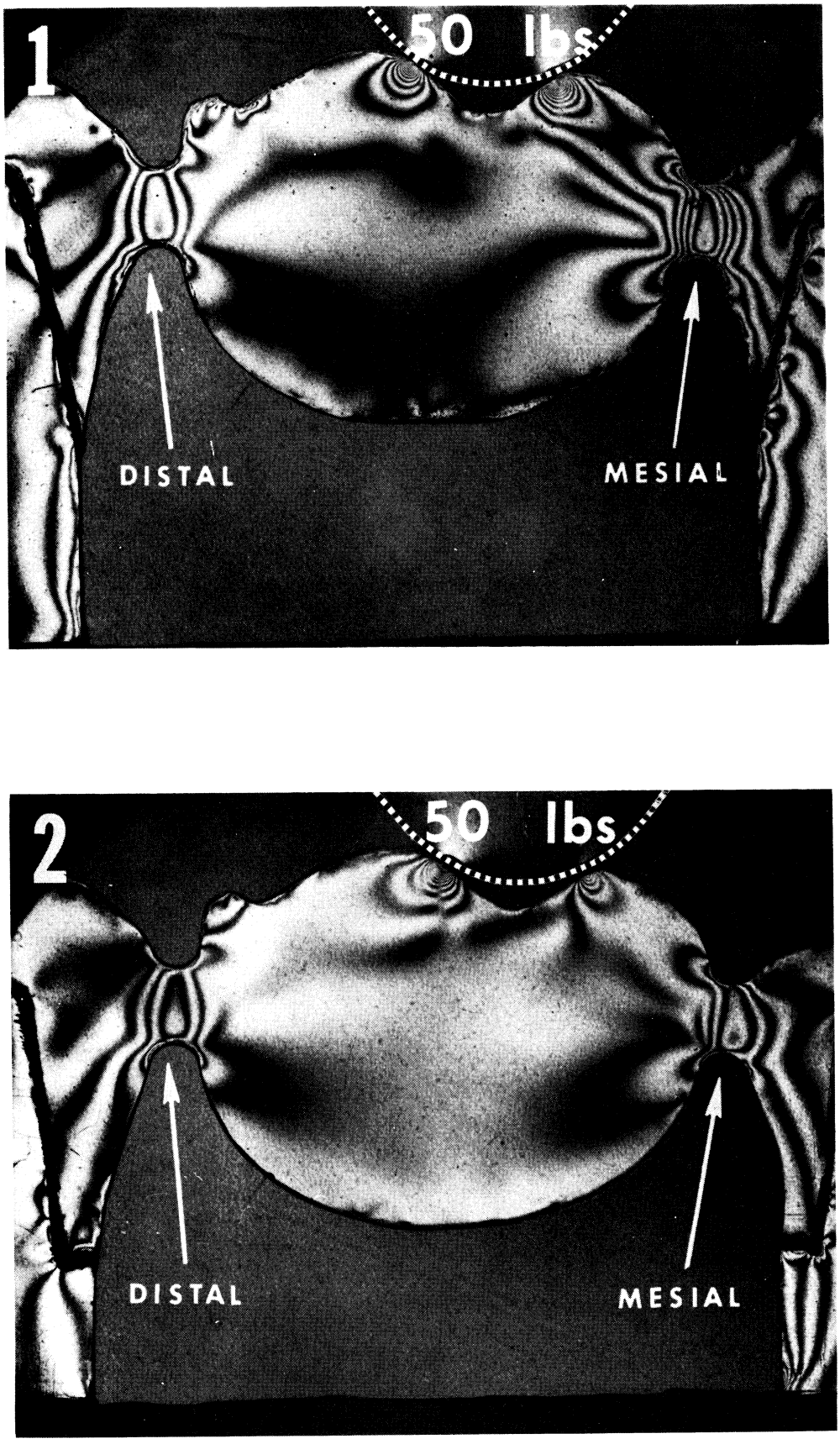

Figure 48. Bridges 1 and 2 Were Loaded at the Pontic, 50 Pounds Concentrated Load.

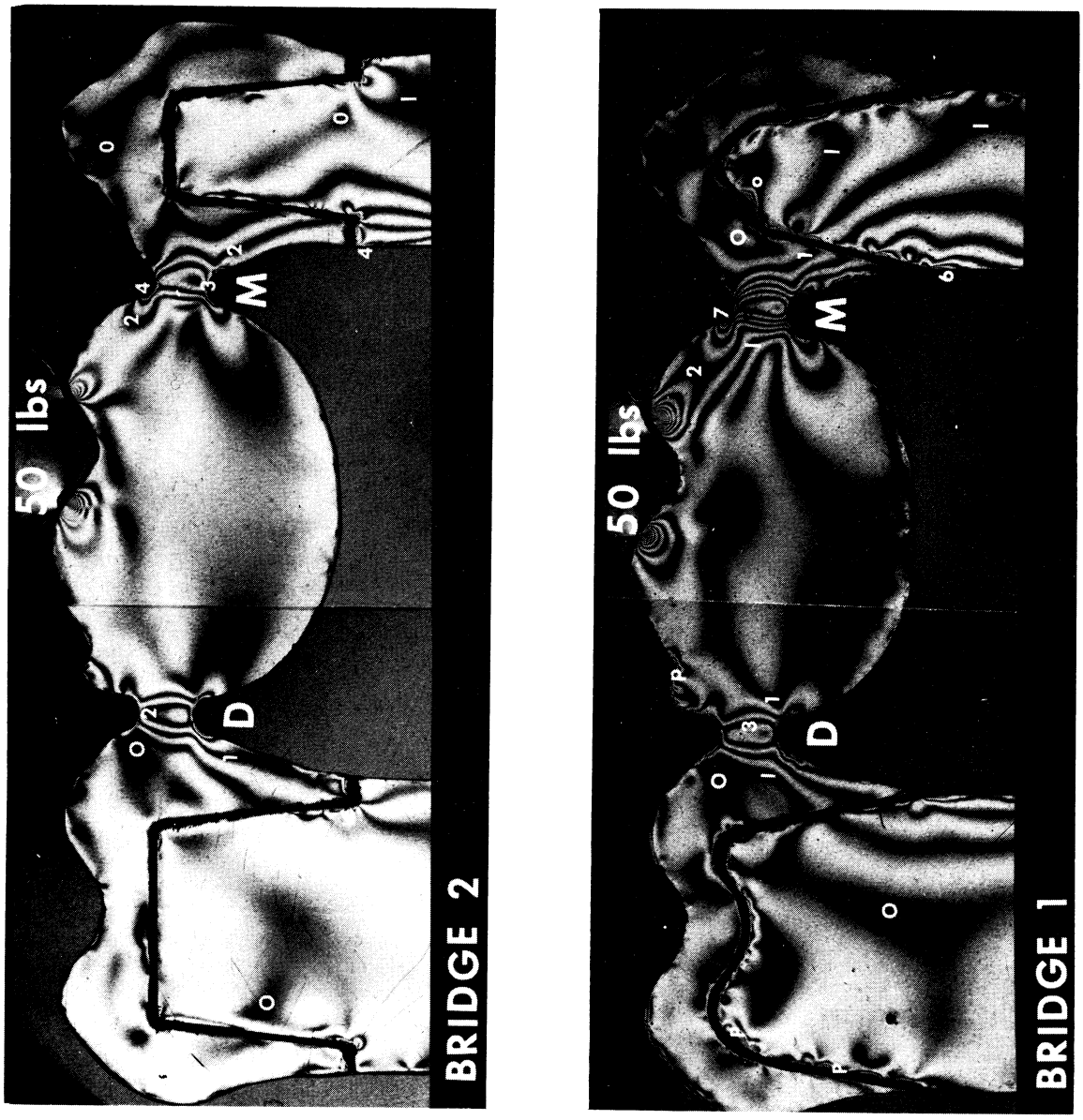

Figure 49. Composite Dark-field Photographs of Bridges 1 and 2, Loaded with 50 Pound Concentrated Load on the Pontic.

of the retainer to the tooth structure. Comparing the mesial fixed joint (M) in both bridges, bridge 2 had three isochromatic fringes while bridge 1 had five isochromatic fringes at the center of the mesial joint. A fourth fringe was detected at the base of the U notch above the mesial joint in bridge 2, while an isochromatic fringe of an order of 7 was detected at the same site in bridge 1, although all rounded U notches had the same radius, and r/d was equal to 0.392 in both bridges.

Since in the mouth the ratio r/d is not precisely duplicated, another bridge similar to bridge 2 was used with V notches at the molar-pontic contact area, and the U notches were not uniform at the bicuspid-pontic contact area, as shown in Figure 50. A "loader" was cut to represent upper teeth, and seven contact areas were established between the "loader" and the bridge model, as indicated by the seven arrows. The areas of the fixed joints again showed high stress concentrations. Since the isochromatic fringes were highly complicated in both photographs, a diagram was drawn to demonstrate the fringe orders along the free boundaries of the bridge 2 as shown in Figure 51 (lower picture). It was shown that alternate areas of tension and compression existed on both the upper and lower surfaces of the bridge. The numbers on the diagram indicate the fringe order, while + and - denote tension and compression respectively. This behavior of the dental bridge will be contrasted later with stress distribution in bending in a symmetrical beam, which is shown in upper picture of Figure 51.

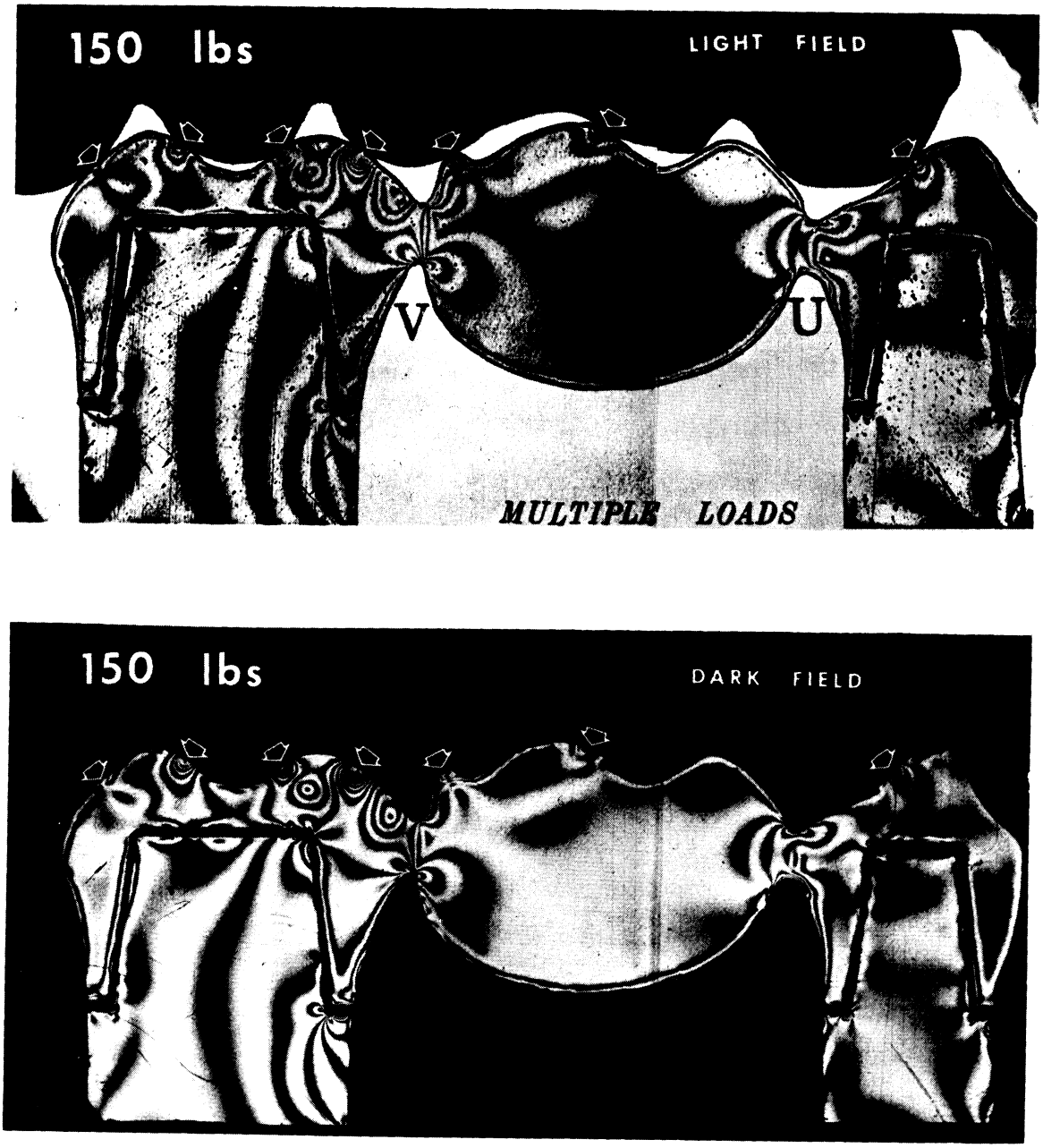

Figure 50. Bridge Model Similar to Bridge 2, Except for the Inclusion of U and V Notches at the Fixed Joints. The r/d Ratio Was Not 0.392.

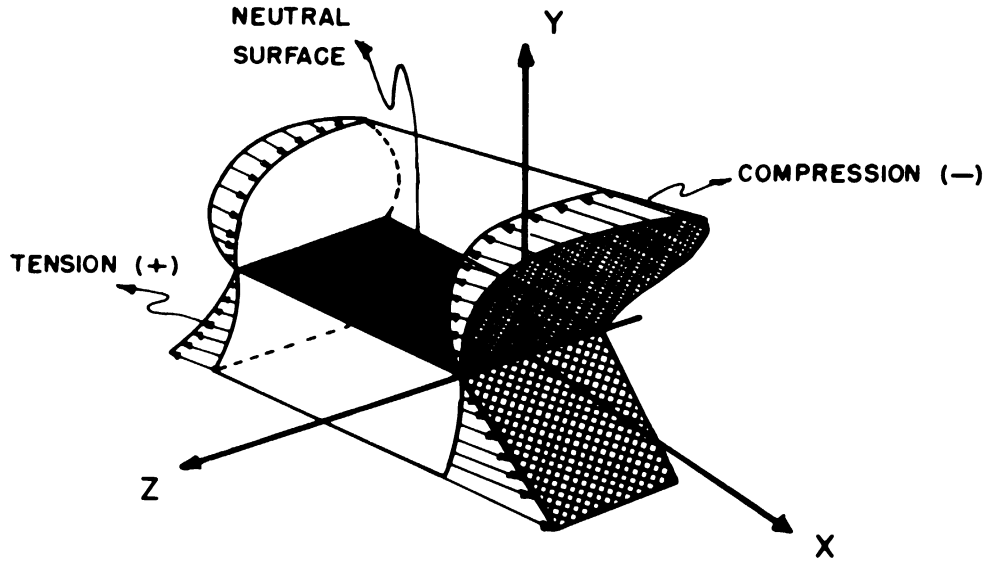

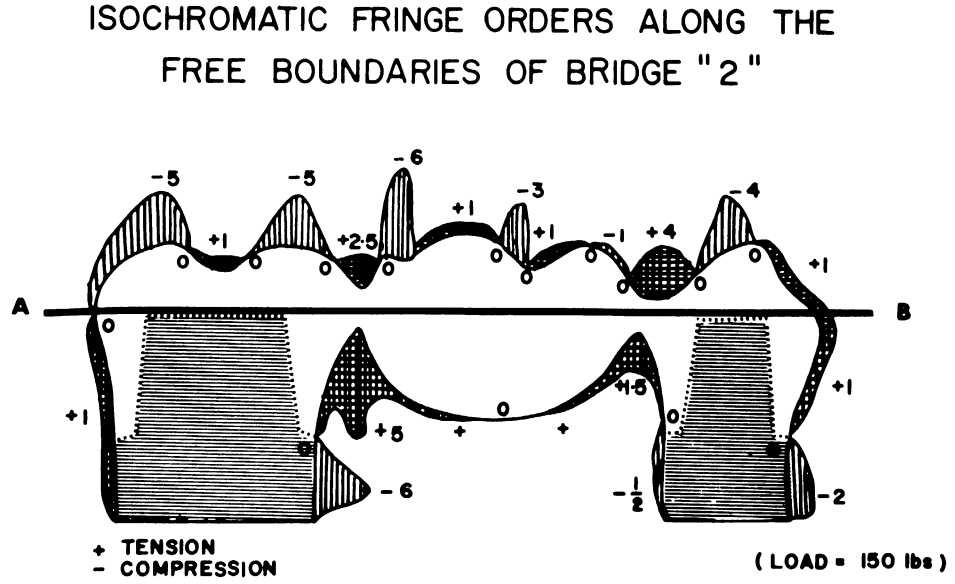

Figure 51. Bending Stress Distribution in A Symmetrical Beam (Upper Diagram) Contrasted with the Complicated Stress Distribution in Modified Bridge 2, with U and V Notches (Lower Diagram).

In the cantilever bridge 3, a sharp V notch was used above and below the fixed joint, as shown in the upper photograph of Figure 52. A load of 10 pounds was used to produce a bending moment of 21 pound-inch. Ten and one-half fringes were counted at the tip of the V notch. The same bridge was filed, in order to produce an r/d ratio of 0.392, as in the previous two bridges (r = 0.094 inch, and d = 0.240 inch) . This simple modification resulted in a reduction of the number of isochromatic fringes, from 10.5 to 5.5, as shown in the lower photograph in Figure 52. When the bending moment was increased to 40 pound-inch (Figure 53) the number of the isochromatic fringes almost tripled, from 5.5 to 14. In both photographs in Figure 53, r/d ratio remained the same as in bridges 1 and 2, i.e., 0.392. By applying three as nearly equal moments as possible, but varying the site of the load, the absolute number of the fringes remained approximately the same, as shown in Figure 54. The fringes were counted along the line AB. In general, the crowding of fringes at the fixed joint in the cantilever bridge 3 was more than the corresponding crowding in bridges 1 and 2. The letter H in Figure 53 denotes an area of high stress concentration in bending.

2. Stress Analysis of Modified Bridge 2 and Bridge 2.

Modified bridge 2 (with U and V notches) was chosen for the complete stress analysis, in order to compare it with bridge 2 with r/d ratio of 0.392. τ_{xy} was computed along

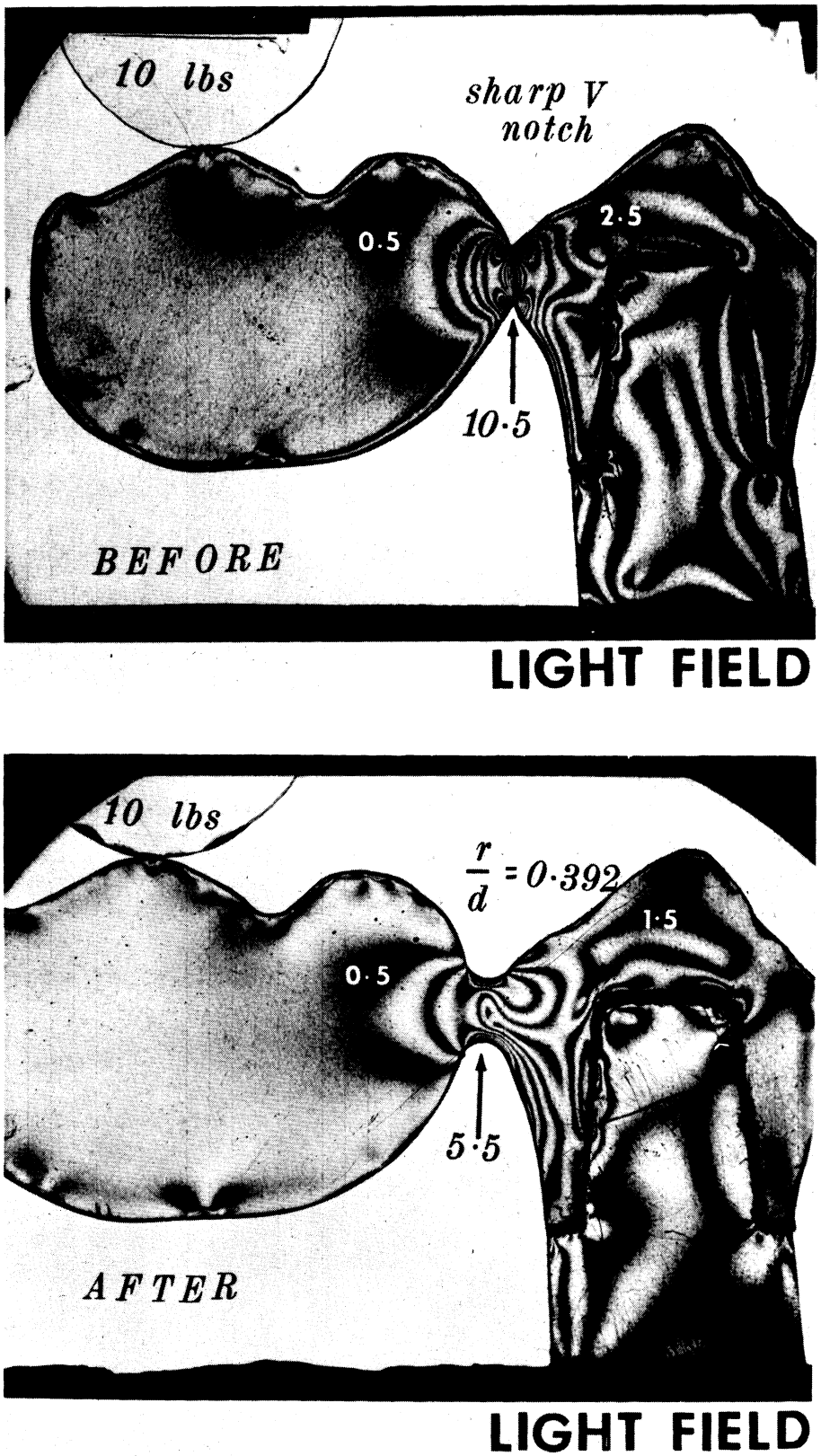

Figure 52. Cantilever Bridge 3, with Sharp V Notch (Upper Photograph), Contrasted to Same Bridge with r/d Ratio of 0.392 (Lower Photograph).

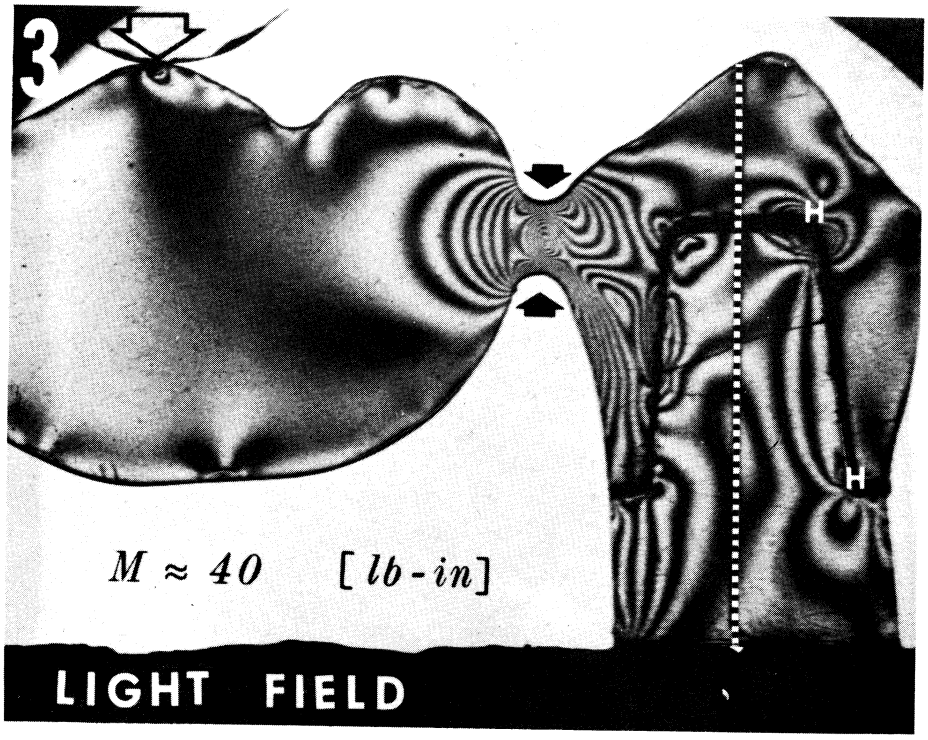

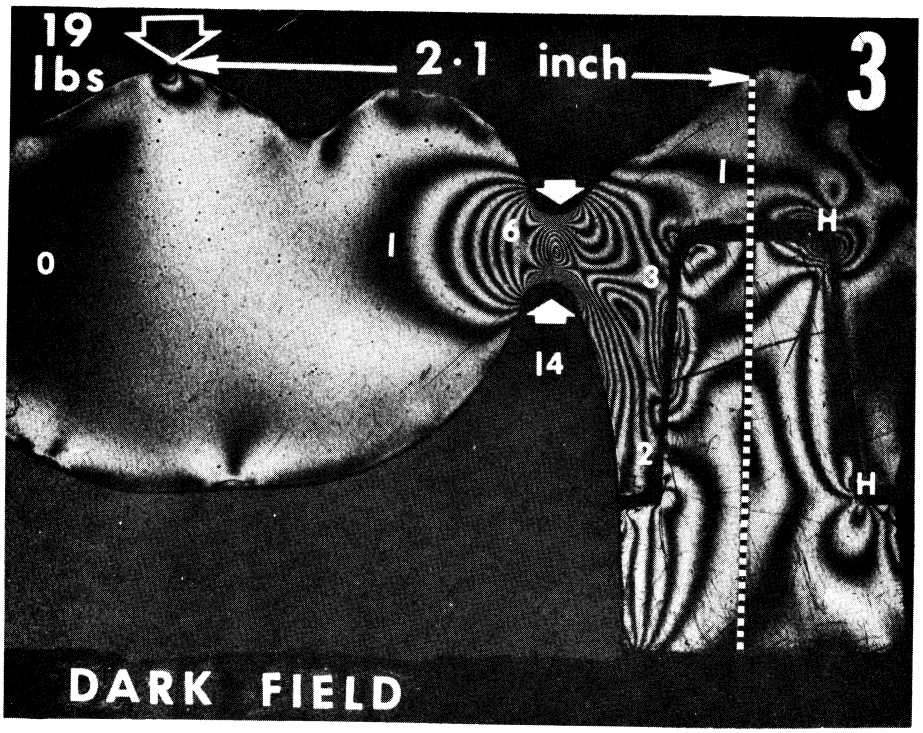

Figure 53. Cantilever Bridge 3 Subjected to 40 Pound-inch Bending Moment. Both Light and Dark Field Isochromatics are Shown.

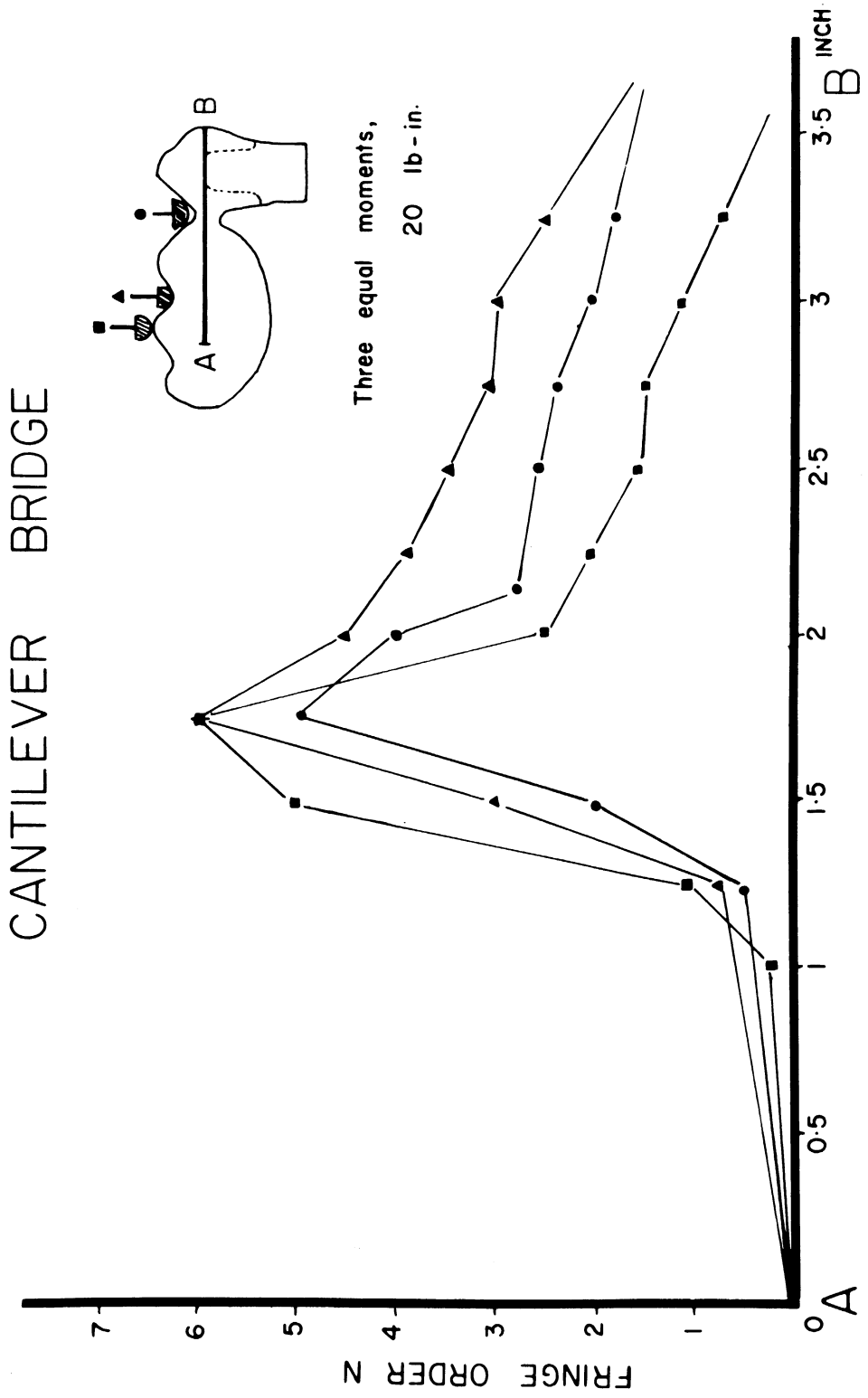

Figure 54. Cantilever Bridge 3 Subjected to Three Approximately Equal Bending Moments.

the line AB and CD, as shown in Figure 55. The multiple point loader was used for loading the bridge, because it represents a realistic loading device similar to the oral conditions of loading. Lines AB and CD passed from one proximal end of the bridge to the other, and both passed through the two fixed joints. The beam (bridge) did not transmit a constant bending moment, and it could not be considered to be in pure bending, therefore, the shear stress component did not vanish. τ_{xy} was computed from the photoelastic data, and it ranged from - 200 psi to + 410 psi, i.e., shear stresses were not constant along the length of the beam, because the unsymmetrical beam was loaded unsymmetrically. The principal stresses were separated along line OP, which lies between AB and CD, and they are shown in Figure 56. The difference between the principal stresses ($\sigma_1 - \sigma_2$) is shown as the solid-line curve, σ_2 is denoted by the finely-dotted line curve, and σ_1 is denoted by the interrupted black line curve. σ_2 was compressive (- 890 psi) near the distal contact area of the pontic (point 7 on the x-axis), while σ_1 was tensile (+ 850 psi) at the same point. Both σ_1 and σ_2 were compressive in the area near mesial contact area of the pontic, (point 20 on the x-axis). σ_2 had the largest algebraic value.

The principal stresses were separated for bridge 2 (with r/d ratio of 0.392), along line OP which passes through the three components of the bridge between lines AB and CD (as shown in Figure 57). On comparing Figures 56 and 57, it is clear that there is a marked improvement of the design, which

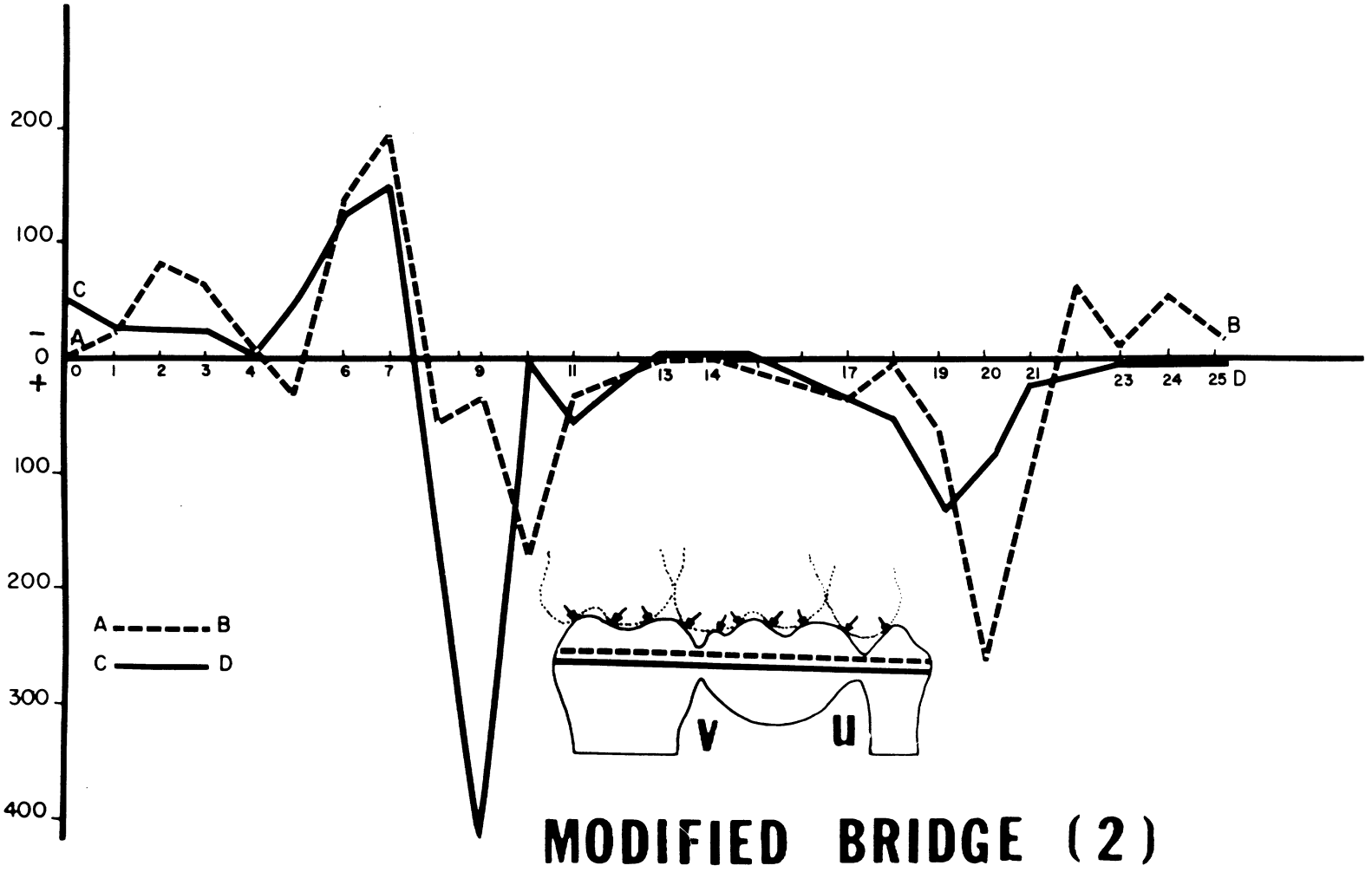

Figure 55. τ_{xy} Computed Along AB and CD Lines in Modified Bridge 2 with U and V Notches.

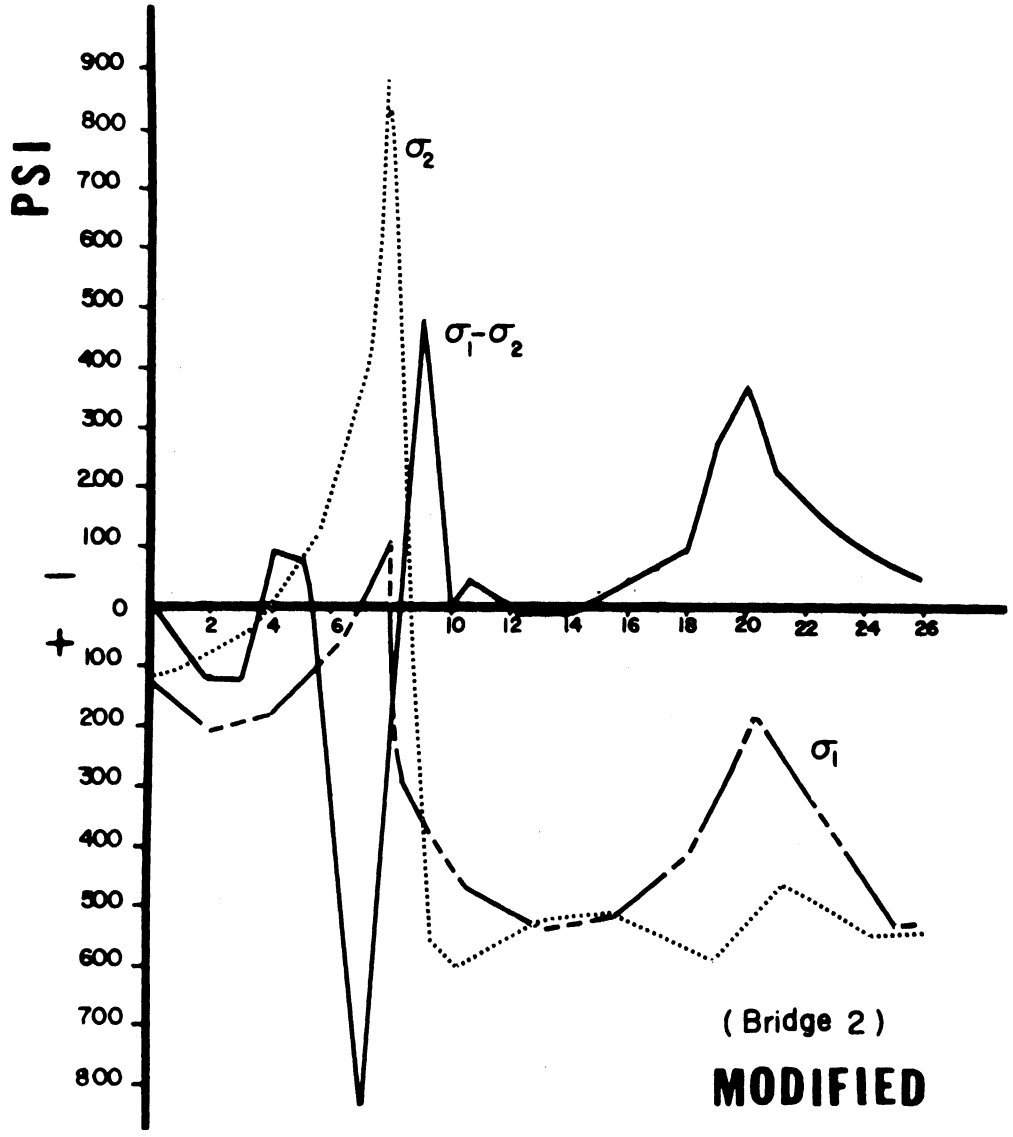

Figure 56. Principal Stress Along OP Line in Modified Bridge 2 with U and V Notches.

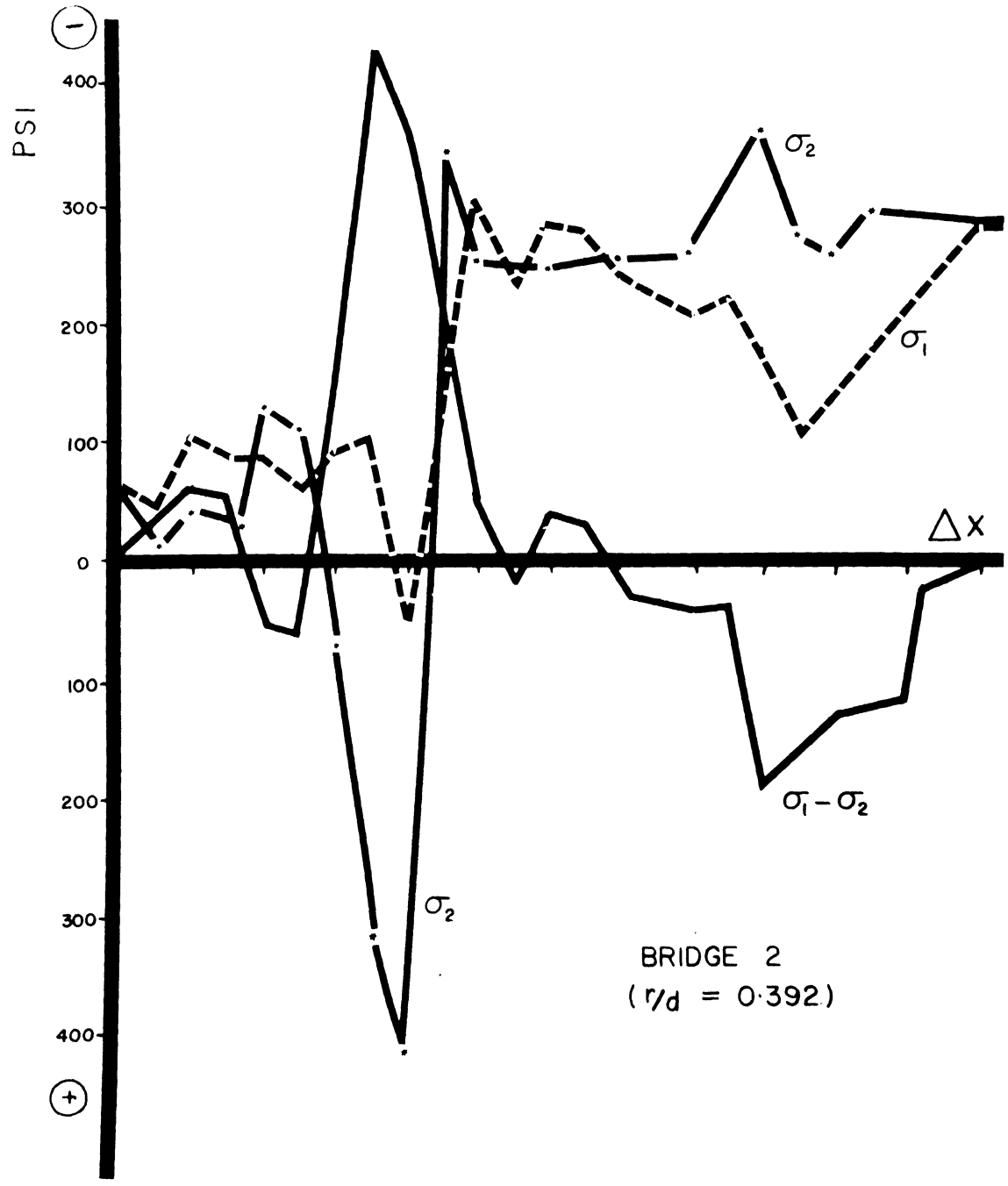

Figure 57. Principal Stresses in Bridge 2 with r/d Ratio of 0.392.

is mainly due to the elimination of U and V notches which were present to the fixed joint areas in the modified bridge 2. The shear stress at point 7 (modified bridge 2 with U and V notches) was about 850 psi, and at the same point 7 (bridge 2, r/d = 0.392) it was reduced to 420 psi, or a 50 percent reduction. The same was found for σ_1 and σ_2 values, on comparing both bridges, e.g., at point 20, σ_1 was +195 psi (in modified bridge), and it was reduced to - 100 psi (in bridge with r/d = 0.392).

G. Experimental Verification of the Reproductability of Photoelastic Results

Three models were cut, similar to occlusal reduction Model 2, and were given the code names X , Y, and Z in order not to confuse them with the other models. The three models were constructed in the same way as the experimental models.

Each model was loaded with a central load of 75 pounds, as shown in Figure 58. Two photographs were taken for each model at the same magnification, using light and dark field photography. The pictures were cut into one-half, along the vertical axis of the models. Composite pictures were made, using dark field (D) halves on the right side, and light field (L) halves on the left side.

The area marked Ω in the three pictures has the same retardation. The area marked $\sum$ also had the same retardation, except that in Model X the 1.5 fringe covered less area than that for both Models Y and Z. The corner of the wall of the restoration with the floor was marked Δ , and again

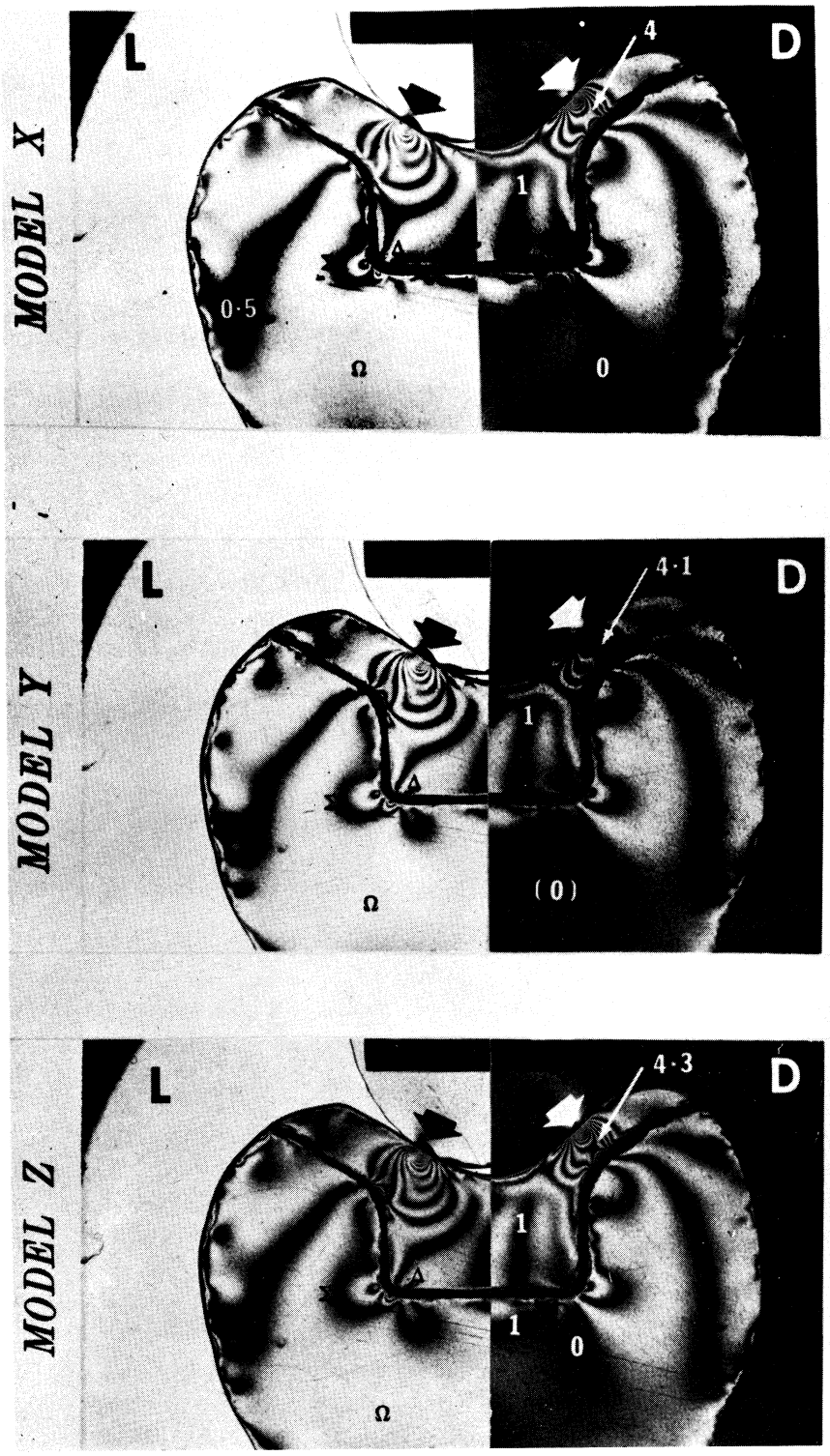

Figure 58. Photoelastic Recording for Models x, y, and z, Used for Experimental Verification of the Accuracy of the Results. 75 Pounds Concentrated Load, D = Dark Field Photography and L = Light Field Photography.

the order of the fringe (0.5) was the same, but in Model X the fringe covered slightly more area than that in Models Y and Z.

Comparing the dark halves, the zero fringe in Model X covered less area than that in Models Y and Z. In Model Z fringe order 1 appeared below the base of the restoration, and it is not present in Models X or Y. The order of the fringe in the center of the restoration for all models was one. On comparing the three areas directly under the loads (pointed to by the white arrows) the orders of the isochromatics were 4.0, 4.1, and 4.3 for Models X, Y and Z respectively. The variation was about seven percent, which is rather low. N_{max} under the load (indicated by the thick white arrow) was 11, 11.3, and 11.65 for Models X, Y and Z respectively. The variation in this particular area was about six percent.

It could be deduced that in constructing a series of photoelastic models, photoelastic results would vary between five and seven percent, which agrees with previous engineering papers discussing the accuracy of photoelasticity.[162,201]

CHAPTER VI

DISCUSSION AND APPLICATION OF RESULTS

Structural design in dentistry is controlled by three main factors, mechanical, esthetical, and biological. Mechanical structures such as a crown or fixed bridge, serving as substitutes for lost teeth, rest on and are supported by foundations which are responsive biologically. Discussion of the biological and esthetical limitations of design, as well as evaluation and practical applications of the experimental results will be presented.

A. General Discussion.

There are three main factors that influence the load carrying capacity of a dental structure, namely: (1) Oral forces which are exerted upon dental structures, which are primarily forces of occlusion,[108,180,217,218] (2) The form and the shape of the dental structure which receives the loads; the site of load application and the consequent stresses induced within the structure, and (3) The ability of the material from which the mechanical structure is built to withstand the stresses induced within it.[29,176]

The problems investigated could not be solved analytically, because they are statically indeterminate, and because of the complicated and irregular morphology of teeth which currently defied mathematical analysis. If a beam is subjected to pure bending, its fibers are in a state of unaxial stress.

If, further, a beam is prismatic, i.e., of a constant cross-sectional area and shape, the critical section occurs at the section of the greatest bending. Another critical section for any prismatic beam occurs where the shear is maximum.(118) Maximum or minimum moment occurs at a point where the shear is zero. If no shear occurs along a certain portion of a beam, no change in moment takes place. Dental beams are not prismatic in nature, therefore, they were investigated using experimental stress-analysis procedures. Idealization of dental beams has been attempted, but the results were of little value to restorative dentistry.(17)

Brittle materials fracture with little plastic deformation (a linear relationship between σ and ϵ). These materials exhibit little ultimate elongation. In ductile materials there is marked plastic deformation which commences at a fairly definite stress (e.g. yield point, possibly elastic limit), there is also a considerable ultimate elongation. The strength of a gold casting (polycrystalline solid) is great due to the interaction of grains and grain boundaries, but the theoretical strength is never attained because of the innumerable stress raisers. The segregation of grain boundaries, gas bubbles, shrink spots, and similar factors act as stress raisers in the structure. Another form of fracture arises when stresses perhaps even less than the yield strength, are applied repeatedly. The repetitions of stresses may eventually produce fine cracks which grow very slowly first, then extend rapidly across the entire part, giving very little warning of the impending

failure. This process is known as fatigue.[145] This phenomenon occurs intraorally at the soldered joint, especially when the soldered joint is pitted (overheated), and not deep enough gingivally. Corrosion and wear could contribute significantly to dental failures. It could be now assumed safely that the failure of dental restorations in function is a complex phenomenon, where any one of the critical factors cited, or a combination of them, could play a significant role in failure.

Fatigue cracks are most likely to form and grow from locations where stress concentrations are present. In engineering, a stress concentration factor (K) of three or more is quite common.[66] If the stress concentration is such as to raise the local stress up to the tensile strength, then fracture will occur. This consideration is important for both brittle and ductile materials. The proportional limit of dentin is about 24,000 psi, of enamel is about 54,000 psi, and that of zinc phosphate cement is about 11,000 psi.[176] The last material is unfortunately used to cement gold structures to natural teeth, and it is important to note that its strength is lower than dentin in compression. Failure could be due to failure of the cement, microscopically or macroscopically, which would lead to failure of the gold restroation. The failure cited here is engineering failure, clinical failure will be discussed later.

B. Evaluation of the Present Study.

1. Experimental Procedures.

Photoelasticity is a whole-field technique, which helps in the understanding of the total stress fields in the examined birefringent models. In general, it is easy to obtain two-dimensional photoelastic measurements with sufficient sensitivity and precision. The appropriate manufacturing of three-dimensional models requires special techniques, but the evaluation of the stresses at free boundaries is very simple.

The construction of the photoelastic models in the present study involved using of two different birefringent materials, i.e., composite models. The two parts, representing the restoration and tooth structure were cut separately, and then were stress annealed. The use of improved dental stone to represent the zinc phosphate cement caused some parasitic birefringency due to a setting expansion (0.05 to 0.09 percent). This was part of the experimental error in the present study which affected the precision of the results. The compressive strength of the dental stone is about 12,000 psi (dry) while that of dental cement is about 23,000 psi (one week),[176] which would yield a ratio of about 1.9 in comparison with a ratio of about 1.31, which was used in scaling of the photoelastic materials. It was considered that the discrepency in the scaling ratio was negligible, considering the thickness of the stone in the constructed models.

In the construction of three two-dimensional models of dental bridges, all models well held together with double adhesive tape, and a fine file 0.185 inch in diameter, was used to file the notches below and above the contact areas. This resulted in the reproduction of constant radii of the U-notches in the bridges. Since any variation in the r/d ratio would change the stress distribution, r/d was also kept constant in all bridges, except those having deliberate U or V notches.

It is important to mention that all the loads used in this investigation were vertical, and no diametrical compressive loads were utilized. Some vertical loads were used in the dental bridges section, which were deliberately planned to induce bending moments (as shown in Figure 53) to compare the stress distribution in certain structural features.

2. Photoelastic Findings.

It is clear that the change of design from a rounded shoulder (Model 3) to a sharp knife edge (Model 1) increased the number of the isochromatics from 10 to 17, as seen in Figure 21. This particular result completely disagreed with that of Rumetsch, Schreiber and Motsch.[189] They compared four models, resembling jacket crowns on anterior upper teeth. Under identical loads, they reported that a rounded shoulder (comparable to Model 3) had 18 isochromatics, and a sharp knife edge shoulder (comparable to Model 1) had five fringes only. They did not present any explanation for this controversial result.

In Figure 22, Models 6 (-15°) and 4 (flat shoulder) were compared. Although the load was moved from one proximal side of the models to the other, analogous areas of high stress concentration were demonstrated (lower right corner of both pictures in Figure 22). Both areas represent the development of tensile stresses between the restoration and the tooth structure, which are contraindicated in this particular area. The photoelastic analyses allow in a relatively easy manner the determination of the shoulder type that would produce the minimum stress. This could be done in a rather empirical way[64] by observing zones at the gingival areas of the margins at which the fringes are concentrated.

In the axial wall models (Figures 27 and 28) there was a symmetry around the central line of the models which was not the case with the shoulder geometry models. A load of 150 pounds was used in Figure 27, (axial wall Models 1 and 2), midway between the center and the edge of the model. It was interesting to find that the isochromatics converged along the cement then diverged, giving the illusion of continuity. When the angle of convergence was increased from 0° (Model 1) to 2.5° (Model 2) the order of the isochromatics changed at the axio-gingival areas (A-G) from 3 to 4.5 respectively. The stress distribution in the tooth structure in Models 1 and 2 was more or less the same. No evidence of tensile stress was noticed in the axio-gingival line angles away from the loading site. Axial wall Models 4 (2α = 15°) and 5 (2α = 20°) are shown in Figure 28, with identical loading sites but with two different loads. In the upper picture,

two black arrows point at the axio-gingival line-angles. The fringe order was one-half in the upper picture, while in the lower picture is increased to 2.5, although the load was decreased from 150 pounds to 100 pounds respectively.

In occlusal reduction models (Figures 32, 33 and 34) variations of the cusp coverage are shown. A concentrated load of 150 pounds was applied to the lingual cusp of both occlusal reduction Models 1 and 2. The basic difference between the two models is the extension of the small cavosurface bevel in Model 1 to cover part of the cusp in Model 2. A change of the stress distribution took place with this modification in design. No isochromatic fringes were detected in Model 1, while 18.5 fringes (N_{max}) were observed in Model 2. The stresses in the tooth structure also changed; 19.5 fringes were counted directly under the load in Model 1, and only 10.5 fringes were detected in Model 2, or about 50 percent reduction. This was one of the most interesting observations in this group of experiments. It seems that a simple criterion for design could be deduced. If the cusp height is higher than its base is broad, then it requires protection with gold, if not, then there is no real need for gold coverage. If cusp protection with gold is indicated, the optimum thickness is partially answered by Figure 33, (occlusal reduction Models 3 and 9). When the gold part of the restoration was extended to cover the cusp completely, there was a considerable decrease in the isochromatic fringes to 7.5. A new problem was encountered in the form of a high stress gradient, indicated by the letter

H in occlusal reduction Model 3. This concentration was due to the presence of a sharp corner in both the restoration and the preparation, which was modified in other models. In occlusal reduction Model 9 (theoretical), when the gold coverage was extended to cover the whole tooth, the stress pattern changed completely. In the tooth structure, in the area immediately below the load, 14.5 fringes were present. There was also an area of high stress concentration in the gingival part of the restoration, indicated by the fringe order of 16.5, which is due to the induced undercut in the restoration.

When the occlusal reduction models are loaded at the buccal or lingual cusps, compressive stresses will generally result on the surface of the respective cusps, and in the adjacent tooth structure. When the load is moved to the center (Figure 34), the components of the applied force may be resolved in a horizontal direction, and conceivably produce tension, as indicated by the letter T (Figure 34). The upper picture in Figure 34 shows the superposition of the isoclinics on the isochromatics, when the quarter-wave plates were removed from the polariscope. Occlusal reduction Model 7 (Figure 34) when loaded on the buccal cusp, using 100 pounds concentrated load, showed a considerable reduction in the order of isochromatics is tooth structure, with a high value of 3.5 compared to 14.5 in Model 9, and 7.5 in Model 3. This was a result of the interface between the gold restoration and the tooth structure being flat, and to the absence of sharp angles or corners, along with the increased thickness of the restoration.

In the vertical pin experiments, a paired approach was adopted in order to investigate the effect of pins on the structural design of posterior restorations. Vertical pin Model 4 is shown in Figure 38, when 100 pounds load was moved from the buccal cusp to the inclines of the cusps in the center. Tensile stress (T) was present at both side of loads, but the bulk of the restoration at the tensile areas would be enough to neutralize it. Generally, there was no marked stress-concentration around the pins, although the long pin usually had a higher order of fringes than the short one. N_{max} in the upper picture (Figure 38) was about 16, and in the lower picture was 11 fringes. In Figure 39, N_{max} was reduced from 14.5 (Model 6) to 13.5 (Model 8) when the thickness of the restoration increased. The stress distribution in the tooth structure in both models was comparative. By comparing Figures 34 and 38, both vertical pin Model 4 and occlusal reduction Model 7 were subjected to 100 pounds load buccally. It is evident that the stress distribution in the latter model was better than the former, both in the restoration and the tooth structure areas. It is important to mention that only vertical loading was used, and no bending was involved.

In the proximal reduction experiments, one loading site was chosen for all models, that of the contact area. Proximal reduction Model 1 is shown in Figure 40, and an area of high stress concentration (H) was detected in both

upper and lower photographs. It is logical to recommend an increase in the bulk of the restoration in this particular area, in order to redistribute the stresses. There is a similar area in proximal reduction Model 2, as shown in Figure 41. The shear-stress, as indicated by the isochromatic fringes for Model 2 in the tooth structure is similar to that in Model 1. There is one major difference between Models 1 and 2, which is the area of the restoration. The restoration in proximal reduction Model 2 is larger than that in Model 1, and there is no marked crowding of fringes along the junction of the proximal and occlusal parts of the restoration. In Figure 42, proximal reduction Model 3 is shown, with two areas of high stress concentration (H) comparable to those shown in Figure 40.

3. Effect of Design Variations on the Stress Concentration Factors.

Under ordinary conditions a ductile structure when loaded with a "steady stress" (i.e., a steadily increasing uniaxial stress) does not suffer loss of strength due to presence of a stress raiser, e.g., a notch. If a member is loaded statically (steady load) but may also be subjected to shock loading, or if the part contains sharp discontinuities, a ductile material may behave in the manner of a brittle material, and the computation of stress concentration factor, (K) , becomes an important prerequisite to design.[182]

The present investigation included many variations of dental designs and their influence on K . In shoulder geometry experiments, K ranged from 2.39 to 5.1. It was evident

that stress concentrations will always be found at sudden changes of section, which could be reduced by modifying the design to include a round margin. The difference between shoulder geometry Models 3 and 2 (K = 2.39 and 2.48, respectively) results from a difference in the radius of curvature. It has been established in engineering that as the radius of the fillet increase, the stress concentration factor decreases.[182] There is a biological limitation in the anatomy of teeth, when this last rule is applied. If the radius is increased more than that incorporated in shoulder geometry Model 3, the danger of exposing the pulp tissues at the axio-gingival line angle becomes eminent. Based on the different values for K in shoulder geometry designs, it is clear that modifying the sharp knife-edged shoulder (Model 1) by increasing the bulk at the proximal margin, and rounding the axio-gingival angle reduced K by 50 percent, as seen in Models 2 and 3. The dotted line in Figure 24 represents the mean stress concentration factor, which could be thought of as a boundary line, with all designs falling below it being acceptable. The clinician could choose any of the designs with a low K . It is assumed that designs above the dotted line would be unacceptable, from the strength and stress viewpoint.

In axial wall convergence experiments, K ranged from 2.41 (Model 2:2 α = 5°) to 4.79 (Model 5:2 α = 20°), as shown in Figure 29. The mean K was computed as 3.0, which is represented by the dotted line.

In the occlusal reduction models, K were computed, and they ranged from 3.25 (Model 7) to 7.8 (Model 9), as shown in Figure 35. It was found that the stress concentration factor decreased, as the occlusal thickness of the restoration increased. The so-called anatomical reduction (Models 3 and 5) created sharp corners and irregularities that were eliminated in the optimum design, Model 7, by flattening the cusps. The mean K was found to be 4.5, and is represented by the dotted line in Figure 35.

In vertical pin experiments, it was found that the models that incorporated pins, had increased K values, e.g., vertical pin Model 4 had K of 3.9. When the thickness of occlusal protection was increased (doubled from 1 to 2 mm) and the pins eliminated, K dropped to 3.3. All vertical pin models fell below the mean K of 4.5 as shown in Figure 35.

In proximal reduction models, it was found that, for practical purposes, the three tested designs had the same stress concentration factor, and the stress distribution in the three models was comparable. Concerning the principal stresses, σ_1 and σ_2 in proximal reduction Model 1, Figure 45, it was interesting to find σ_1 and σ_2 at or near B became tensile in nature, and σ_2 at the other end,

was also tensile. The small part (gold) that covers the extreme proximo-buccal and proximo-lingual areas needs some design modifications, because of the presence of tensile stresses at these thin structures, which may cause brittle failure of the cement in the mouth.

The analytical determination of K for dental designs, will help in understanding why some dental restorations fail. It should be mentioned that K is different for different types of loading, that they must be applied to nominal stresses, and that K is a dimensionless product. In dealing with dental designs, it is important to know not only the maximum stresses at the surface, but also stress magnitudes at various levels below the surface. Photoelasticity is one of the best methods that provides an over-all picture of stress gradients. Since fatigue failures almost invariably originate at stress raisers, the matter of minimizing stress concentration is of utmost importance.[9] When there is a choice in the placement of a stress raiser, e.g., a pin hole, it should be located in a region of low nominal stress. It is also important to increase the bulk of the structure at areas of high stress. Recently, it was proved that computations of K were different for tensile and compressive loadings,[66] the compressive stress concentrations were higher than those in tension, and their influence was observable a greater distance away from the stress raiser. It should also be mentioned that values of K computed from two-dimensional photoelasticity are slightly

higher than those computed using three dimensional photoelasticity, due to the lack of the reinforcing effect present in three-dimensional photoelasticity.[64]

From the current study, it was found that structural design in dentistry could be improved substantially if many of the stress raisers are modified. The pertinent stress raisers and means of minimizing their effects are listed briefly:

(1) Sharp line angles in the preparation of teeth, they should be rounded to reduce stress concentration.

(2) Sharp notches in dental bridge construction, especially near the fixed joints, V notches should be replaced by U notches, and the larger the radius the better the design.

(3) Sharp shoulders (e.g. knife-edge) are considered as stress raisers, rounding of the gingival margin will reduce the stresses both in the dental restoration and the tooth structure.

(4) Occlusal cavosurface bevels should not be extended to cover part of the corresponding cusps, since the thin gold margin will weaken the restoration considerably. If the cusps are to be protected, the cusps should be reduced enough in order to allow for 2 to 2.5 mms of gold.

(5) Pins should be placed in areas of low stress gradient, e.g., occlusally but not gingivally where they would enhance the failure of the restoration.

(6) Holes for vertical pins should be rounded at the bottom, and threaded pins in tooth structure should be discarded, as engineering research recently pointed out that stress concentration factors in both threaded roots were rather high (2.7 - 4.0).[22]

(7) In proximal reduction, enough gold bulk should be incorporated in slice preparations, since the proximo-buccal and proximo-lingual margins are thin and could not resist tensile stresses.

(8) U-shaped members (M.O.D. restorations) are better than L-shaped members (M.O. or D.O. restorations) when used on abutment teeth, in order to decrease the effects of bending moments and torque.

(9) Depth along with the radius of the notches above and below the fixed joint are the most important criteria in the design of fixed joints of dental bridges. The aim should be to increase the r/d ratio (Figure 47) in order to decrease the stress concentration factors.

Other stress raisers in dentistry include deep developmental grooves in restorations, especially gold and amalgam individual restorations,[149] V notches in circular shafts

(e.g. threaded pins used in restorative dentistry),[182] undercuts induced by inverted-cone burs, occlusal and proximal grooves (V shaped), and locks in the slice preparations on anterior and posterior teeth.

4. Dimensional Analysis.

Using dimensional analysis methods in experimental stress analysis, provides an important tool for the interpretation of the experimental results.[131] Geometrical similarity of the models to the prototype is the most important assumption, along with isotropy and homogeneity. Equation 18 as shown in Figure 20, was derived[45] in order to compute the corresponding stresses in the prototype. The derived equation should have a limited application, until the visco-elastic behavior of tooth structure is completely investigated. In deriving Equation (18), isotropy and homogeneity were assumed in the tooth structure, as a generalization. It is hoped, in the future, that experimental stress analysis of dental structures, be carried intraorally using some new technics, such as birefringent coatings and fatigue prediction by ultrasound.

It would have been desirable to use full scale models. Even more important, it would have been a far reaching achievement to use birefringent photoelastic materials with E and μ of nearly the same magnitudes as those of dental gold and tooth structure. This was obviously impossible in view of the nature of the available photoelastic materials.

Applying Equation (18) to the experimental results, would transform the stresses from the photoelastic model to prototype, e.g. the stresses in occlusal reduction Model 7 (3.0 mms of occlusal gold, flat without occlusal anatomical reduction) were analyzed, as shown in Figure 37. Point 14 along the line A B was chosen, since it is midway between the buccal lingual surfaces, and lies within the gold structure. The principal stresses in the prototype were estimated: σ_1 = - 3520 psi, σ_2 = - 1228 psi, and τ_{max} = - 1127 psi. The values of the principal stresses are much lower than the proportional limit of type C dental gold (30 - 60,000 psi, for the soft and hardened alloys, respectively).[176]

By repeating the same procedure for proximal reduction Model 1 (slice-restoration, Figure 44), the stresses were computed for point 4 along the A B plane. σ_1 was -1155 psi, and σ_2 was +625 psi. This is an indication for redesign of this part of the restoration, since there is usually a thin film of luting medium under it, which will be discussed later.

5. Correlation of Dental Cavity Design to Experimental Stress Analysis, and Application of Results in Dentistry.

Structural design in dentistry is abundant with controversies, which were pointed out in the literature review. The results of this study emphasize that a fixed dental bridge with soldered joints does not perform like a simply-supported beam, as its abutment reactions are somewhat more complicated.

It is impossible to consider, any longer, that a shoulderless preparation is the same as that with shoulders, hence the former was shown less able to withstand vertical occlusal forces as compared with the latter. This finding could be extended to include porcelain jacket crowns. As early as 1927, McCloskey (Reference 155) found that "a good, clean-cut, well defined shoulder is absolutely necessary for strength in a crown." He found that resistance to crushing of crowns with shoulders was higher than those without shoulders, where they crushed at 116.92 pounds and 43.44 respectively. Lehman arrived at the same conclusions, in 1967.[138] The fallacy of gingival locks and/or bevelled gingival margins was shown clearly in the results. There were significant differences in the results of shoulder geometry experiments, showing that the different margins had different stress concentration factors. It is clear from the results, that a rounded shoulder (shoulder geometry Model 3) represented the optimum design, which did not agree with Rumtesch's results.[189]

The relationship between the retentive forces and the angle of convergence in dental restorations was established to be a "hyperbola",[117] with parallel axial walls showing the highest retention. The elimination of the right angle between the pulpal and axial walls, and between the axial and gingival walls was shown to contribute to the reduction of the shear stresses in both the tooth structure and the restoration. It is believed that the optimum convergence angle of axial walls should be 2.5° to 6.5°, which agrees completely with

Jørgensen's[117] experiments correlating convergence to retention.

It was established that short dental pins did not change the stress picture in dental structures. Jeanneret[106] showed that the combination of vertical pins with cusp protection would supply a significant increase to any displacing tensile forces, thus augmenting the anchorage of the restoration. The results of the present investigation showed that the stress concentration factor decreased as the thickness of dental gold protecting the cusps increased. It was hypothesized, that cusp protection with gold is important when a cusp is higher than its base is broad, as shown in Figure 59, because the stress distribution would be improved considerably, preventing sudden increases of tensile stresses at the angle of the vertical walls of the cavity with its floor. Another factor to be considered in dental design is the angle of the gold-protected cusp. By reduction of the cusp angle, the components of applied forces and the resultants would be lower, as shown in Figure 60. On the left cusp $\bar{N}$ was computed as 28.7 pounds, and on the right cusp $\bar{N}$ was 32.1 pounds, which is an important difference.

The shape and design of proximal portions in compound restorations is an important part of structural design both in individual restorations and in abutment restorations. If the slice preparation is to be used, more tooth structure should be removed proximo-buccally and proximo-lingually, as more gold bulk is needed in the areas where tensile stresses

A

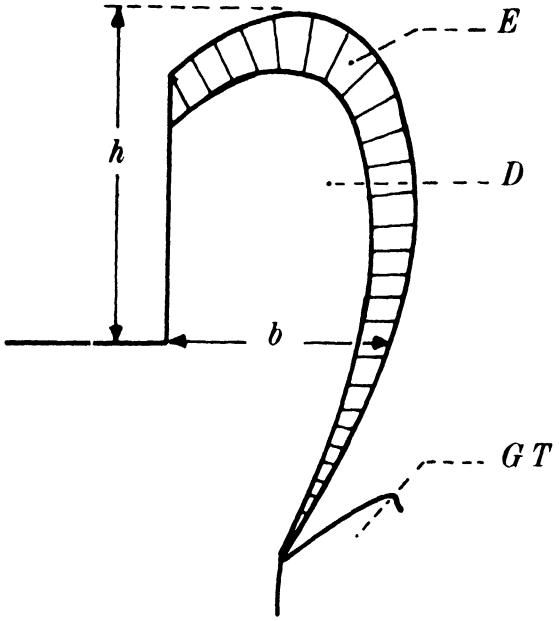

E : *Enamel*
D : *Dentin*
GT : *Gingival Tissues*
h : *Cusp Height*
b : *Cusp Breadth*

B

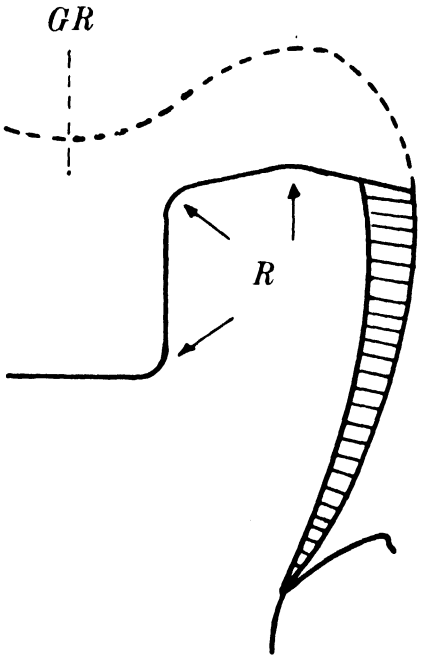

GR : *Gold Restoration*
R : *Rounded Corners*

Figure 59. Criterion for Cusp Protection With Gold.

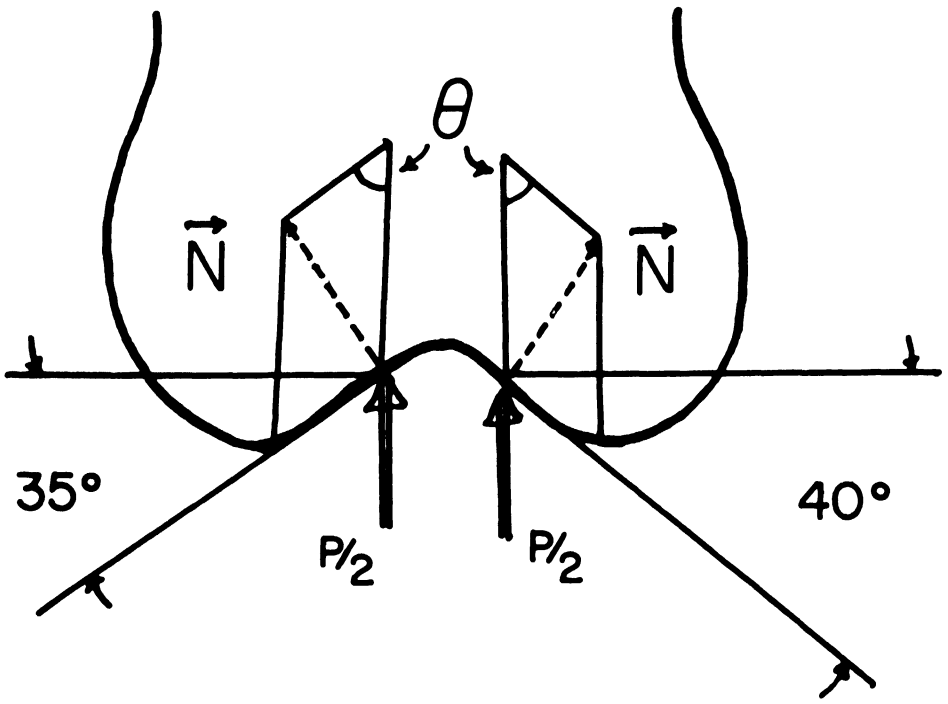

OCCLUSAL FORCE = 100 lbs.

$P/2 = 50$ lbs, $\vec{N} = (P/2) \cdot \text{Sine}\,\theta$

Figure 60. Effect of Cusp Angle on Force Components.

were detected. The choice between a proximal box or a slice would depend on the tooth form proximally, since both designs had the same stress concentration factor. If a "slice-lock" is adopted,[18] the lock should have a large radius, to eliminate a potential source of stress concentration. If a proximal box is used, with or without parallel walls, a gingival pin should not be incorporated, as the gingival area of proximal restorations is considered an area of high stress concentrations. Pins should be used occlusally and not proximally. It is absolutely important to point out that sharp ledges or corners in preparations or restorations, are primary sources for weakened areas. As a rule of thumb, all line and point angles in dental preparations should be rounded.

The problem of structural design of dental bridges was investigated, but not in great depth. It was established that dental bridges which are fixed at both ends had a more favorable stress distribution, than dental bridges which are fixed at one end only, i.e. cantilever bridges. If cantilever bridges need to be used intraorally, double abutments for their support (splinting) must be used, in order to reduce the hazardous effects of the induced bending moments, both on the dental restoration and tooth structure. It was also interesting to find that doubling the bending moment at the free end of the cantilever bridge, the number of fringes at the contact area (fixed joint) almost tripled.

The contact area (fixed joint) in dental bridges was the weakest structural area of the bridges investigated. It is generally important to avoid any V-notches in the vicinity of the contact area, and rounding of the notches above and below the fixed joint becomes mandatory. This effect was clearly demonstrated in Figure 53; when the V-notch was transformed to a U-notch in the same bridge, the shear stress was reduced to one-half the previous value. The ratio r/d (Figure 47) is extremely important in the design of this weak area. There is some effort to control the radius of r in dentistry, but the effort should be increased. Roark[182] demonstrated that when r/d was increased from 0.025 to 0.50 for two V notches in member of rectangular section, K (in bending) was reduced from 3.6 to 1.3. For two U notches in a member of rectangular section, when r/d was increased from 0.05 to 0.75, K (in bending) was reduced from 2.20 to only 1.18. He showed K would be reduced further, if there was only one notch. The r/d ratio used in all bridges in the present investigation was 0.392; if it is assumed the bridges investigated were rectangular sections, K in tension, according to Roark,[182] would be 1.60 to 1.65, and K in bending would be 1.38 to 1.42, which are quite low. It was assumed that U-notches in a circular shaft, would have the same theoretical stress concentration factors. In dentistry, there is slight control of the dimension d (Figure 47), because of the biological considerations of the periodontal ligament, which would prevent increasing the depth of the fixed joint.

It would be advantageous to cast dental bridges as a one unit casting, thus avoiding any incorporation of soldered joints, and the introduction of an alloy with a lower proportional limit. If soldered joints are made, over-heating should be avoided in order to avoid the presence of pits or porosities in the joint, which would weaken it considerably.

It is assumed that fixed bridges should be placed in any situation where a common line of insertion can be prepared for all teeth. This ruling should be valid for both long and short span bridges, to avoid the problem of adverse leverage which might arise with a fixed-movable bridge (the so-called stress breakers). Movable bridge joints, however, were not investigated in the present research. No variations in the design of the suspended members of the bridges (pontics) were attempted in the current work, and all restorations and pontics were constructed as one piece of plastic, representing dental gold alloy. Finally, it is important to point out that all experiments dealing with individual design factors were completed before the construction of the photoelastic models representing dental bridges. This approach was adopted so that designs exhibiting low stress concentration factors could be incorporated in Bridge 2, as compared to those of high stress concentration factors, which were incorporated in Bridge 1.

Failure of dental restorations during oral service, is attributed to many factors such as improper handling of restorative materials, but improper cavity design has been considered as a major cause. The importance of properly

prepared cavities has been recognized in the dental literature, (References 150 and 151) and numerous articles have outlined the essential mechanical principles as applied to cavity preparation in relation to restorative materials. The experimental approach has found its place in dentistry recently, with the main objective of improving structural design. Dental restorations, however, continue to fail because cavity designs (preparations) do not adequately minimize or compensate the intrinsic weaknesses in restorative dental materials and tooth structure, and because dentists have found it arduous to use the mechanical principles of cavity design as idealistically as they are employed in the research laboratory. At the same time, biological factors should be considered in the application of sound principles of engineering design to dentistry.

Failure can occur in the tooth-restoration interface, in the restoration itself, or even in the remaining tooth structure. The concept that restorative dentistry is a procedure based solely upon an understanding and application of mechanical processes is just as untenable as the view which holds that it is entirely biological. It has been established that, in order to make a dental restoration acceptable biologically, its design must also conform to, and respect the basic laws of mechanics, engineering design and physics. (Reference 208). Therefore, a structural consideration of

the integrity of the restored tooth must include the tooth structure, the restorative material and the relationship of the restorative material to the residual tooth tissues.

There are several types of dental restorative failures, some are directly related to cavity design, others are indirectly; and they include:

(1) The presence of high shear stresses at the margins of the restoration, would lead to a marginal failure and loss of integrity between the restoration and the tooth structure. Since zinc-phosphate cements have little transverse strength, it should not be used where bending stresses are present.[151]

(2) Fractures may occur in association with occlusal wearing of the central fossa of restorations made of brittle materials (silver amalgam), leaving hard cusp tips in occlusal interference. In other words, fracture here is a brittle fracture, which occurs with very little permanent deformation soon after the elastic limit is exceeded.[206,207]

(3) Fracture is promoted by the stress concentration factor, especially of tooth structure. Sharp angles and sudden change of cross-sectional areas are the main factors responsible for tooth structure failure.

(4) If the yield strength in tension of a ductile restorative material is exceeded, the material will fail by yielding. This ductile fracture is especially exhibited in a faulty soldered joint in a bridge framework. Imperfections in soldered joints or from casting technique, and overwork or strain hardening due to a span being too long, with springing in the center of the beam, may result in brittleness, loss of strength and ductility, and subsequent fracture.[118]

(5) There are instances when the wrong design is used on the wrong tooth under unfavorable occlusal forces. Design failure is due to a combination of one or more of the previous factors, incorporating, e.g., cast gold (Type A), in an L-shaped member (restoration) on an abutment tooth in five-unit fixed bridge. (This is an extreme case of abusing a restorative material, combined with the wrong choice of design.)

(6) The axial contour of a restoration, regardless of the material used, should restore the original anatomy of a tooth. Interproximally this means adequate finishing of a restoration to prevent any overhang or bulbous curvatures. If the restoration impinges on the interdental tissues in this area, a periodontal failure will be

encountered. This is a failure of the supporting tissues of the tooth, although the strength of the restoration may be adequate.[95,208,226]

On the basis of these types of failures, the cavity preparation must be designed to take into account the nature and properties of the materials involved, i.e., tooth structure and the restorative material. Biological and esthetical limitations of proper mechanical structural design principles, should be respected. The design parameter of ductile materials is the proportional limit, while the design parameter of brittle material is the ultimate strength. It is interesting to note that the proportional limit of both dentin and cast gold (type C) is about the same (25,000 psi), however, the tensile strength of dentin does not exceed 7,000 psi.[137,215] This means that the ultimate compressive strength of dentin (43,000 psi) is six times as great as its tensile strength, so as much dentin as possible must be preserved to prevent marginal failures, and proper restorative design should compensate for this structural deficiency of dentin. It should be remembered, however, that bulk in a dental restoration can be accommodated only at the expense of tooth structure (especially dentin), so care should be exercised to avoid the indiscriminate removal of tooth material.

Since cavity design influences the nature and magnitude of the stress in the structure, the design should be chosen to avoid high stresses, especially tensile or bending

stresses. The selection of a restorative material for a certain restorative design should be guided by the fact that differences in elastic moduli between the tooth structure and the restorative material can produce a marginal discrepancy along the interface, under occlusal loading. Also the relative difference in bulk of the restoration and the tooth can result in differential deformation.[150,198] Complicated cases involving combination of simple conditions are apt to be encountered, and until further laboratory work has been done, it is necessary to use judgment based on considerations of stress analysis.

C. Recommendations for Further Work.

If further work is to be done in experimental stress analysis of dental structures, three dimensional stress analysis of the models would be more favorable for combining different design factors. It would be extremely difficult to compute all the components of stress using that method alone, therefore, it is recommended to combine it with the Moiré method. Scaling, would present problems, since the available epoxies do not have a wide range of moduli of elasticity and Poisson's ratios.

Birefringent coatings on scaled metal dental restorations would present a general survey of the surface strains present on the restorations. Birefringent coatings, however, would present difficulties when natural tooth structure or on plastic models representing teeth, because of the encountered creep problems.

Pontics in fixed bridges should be investigated, with more emphasis on the combination of different photoelastic materials to represent gold-acrylic and gold-porcelain combinations. Also, variations in the joints of the retainers to the pontics should be investigated, comparing fixed and movable joints, along with variations of r/d ratio and its effect on bending and tensile stresses.

The viscoelastic properties of dentin are still not defined, and more research is needed to improve the current understanding of the behavior of the total tooth structure. The modulus of elasticity and Poisson's ratio of the periodontal ligament of human teeth are not known yet, and if their values were known, the stress distribution in dental models could be modified greatly.

Experimental stress analysis methods could be used to investigate many dental problems, such as design of retainers in partial dentures, complete dentures with or without metallic bases, some orthodontic appliances and maxillofacial prostheses.

CHAPTER VII

GENERAL SUMMARY

The problem outlined in the present investigation involved the detailed experimental stress analysis of several dental restorations through the computation of geometrical stress concentration factors, and the experimental surveying of different mechanical factors affecting restorative designs in dentistry.

Structural design factors investigated were the shoulder geometry of posterior compound restorations, the degree of convergence of axial walls, the extent of occlusal reduction of posterior abutment teeth, the effect of vertical pins on stress distribution in posterior restorations and the magnitude of proximal reduction in compound posterior restorations. Certain posterior bridges were tested in order to detect areas of weakness suitable for redesign.

The photoelastic method of experimental stress analysis was used in this research, for the determination and improvement of mechanical strength of investigated structures. Pursuant to this aim, an attempt was made to assess the overall stress distribution in different dental designs and to compare them using photoelasticity, as well as statistical inference techniques.

The conventional two-dimensional photoelastic method involved the fabrication of a suitable model for each tested

design, which was loaded and placed in a circular transmission polariscope, and the resulting fringe pattern was traced and photographed. Composite photoelastic models were constructed of two birefringent materials, and improved dental stone representing dental cement was used to lute them. The ratio of moduli of elasticity of gold to tooth structure was estimated to be 1.4. The ratio of the moduli of the two birefringent materials representing gold and tooth structure, was 1.31, which resulted in an error in scaling of about 6.3 percent.

Seven designs were tested, in the investigation of shoulder geometry designs. The models were loaded at four different sites, using two different loads at each site for each model. Significant statistical differences were detected in the stress distribution of the seven shoulder designs ($p \leq 0.005$)***. The rounded shoulder (Model 3) had the lowest value, $K = 2.39$, while the knife edged shoulder (Model 1) had the highest value, $K = 5.1$.

Five axial wall convergence designs were investigated, and the convergence angle (α) ranged from 0° to 10°. Two loads were used at three different sites, in accordance with occlusal loadings. Significant statistical differences were detected in the stress distribution of the five convergence angles, ($p < 0.0005$)***. Model 2 (convergence angle = 2.5°) had the lowest K of 2.41.

Nine occlusal reduction designs were investigated, to assess the relationship between structural strength and thickness of occlusal gold. All photoelastic models were loaded at three different anatomical sites using three different concentrated loads. Significant statistical differences were detected in the nine tested designs, ($p < 0.005$)***. It was shown that increasing the occlusal "gold" thickness, decreased the stress concentration factor. Model 7 (3 mm in the prototype) showed the lowest K of 3.25, while Model 9 (1 mm in the prototype) showed the highest K of 7.8.

In vertical pin experiments involving six designs, a paired approach was used. The same design was tested twice, with and without pins. The loading procedure was identical to that used in occlusal reduction experiments. It was found that there was no statistical difference between restorations with or without vertical pins, as far as the stress distribution was concerned, but there were significant differences between models having different occlusal thickness. This result agreed with those deduced from occlusal reduction experiments.

In experiments related to proximal reduction in compound restorations, three basic designs were loaded at the area of proximal contact using three different concentrated loads. There was no difference between the computed stress concentration factors (K ranged from 2.78 to 2.81). Statistical inference technics agreed with these results, and no significant differences were detected, ($p < 0.005$).

In posterior fixed bridges experiments, three basic models were constructed, and loaded using one concentrated load at different sites. For all bridges, the r/d ratio was kept at 0.392 at the fixed joints areas. Optimum design features were incorporated in bridge 2, while some stress raisers were incorporated in bridge 1. Bridge 3 represented a dental cantilever bridge similar to bridge 2. Composite photoelastic recordings showed that the fixed joint areas (soldered joints in dentistry), possessed high stress concentrations. A modified bridge 2 was built, with U and V notches in these areas. It was shown that bridge 2 with r/d ratio of 0.392 had approximately 50 percent less concentration of stress at the critical fixed joint areas than the modified bridge 2 (with U and V notches), when a multiple loader was used.

CONCLUSIONS

The following conclusions may be drawn from this study:

(1) The stresses in the proximal portions of all seven shoulder models were compressive in nature, when the proximal shoulders were loaded occlusally on the same proximal marginal ridge.

(2) The chamfer-type was the optimum design in proximo-occlusal posterior restorations, where it showed the lowest stress concentration factor.

(3) Rounding the axio-gingival line angle in shoulder geometry experiments reduced the stress concentration factor up to 50 percent.

(4) The gingival area of proximal shoulders was a critical area, extra retentive features (pins or grooves) should not be placed in this area.

(5) Sloping the two axial walls of the proximal portions increased the stress concentration factor in axial wall restorations, and the optimum convergence angle was between 2.5° and 6.5°. Stress concentration factor increased as the convergence angle increased.

(6) The tensile stress at the axio-gingival line angle is small, when the occlusal load is applied on the opposite occluso-axial line angle.

(7) Buccal and lingual cusps, on posterior teeth to be used as abutments in restorative dentistry, should be protected

with occlusal gold, if the cusp length exceeds the breadth measured at the base.

(8) Stress concentration factor computed for flat cuspal reduction was 40 percent less than that for anatomical cuspal reduction, because of the increase in the thickness of the restoration.

(9) There is a definite relationship between the extent of cuspal protection and stress concentration factors, increasing the thickness of occlusal gold decreases the stress concentration factor.

(10) In two-point central occlusal loading of posterior restored teeth, the stresses in the restoration in the region of the central fossa were tensile in nature. Deep developmental grooves in this area should be avoided.

(11) The tensile stress at the central fossa was small in magnitude and could be reduced by decreasing the corresponding cusp angles.

(12) Non-tapered vertical occlusal pins did not alter the stress distribution of posterior restorations, and the residual tooth structure. In comparing long versus short pins, the former had a higher stress concentration factor than the latter.

(13) There are no significant structural differences between the slice restoration, proximal boxes with parallel walls, and proximal boxes with 45°. These three designs showed the same stress concentration factor.

(14) If slice restorations are to be used, more reduction of tooth structure is recommended at the proximo-lingual-occlusal point angles, which would increase the bulk of dental gold at these critical areas (from one to two millimeters). This would minimize the tensile stresses developed at these areas in the restoration.

(15) Dental fixed bridges did not function in bending as a symmetrical beam, but alternate areas of tension and compression were demonstrated when multiple contact loading was used.

(16) The weakest area in posterior fixed bridges is the fixed joint (soldered area), since it exhibited high concentration of tensile and shear stresses.

(17) V-grooves should be avoided, at the fixed joint areas, and they should be replaced by U-grooves. The ratio of the radius of the groove to its depth (r/d) should be as large as possible in order to reduce the tensile and shear stresses at these critical areas.

(18) Bridges with chamfers and flat occlusal protection (2) were structurally stronger than bridges with knife-edged proximal margins and anatomical occlusal protection (1), based on the number of isochromatics at the fixed joint areas.

(19) Comparing bridge (2) with r/d ratio of 0.392 with a modified bridge 2 with V and U notches, stress concentration in the former was about 50 percent less than the latter.

(20) Cantilever dental bridges should not be constructed in the oral cavity.

(21) Other structural design studies using experimental stress analysis methods should follow to investigate more restorative dental problems, such as fracture of clasp arms, the use of threaded pins, and the effect of grooves and locks on the stress concentration factor.

REFERENCES

1. Adams, J. D. "Planning Posterior Bridges." Am. Dent. A. J., 53, 647-654, 1956.

2. Alexander, Nicholas. Photoelasticity. Kingston, R. I., Rhode Island State College, 1936, 76 p. (p. C20).

3. Ante, I. H. "The Fundamental Principles, Design, and Construction of Bridge Prosthesis." Canad. Dent. A. J., 3, 237-248, 1937.

4. Barnett, R. L. "Survey of Optimum Structural Design." Exp. Mech., 6, 19A-26A, 1966.

5. Bartels, J. C. "Full Porcelain Veneer Crowns." J. Prosth. Dent., 7, 533-540, 1954.

6. Baud, R. V. "Fillet Profiles for Constant Stress." Prod. Eng., 5, 133-134, 1934.

7. Beaudreau, D. E. "The Role of the Posterior Fixed Bridge in Occlusion." p. 13-24 (In Miller, C. J. ed., Dent. Clin. No. Am., Symposium on Crown and Bridge Prosthodontics., Philadelphia, Saunders, March 1965, 266 p.).

8. Beke, A. L. "Margins of Safety for Forces on the Human Dentition." J. Prosth. Dent., 18, 261-267, 1967.

9. Benaim, L. "Essai de Mechanique Appliquée a l'Art Dentaire et a l'Implantologie." Rev. Fran. Odonto-Stomat., 14, 1135-1186, 1967.

10. Bowen, R. L. and Rodriguez, M. S. "Tensile Strength and Modulus of Elasticity of Tooth Structure and Several Restorative Materials." Am. Dent. A. J., 64, 378-387, 1962.

11. Brass, G. A. "Common Problems Arising from the New Developments in Operative Dentistry." Canad. Dent. A. J., 30, 297-303, 1964.

12. Brewster, David. "On the Communication of Structure of Doubly Refracting Crystals to Glass, Flour Spar and Other Substances, by Mechanical Compression and Dilatation." Phil. Trans., 156-178, 1816.

13. Brownlee, M. A. Industrial Experimentation. New York, Chemical Publishing Co., 1953, 194 p. (p 86-122).

14. _____. Statistical Theory and Methodology in Science and Engineering. New York, Wiley, 1965, 590 p. (p. 309-327).

15. Brumfield, R. C. Dental Gold Structures. Ann Arbor, Edwards Brothers Inc., 1949, 184 p. (p. 29-72).

16. _____. "Load Capacities of Posterior Dental Bridges." J. Prosth. Dent., 4, 530-547, 1954.

17. _____. "Fundamental Mechanics of Dental Bridges." p. 1118-1196 (In Tylman, S. D., and Tylman, S. G., Theory and Practice of Crown and Bridge Prosthodontics. Saint Louis, Mosby. 1965, 1249 p.).

18. Brunel, A. L., and Lakermance, J. Inlays D'Obturation: Inlays d'Or et Inlays de Porcelaine. Paris, Mason et Cie, 1963, 270 p., (p. 120-129).

19. Buckingham, E. "Model Experiments and the Form of Empirical Equations." Trans. A.S.M.E., 37, p. 263-269, 1915.

20. Burns, B. B. "Pin Retention of Cast Gold Restorations." J. Prosth. Dent. 15, 1101-1108, 1965.

21. Castro, M. E. Photoelasticity Applied in a Compressive Study of Four Types of Cavity Preparations for Primary Molars. Ann Arbor, University of Michigan, School of Dentistry, thesis, 31 p., (p. 26-28), 1952.

22. Chalupnik, J. D. Stress Concentrations in Bolt Threaded Roots. Society for Experimental Stress Analysis, Gen. Meeting, Oct. 1967.

23. Chilton, N. W., and Fertig, J. W. "Studies in the Design and Analysis of Dental Experiments, 1. The Importance of Equal Sample Sizes in Experiments." J. Dent. Res. 39, 53-62, 1960.

24. Chilton, N. W. "Studies in Design and Analysis of Dental Experiments, 2. A Four-Way Analysis of Variance." J. Dent. Res., 39, 344-360, 1960.

25. Clark, A. B. J. "Static and Dynamic Calibration of a Photoelastic Model Material, CR-39." Proc. Soc. Exp. Stress Anal., 14, p. 195-204, 1956.

26. Clayton, J. A. A Study of a Telemetric System for Measuring Vertical and Lateral Occlusal Forces. Ann Arbor, University of Michigan, School of Dentistry, thesis, 65 p., (p. 52-59), 1967.

27. Clutterbuck, M. "The Dependence of Stress Distribution on Elastic Constants." Brit. J. Appl. Phys., 9, p. 323-329, 1958.

28. Cochran, W. G., and Cox, G. M. Experimental Designs. New York, Wiley, 1966, 611 p. (p. 148-234).

29. Coker, E. G., and Filon, L. A Treatise on Photoelasticity. Cambridge, Cambridge Univ. Press, 1931, 720 p. (p. 481-510).

30. Colin, L., Kaufman, E. G., and Paprino, R. "Stress Concentrations in Full Crown Restorations." N. Y. S. Dent. J., 29, 370-373, 1963.

31. Conod, H. "Etude sur la Statique de la Couronne Jaquette." Act. Odontostomat., 14, 193-231, 1951.

32. Coolidge, D. J., Jr. "An Investigation of the Mechanical and Stress-Optical Properties of Columbia Resin, CR-39." Proc. Soc. Exp. Stress Anal., 6, 74-82, 1948.

33. Craig, R. G., and Peyton, F. A. "The Microhardness of Enamel and Dentin." J. Dent. Res., 37, 661-668, 1958.

34. _____. "Elastic and Mechanical Properties of Human Dentin." J. Dent. Res., 37, 710-718, 1958.

35. Craig, R. G., Gehring, P. E., and Peyton, F. A. "Relation of Structure to the Microhardness of Human Dentin." J. Dent. Res., 38, 624-630, 1959.

36. Craig, R. G., Peyton, F. A., and Johnson, D. W. "Compressive Properties of Enamel, Dental Cements, and Gold." J. Dent. Res., 40, 936-945, 1961.

37. Craig, R. G., and Peyton, F. A. "Measurement of Stresses in Fixed Bridge Restorations Using a Brittle-Coating Technique." J. Dent. Res., 44, 756-762, 1965.

38. Craig, R. G., El-Ebrashi, M. K., and Peyton, F. A. Experimental Stress Analysis of Dental Restorations. I. A. D. R. Gen. Meeting, 1967, Abstracts, p. 176.

39. _____. "Two-Dimensional Photoelastic Stress Analysis of Crowns." J. Prosth. Dent., 17, 292-302, 1967.

40. _____. "Two-Dimensional Photoelastic Stress Analysis of Inlays." J. Prosth. Dent., 17, 277-291, 1967.

41. Crandall, S. H., and Dahl, N. C. An Introduction to the Mechanics of Solids. New York, McGraw Hill, 1959, 444 p. (p. 281-305).

42. Crites, N. A., Grover, Horace, and Hunter, A. R. Experimental Stress Analysis by Photoelastic Techniques. Prod. Eng., 33, 57-69, 1962.

43. Dagostino, J., Drucker, D. C., Lin, C. K., and Mylonas, C. "Epoxy Adhesives and Casting Resins as Photoelastic Plastics." Proc. Soc. Exp. Stress Anal., 12, 123-128, 1955.

44. Dally, J. W., and Ahimaz, F. A. "Photographic Method to Sharpen and Double Isochromatic Fringes." Exp. Mech., 2, 170-175, 1962.

45. Dally, J. W., and Riley, W. F. Experimental Stress Analysis. New York, McGraw-Hill, 1965, 520 p. (p. 200-221).

46. Davies, O. L. The Design and Analysis of Industrial Experiments. New York, Haefner Publishing Co., 1963, 636 p. (p. 247-366).

47. Dempster, W. T., and Liddicoat, R. T. "Compact Bone as a Non-Isotropic Material." Amer. J. Anat., 91, 331-339, 1952.

48. Dempster, W. T., and Duddles, R. A. "Tooth Statics: Equilibrium of a Free Body." Am. Dent. A. J., 68, 652-666, 1964.

49. Dixon, W. J., and Massey, F. J., Jr. Introduction to Statistical Analysis. New York, McGraw-Hill, 1957, 488 p. (p. 250-254).

50. Dolan, T. J., and Richards, D. G. "A Photoelastic Study of the Stresses in Wing Ribs." J. Aero. Sci., 7, 340-346, 1940.

51. Dolan, T. J., and Levine, R. E. "A Study of the Stresses in Curved Beams." Proc. 13th Eastern Photoelasticity Center., p. 90-98, June 1941.

52. _____. "Influence of Certain Variables on the Stresses in Gear Teeth." J. Appl. Phys., 12, 584-591, 1941.

53. Drucker, D. C. "Photoelastic Separation of Principal Stresses by Obilque-Incidence." J. Appl. Mech., 10, 156-160, 1943.

54. _____. "The Method of Oblique-Incidence in Photoelasticity." Proc. Soc. Exp. Stress Anal., 8, 51-66, 1950.

55. Duncan, D. B. "Multiple Range and Multiple F Test." Biometrics, 11, 1-42, 1955.

56. Dumont, M. A. "L'Ancrage a Tenons: Principles, Application et Realization." Rev. Fr. Odont., 13, 779-792, 1966.

57. Durelli, A. J., and Murray, W. M. "Stress Distribution Around a Circular Discontinuity in Any Two-Dimensional System of Combined Stress." Proc. 14th Eastern Photoelasticity Confer., 21-36, 1941.

58. Durelli, A. J., Lake, R. L., and Phillips, E. A. "Stress Concentrations Produced by Multiple Semi-Circular Notches in Infinite Plates Under Uniaxial State of Stress." Proc. Soc. Exp. Stress Anal., 10, 53-64, 1952.

59. Durelli, A. J., Phillips, E. A., and Tsao, C. H. Introduction to Theoretical and Experimental Analysis of Stress and Strain. New York, McGraw-Hill, 1958, 498 p. (p. 250-277).

60. Durelli, A. J., Dally, J. W., and Riley, W. F. "Stress and Strength Studies on Turbine Blade Attachments." Proc. Soc. Exp. Stress Anal., 16, 171-182, 1958.

61. Durelli, A. J., and Dally, J. W. "Stress Concentration Factors Under Dynamic Conditions." J. Mech. Eng. Sci., 1, 1-5, 1959.

62. Durelli, A. J., and Murray, W. M. "Stress Distribution Around an Elliptical Discontinuity in Any Two-Dimensional, Uniform, and Axial System of Combined Stress." Proc. Soc. Exp. Stress Anal., 19, 19-29, 1961.

63. Durelli, A. J., and Riley, W. F. Introduction to Photomechanics. Englewood Cliffs, N. J., Prentice Hall, 1965, 402 p. (p. 254-291).

64. Durelli, A. J. Applied Stress Analysis. Englewood Cliffs, N. J., Prentice Hall, 1967, 180 p. (p. 38-51).

65. Durelli, A. J., and Parks, V. J. "Experimental Stress Analysis of Loaded Boundaries in Two-Dimensional Second-Boundary Value Problems." Exp. Mech., 7, 381-385, 1967.

66. Edelman, W. E. Photomechanics of Stress Transfer Mechanisms in Composite Materials. At Society for Experimental Stress Analysis, Annual Meeting, Chicago, 1967.

67. Embrell, K. A. Retentive Qualities of Pin Retained Castings. Ann Arbor, University of Michigan, School of Dentistry, thesis, 38 p., 1965.

68. Ewing, J. E. "Re-evaluation of the Cantilever Principle. J. Prosth. Dent., 7, 78-92, 1957.

69. Faupel, F. H. Engineering Design: A Synthesis of Stress Analysis and Materials Engineering., New York, Wiley, 1964, 980 p., (p. 711-798).

70. Favre, H. "Sur une Nouvelle Methode Optique de Determination des Tensions Interieurs." Revue d'Optique, 8, 193-213, 241-261, 1929.

71. Fisher, R. A. The Design of Experiments. Edinburgh, Oliver and Boyd, 4th ed., 1946, 213 p., p. (9-25).

72. Flanagan, J. H. "Photoelastic Photography." Proc. Soc. Exp. Stress Anal., 15, 1-10, 1958.

73. Flynn, P. D., and Roll, A. A. "A Comparison of Stress Concentration Factors in Hyperbolic and U-Shaped Grooves." Exp. Mech., 7, 272-275, 1967.

74. Foeppel, L., and Moench, E. M. Praktische Spannungsoptik. Berlin, Springer, 1950, 162 p. (p. 114-129).

75. Frocht, M. M. "Factors of Stress Concentration Photoelastically Determined." J. Appl. Mech., 2, 67-77, 1935.

76. _____. "A Rapid Method for the Determination of Principal Stresses Across Sections of Symmetry from Photoelastic Data." J. Appl. Mech., 5, 24-28, 1938.

77. _____. "The Shear-Difference Method." Proc. 13th Eastern Photoelasticity Confer., p. 51-95, June 1941.

78. _____. Photoelasticity. Volume I, New York, Wiley, 1941, 401 p. (p. 129-249).

79. _____. Photoelasticity. Volume II, New York, Wiley, 1948, 505 p. (p. 137-198).

80. Frocht, M. M., and Landberg, D. M. "Factors of Stress Concentration in Bars with Deep Sharp Grooves and Fillets in Tension." Proc. Soc. Exp. Stress Anal., 9, 149-162, 1951.

81. Frocht, M. M., Guernsey, R. L., Jr., and Landberg, D. M. "Photoelasticity - A Precision Instrument of Stress Analysis." Proc. Soc. Exp. Stress Anal., 11, 105-112, 1953.

82. Frocht, M. M., and Pih, Hui. "A New Cementable Material for Two- and Three-Dimensional Photoelastic Research." Proc. Soc. Exp. Stress Anal., 12, 55-64, 1954.

83. Frocht, M. M., and Thomson, R. A. "Experiments in Mechanical and Optical Coincidence in Photoelasticity." Exp. Mech., 1, 43-47, 1961.

84. Fusayama, Takao."Chamfered Preparation of Veneer Three-Quarter Crowns." Shikaitenho (The Nippon Dental Review), 5, 17-22, 1948.

85. Fusayama, Takao, Ide, Kimiko, and Hosoda. Hiroyasu, "Relief of Resistance of Cement of Full Cast Crown." J. Prosth. Dent., 14, 94-106, 1964.

86. Gabel, A. B. The American Textbook of Operative Dentistry, 9th. ed., Philadelphia, Lea and Febiger, 1954, 626 p. (p. 154-214).

87. Granath, L. R. "Photoelastic Model Experiments on Class II Cavity Restorations of Dental Amalgam." Odont. Revy, 16, Supplement 9, p. 1-38, 1965.

88. Guard, W. F., Haack, D. C., and Ireland, R. L. "Photoelastic Stress Analysis of Buccolingual Sections Class II Cavity Restorations." Am. Dent. A. J., 57, 631-635, 1958.

89. Guard, W. F. "Photoelastic Stress Analysis of Buccolingual Sections of Class II Cavity Restorations." Colo. S. Dent. A. J., 42, 31-35, 1964.

90. Guenther, W. C. Analysis of Variance. Englewood Cliffs, Prentice Hall, 1966, 199 p. (p. 99-141).

91. Hampson, E. L. Textbook of Operative Dentistry. London, William Heinmann Medical Books, 1964, 329 p. (p. 101-153).

92. Harmon, C. B. "Pontic Design." J. Prosth. Dent., 8, 496-503, 1958.

93. Haskins, R. C., Haack, D. C., and Ireland, R. L. "A Study of Stress Pattern Variation in Class II Cavity Restorations asaResult of Different Cavity Designs." J. Dent. Res., 33, 757-766, 1954.

94. Havard, D. G. "Photographic Display of Stress Directions in Plane Photoelasticity." Exp. Mech., 7, 407-408, 1967.

95. Hazen, S. P., and Osborne, J. W. "Relationship of Operative Dentistry to Periodontal Health." p. 245-254. (In Ferguson, G. W., ed., Dent. Clin. No. Am., Symposium on Operative Dentistry, Philadelphia, Saunders, March 1967, 276 p.)

96. Hendrick, R. M. A Comparative Study of the Relative Merits of the Box and Slice Types of Cavity Preparations. Ann Arbor, University of Michigan, School of Dentistry, thesis, 31 p. 1938.

97. Herlands, R. E., Lucca, J. L., and Morris, M. L. "Forms, Contours, and Extensions of Full Coverage Restorations in Occlusal Reconstruction." p. 147-162. (In Giordano, J. V., ed., Dent. Clin. No. Am., Symposium on Occlusion., Philadelphia, Saunders, March 1967, 286 p.)

98. Hetenyi, M. "The Distribution of Stress in Threaded Connections." Proc. Soc. Exp. Stress Anal., 1, 147-156, 1943.

99. Hetenyi, M., ed. Handbook of Experimental Stress Analysis. New York, Wiley, 1950. 1077 p. (p. 828-970).

100. Heywood, R. B. "Tensile Fillet Stresses in Loaded Projections." Proc. Inst. Mech. Eng., (London), 159, 384-398, 1948.

101. _____. Designing by Photoelasticity. London, Chapman and Hall, 1952, 414 p. (p. 314-371).

102. Hondo, M., and Miyamoto, H. "Three-Dimensional Photoelasticity of the Rotating Body." Exp. Mech., 6, 559-566, 1966.

103. Howell, A. H., and Manly, R. S. "An Electronic Strain Gage for Measuring Oral Forces." J. Dent. Res., 27, 705-712, 1948.

104. Howland, R. C. J. "Stresses in a Plate Containing an Infinite Row of Holes." Proc. Roy. Soc., 148, 471-477, 1935.

105. Hunter, A. R., and Beiber, R. E. "Stress Concentration Factors for Fatigue Configurations." Exp. Mech., 6, 80-86, 1966.

106. Jeanneret, Max. L'Inlay a Crampons et Ses Applications. Paris, Julien Prelat, 1953, 270 p. (p. 53-73).

107. Jenkins, F. A., and White, H. W. Fundamentals of Optics. 3rd ed., New York, McGraw-Hill, 1957, 637 p., (p. 488-508).

108. Jenkins, G. N. The Physiology of the Mouth. Oxford, Blackwell, 1953, 244 p. (p. 118).

109. Jerrard, H. G. "The Calibration of Quarter-Wave plates." J. Opt. Soc. Am., 42, 159-165, 1952.

110. Jessop, H. T. "The Opticals System in Photoelastic Observations." J. Sci. Instr., 25, 124-126, 1948.

111. _____. "On the Tardy and Senarment Methods of Measuring Relative Retardations." Brit. J. Appl. Phys., 4, 138-141, 1953.

112. Jessop, H. T., and Harris, F. C. Photoelasticity,Principles and Methods. New York, Dover, 1960, 184 p. (p. 89-99).

113. Johnson, E. W. A Three-Dimensional Photoelastic Investigation of Stress Concentrations in Operably Deformed Human Teeth. Edmonton, University of Alberta, School of Engineering, thesis, 89 p., 1965.

114. Johnson, E. W., Wysocki, G. P., and Castaldi, C. R. Three Dimensional Photoelastic Analysis of Stress Concentration in Operatively Prepared Teeth. I.A.D.R. Gen. Meeting, 1966, abstracts, p. 60.

115. Johnston, J. F. "Pontic Form and Bridge Design - A New Survey." Ill. Dent. J., 25, 273-282, 1956.

116. Johnston, J. F., Phillips, R. W., and Dykema, R. W. Modern Practice in Crown and Bridge Prosthodonitcs., Philadelphia, Saunders, 1965, 599 p. (p. 59-73).

117. Jörgensen, Dryer. "The Relationship Between Retention and Convergence Angle in Cemented Veneer Crowns." Acta Odont. Scandinav., 13, 35-40, 1955.

118. Juvinall, R. C. Engineering Considerations of Stress, Strain, and Strength. New York, McGraw-Hill, 1967, 580 p. (p. 467-485).

119. Kanders, R. F. "Simple Technique for Improving the Gingival Bevel of Gold or Acrylic Crowns." N. Y. Univ. J. Dent., 15, 107-108, 1957.

120. Karlstrom, Sam. The Pontostructure Method. Stockholm, A. B. Nordiska Bokhandelns Forlag, 1955, 266 p. (p. 33).

121. Kaufman, E. G., Coelho, D. H., and Colin, Lawrence. "Factors Influencing Retention of Cemented Gold Castings." J. Prosth. Dent., 11, 487-502, 1961.

122. Ketchum, M. S. "Procedures for Recording Data and Calculating Internal Stresses by the Photoelastic Method." Proc. 10th Eastern Photoelasticity Confer., p. 1-66, 1939.

123. Keyes, D. A. "Effect of Cavity and Pattern Design on Structure." Am. Dent. A. J., 30, 1432-1437, 1943.

124. King, R. M. A Method for the Photoelastic Study of Stresses Developed in Dental Structures. Ann Arbor, University of Michigan, School of Dentistry, thesis 71 p., 1953.

125. Klaffenback, A. O. "An Analytical Study of Modern Abutments." Am. Dent. A. J., 23, 2275-2287, 1936.

126. Klotzer, Von W. "Zur Prothesenwiederherstellung. Wege zur Minderung der Bruchanfalligkeit der Kunstoffprothesen." Dent. Zahnarztl. Ztschr., 18, 961-967, 1963.

127. _____. "Spannungsoptische Festigkeitsumter-suchung-enerniger Prothesentypen." Dent. Zahnarztl. Ztschr., 19, 375-384, 1964.

128. _____. "Uber Polarisationsoptische Untersuchungen an Prothesenmodell Korpen." Dent. Zahnarztl Ztschr., 21, 894-901, 1966.

129. Kobayashi, A. S., and Tuppeny, W. H., Jr., ed. Manual on Experimental Stress Analysis. 2nd ed., Westport, Society for Experimental Stress Analysis, 1965, 67 p., (p. 29-44).

130. Koch, W. M., and Szego, L. M. "Use of Double-Exposure Photography in Photoelasticity." J. Appl. Mech., 21, 198-210, 1954.

131. Langhaar, H. L. Dimensional Analysis and Theory of Models. New York, Wiley, 1967, 166 p. (p. 79-97).

132. Leaf, W. F. "The Time-Edge Effect; Its Cause and Prevention." Proc. 15th Semi-Annual Eastern Photoelasticity Confer., p. 20-22, 1942.

133. Ledley, R. S. "A New Method of Determining the Functional Forces Applied to the Prosthetic Appliances and Their Supporting Tissues." J. Prosth. Dent., 5, 546-562, 1955.

134. Lee, G. H. An Introduction to Experimental Stress Analysis. New York, Wiley, 1959, 319 p. (p. 65-85).

135. Lehman, M. L., and Hampson, E. L. "A Study of Strain Patterns in Jacket Crowns on Anterior Teeth Resulting from Different Tooth Preparations." Brit. Dent. J., 113, 337-345, 1962.

136. Lehman, M. L., and Meyer, M. L. "Relationship of Dental Caries and Stress: Concentrations in Teeth as They are Revealed by Photoelastic Tests." J. Dent. Res., 45, 1706-1714, 1966.

137. Lehman, M. L. "Tensile Strength of Human Dentin." J. Dent. Res., 46, 197-201, 1967.

138. _____. "Stability and Durability of Porcelain Jacket Crowns." Brit. Dent. J., 123, 419-426, 1967.

139. Le Huche, Rene. Inlays et Onlays. Paris, Julien Prelat, 1960, 288 p. (p. 12-20).

140. Leven, M. M. "A New Material for Three-Dimensional Photoelasticity." Proc. Soc. Exp. Stress Anal., 6, 19-28 1948.

141. Leven, M. M., and Sampson, R. C. Photoelastic Stress Analysis and Deformation Analysis of Nuclear Reactor Components." Proc. Soc. Exp. Stress Anal., 17, 161-180, 1959.

142. Lewis, R. M., and Owen, M. M. "Mathematical Solution of Problems in Full Crown Construction." Am. Dent. A. J., 59, 943-947, 1959.

143. Li, C. C. Numbers from Experiments. Pittsburg, Boxwood, 1959, 156 p. (p. 74-76).

144. Lipson, Charles, and Juvinall, R. C. Applications of Stress Analysis to Design and Engineering. Ann Arbor, University of Michigan, Engineering Summer Conferences, 1961, 156 p., (p. 35-41).

145. _____. Handbook of Stress and Strength. New York, Macmillian, 1963, 447 p. (p. 27-63).

146. Lorey, R. E., Embrell, K. A., and Myers, G. E., "Retentive Factors in Pin-Retaintd Castings." J. Prosth. Dent., 17, 271-275, 1967.

147. Lucca, J. L. "The Tube Impression Techniques." p. 113-123. (In Trapozzano, V. R., ed., Dent. Clin. No. Am., Symposium on Crown and Bridge Prosthodontics., Philadelphia, Saunders, March 1959, 277 p.).

148. Mahler, D. B., and Peyton, F. A. "Photoelasticity as a Research Technique for Analyzing Stresses in Dental Structures." J. Dent. Res., 34, 831-838, 1955.

149. Mahler, D. B. A Photoelastic Analysis of the Stresses Developed in a Restored Primary Tooth When Subject to Forces of Mastication. Ann Arbor, University of Michigan, Ph.D. Dissertation, 129 p., 1956.

150. Mahler, D. B., and Terkla, L. G. "Analasis of Stress in Dental Structures." p. 789-798. (In Phillips, R. W., ed., Dent. Clin. No. Am., Symposium on Dental Materials., Philadelphia, Saunders, November 1958, p. 545-801).

151. _____. "Relationship of Cavity Design to Restorative Materials." p. 149-157. (In Phillips, R. W., ed., Dent. Clin. No. Am., Symposium on Dental Materials., Philadelphia, Saunders, March 1965, 266 p.).

152. Mann, A. W., Courtade, G. L., and Sanell, Carl. "The Use of Pins in Restorative Dentistry: Part I, Parallel Pin Retention Obtained Without Using Parallel Devices." J. Prosth. Dent., 15, 502-516, 1965.

153. Massa, Hubert, Application de la Photo-elasticite a l'Etude de Problems Relatifs a la Sollicitation de Certains Os et de Certaines Dents., Liege (Belgium), Sciences et Letters S. A., 1957, 151 p. (p. 68-112).

154. Maxwell, J. C. "On the Equilibrium of Elastic Solids. Trans. Roy. Soc., 20, 87-120, 1853.

155. McCloskey, D. F. "Porcelain Jackets Under Stress." J. Dent. Res., 7, 417-423, 1927.

156. McMath, J. F. "The Gingival Groove in Gold Inlay Preparations." Dent. Cosmos, 67, 1162-1164, 1925.

157. Mesnager, A. "Methods of Measuring Internal Stresses In Solids." Budapest Congress of the International Association for Testing Materials. p. 128-190, 1901.

158. Miller, I. F., Belsky, M. W. "The Full Shoulder Preparation for Periodontal Health." p. 83-102. (In Miller, C. J., ed., Dent. Clin. No. Am., Symposium on Crown and Bridge Prosthodontics., Philadelphia, Saunders, March 1965, 266 p.).

159. Mindlin, R. D. "Analysis of Doubly Refracting Materials with Circularly and Elliptically Polarized Light." J. Opt. Soc. Am., 27, 288-291, 1937.

160. _____. "A Review of the Photoelastic Methods of Stress Analysis." J. Appl. Phys., 10, 222-241, 273-294, 1939.

161. Miyauchi, T. "Three-Dimensional Photoelasticity of the Tooth. (Report 2): Static Observations of the Abutment Tooth." Shiawa Gakuho, 59, 306-313, 1959.

162. Moench, E., and Loreck, R. "A Study of the Accuracy and Limits of Application of the Plane Photoelastic Experiments." p. 169-184. (In Proceedings of the First International Symposium of Photoelasticity, Chicago, Illinois, Society for Experimental Stress Analysis. 1961, 293 p.).

163. Morrant, G. A. "Pinlay Preparation as a Bridge Abutment."" Dent. Pract., 2, 328-331, 1952.

164. _____. "Bridges with Particular Relation to the Periodontal Tissues." Dent. Pract., 6, 178-186, 1956.

165. Mumford, J. M., and Storer, Roy. "Modification of the Occlusal Table in Restorative Dentistry." J. Prosth. Dent., 12, 330-338, 1962.

166. Mylonas, C. "The Optical System of Polariscopes." J. Sci. Inst., 25, 77-81, 1948.

167. Natrella, M. G. Experimental Statistics. Washington, D.C., National Bureau of Standards Handbook 91, 1963 (p. 12-1 to 12-21).

168. Neuman, F. E. Die Gesetze der Dopplbrechung des Lichts in Comprimierten Oder Ungleichformig Erwarmten Unkrystallinischen Kopern. Berlin, Abh. d. Kon. Acad. d. Wissenschaftn zu Berlin. 254 p., 1841.

169. Nisida, M., and Saito, H. "Stress Distributions in a Semi-Infinite Plate Due to a Pin, Determined by Interferometric Method." Exp. Mech., 6, 273-279, 1966.

170. Noonan, M. A. "The Use of Photoelasticity in a Study of Cavity Preparations." J. Dent. Child., 16, 24-28, 1949.

171. Oldberg, S., and Lipson, Charles. "Structural Evolution of a Crankshaft." Proc. Soc. Exp. Stress Anal., 2, 118-138, 1944.

172. Peterson, R. E., and Wahl, A. M. "Two and Three Dimensional Cases of Stress Concentration and Comparison with Fatigue Tests." J. Appl. Mech., 3, 324-328, 1936.

173. Peterson, R. E. Stress Concentration Design Factors. New York, Wiley, 1953, 168 p. (p. 1-20).

174. Pettrow, J. N. "Practical Factors in Building and Firing Characteristics of Dental Porcelain." J. Prosth. Dent., 11, 334-344, 1961.

175. Peyton, F. A., Mahler, D. B., and Hershenov, B., "Physical Properties of Dentin." J. Dent. Res., 31, 366-370, 1952.

176. Peyton, F. A., Anthony, D. H., Asgar, Kamal, Charbeneau, G. T., Craig, R. G., and Myers, G. E. Restorative Dental Materials., 2nd ed., Saint Louis, Mosby, 1964, 543 p., (p. 115-148).

177. Pickard, H. M. A Manual of Operative Dentistry. London, Oxford University Press, 1966, 176 p. (p. 130-134).

178. Post, Daniel, "A New Photoelastic Interferometer Suitable for Static and Dynamic Measurements." Proc. Soc. Exp. Stress Anal., 12, 191-202, 1954.

179. _____. "Photoelastic Evaluation of Individual Principal Stresses by Large Field Absolute Retardation Measurements." Proc. Soc. Exp. Stress Anal., 13, 119-132, 1955.

180. Ramfjord, S. P., and Ash, M. M. Occlusion. Philadelphia, Saunders, 1966, 396 p. (p. 92-95).

181. Riley, W. F. "Stresscoat Tunnel Intersections." Proc. Amer Soc. Civil Engr., 90, 167-179, 1964.

182. Roark, R. J. Formulas For Stress and Strain. New York, McGraw-Hill, 1965, 432 p. (p. 382-420).

183. Robinson, A. D. "Photoelastic Recording of Stresses Produced by Expansion of Dental Amalgam." Brit. Dent. J., 117, 145-149, 1964.

184. _____. "Wedging Effect of Dental Restorations." Brit. Dent. J., 121, 16-19, 1966.

185. Rosentiel, E. "The Retention of Inlays and Crowns as a Function of Geometrical Form." Brit. Dent. J., 103, 388-394, 1957.

186. _____. "Marginal Fit of Inlays and Crowns." Brit. Dent. J., 117, 432-442, 1964.

187. Rosner, David. "Function, Placement, and Reproduction of Bevel for Gold Castings." J. Prosth. Dent., 13, 1160-1168, 1963.

188. Roucoules, Leon. Technics de Construction des Elements Inamovibles Classiques en Prothese Dentaire. Paris, Libraire Maloine S. A., 1962, 242, p. (p. 54-63).

189. Rumtesch, Von W., Schreiber, S., and Motsch, A. "Zur Statik der Jacketkrone: Spannungoptische Modellversuche." Schweizerische Mochr. Zahnh., 75, 935-975, 1965.

190. Ryge, Gunnar, Kozak, S. F., and Fairhurst, C. W. "Porosities in Dental Gold Castings." Am. Dent. A. J., 54, 746-754, 1957.

191. Sanell, Carl. Vertical Parallel Pins in Occlusal Rehabilitation. 755-778. (In Courtade, G. L., ed., Dent. Clin. No. Am., Symposium on Occlusal Rehabilitation., Philadelphia, Saunders, November 1963, p. 575-934).

192. Sato, T. "Photoelastic Study of the Traumatic Occlusion as a Cause of Alveolar Pyorrhea." Dainihon Shika Igakuka J., 2, 21-38, 1960.

193. Savin, G. N. Stress Concentration Around Holes. New York, Pergamon, 1961, 310 p. (p. 239-242).

194. Schultz, L. C., Charbeneau, G. T., Doerr, R. E., Comstock, F. W., Kahler, F. W., Jr., Margeson, R. D., Hellman, D. L., and Snyder, D. T. Operative Dentistry. Philadelphia, Lea and Febiger, 1966, 296 p. (p. 147-149).

195. Schwartz, J. R. Inlays and Abutments. New York, Dental Items of Interest, 1956, 478 p. (p. 142-149).

196. Schurcliff, W. A. Polarized Light. Cambridge, Harvard University Press, 1962, 207 p. (p. 157).

197. Shell, J. S., and Hollenback, G. M. "Physical Properties of Dental Gold Castings Closely Approximating Dental Dimensions." South. Calif. S. Dent. A. J., 33, 20-26, 1965.

198. Shell, J. S. Dental Gold and Its Properties. p. 91-106. (In Tocchini, J. J., ed., Restorative Dentistry. New York, McGraw-Hill, 1967, 490 p.).

199. Shimada, Heihachi. "Photoelastic Investigation of Stresses in Composite Models with Notches and Holes." Brit. J. Appl. Phys., 9, 34-37, 1958.

200. Skinner, J. A. "Pinledge Attachments as Aids in Bridge Retention." Dent. Surv., 24, 1577-1580, 1948.

201. Slot, Thomas. "On the Accuracy of Two-Dimensional Photoelastic Experiments in which Uniform Edge Loading is Obtained by the Inflatable-Tubing Technique." Exp. Mech., 7, 189-192, 1967.

202. Smith, G. P. "The Marginal Fit of the Full Cast Shoulderless Crown." J. Prosth. Dent., 7, 231-243, 1957.

203. Smyd, E. S. "Dental Engineering." J. Dent. Res., 27, 649-660, 1948.

204. _____. "Mechanics of the Dental Structures." J. Prosth. Dent., 2, 668-692, 1952.

205. _____. Metal Inlays. p. 372-472. (In Gable, A. B., ed., The American Textbook of Operative Dentistry. London, Henry Kimpton, 1954, 626 p.).

206. Soderberg, C. R. "Factor of Safety and Working Stresses." Trans. A.S.M.E., 52, 206-217, 1930.

207. _____. Working Stresses. p. 438-457. (In Hetenyi, M., ed., Handbook of Experimental Stress Analysis. New York, Wiley, 1950. 1077 p.).

208. Soyer, M. G. "Etude Mecanique des Principaux Ancrages Pour Ponts Fixes." Rev. Franc. Stomat., 5, 1489-1506, 1958.

209. Stanford, J. W., Paffenbarger, G. C., Kumpula, J. W., and Sweeney, W. T. "Determination of Some Compressive Properties of Human Enamel and Dentin." Am. Dent. A. J., 57, 487-495, 1958.

210. Stanford, J. W., Weigel, K. V., Paffenbarger, G. C., and Sweeney, W. T. "Compressive Properties of Hard Tooth Tissues and Some Restorative Materials." Am. Dent. A. J., 60, 746-756, 1960.

211. Steel, R. G. D., and Torrie, J. H. Principles and Procedures of Statistics. New York, McGraw-Hill, 1960, 481 p. (p. 138-149).

212. Tardy, M. H. L. "Methode Pratique d'Examen de Mesure de la Birefringence des Verres d'Optiques." Rev. Optiques, 8, 59-69, 1929.

213. Thom, L. W. "A Discussion of Inlay Preparation and Wax Manipulation." Minneapolis Dist. Dent. J., 35, 3-12, 1951.

214. Timoshenko, S., and Goodier, J. N. Theory of Elasticity. New York, McGraw-Hill, 1951, 506 p. (p. 131-145).

215. Tyldesley, W. R. "The Mechanical Properties of Human Enamel and Dentin." Brit. Dent. J., 106, 269-278, 1959.

216. Tylman, S. D. and Tylman, S. G. Theory and Practice of Crown and Bridge Prosthodontics., 4th ed., Saint Louis, Mosby, 1960, 1063 p. (p. 609-613, 594-608).

217. Tylman, S. D. "Relationship of Structural Design of Dental Bridges to Their Supporting Tissues." Internat. Dent. J., 13, 303-317, 1963.

218. Uhlig, H. "Uber die Kaufraft." Dent. Zahnarztl. Ztschr., 8, 30-38, 1953.

219. Vadovic, Fidrich. "Contribution to the Analysis of Errors in Photoelasticity." Exp. Mech., 5, 413-416, 1965.

220. Vandaele-Dossche, M., and Van Green, R. "La Birefringence Mechanique en Lumiere Ultra-Violette et Ses Applications." Bull. Class. Sci., Acad. Roy. de Belgique, 50, 199-230, 1964.

221. Vicentini, Vittorio. "Stress Concentration Factors for Superposed Notches." Exp. Mech., 7, 117-123, 1967.

222. Wagner, A. W. "Pin Retention for Extensive Posterior Gold Onlays." J. Prosth. Dent., 15, 719-721, 1965.

223. Ward, N. L., and Campbell, V. P. "Design and Construction of Bridges." Dent. Pract., 4, 104-115, 1953.

224. Walton, C. B., and Leven, M. M. "A Preliminary Report of Photoelastic Tests of Strain Patterns within Jacket Crowns." Am. Dent. A. J., 50, 44-48, 1955.

225. Weinberg, L. A. "Force Distribution in Mastication, Clenching, and Bruxism." Dent. Digest, 63, 58-61, 1957.

226. _____. "Axial Inclination and Cuspal Articulation in Relation to Force Distribution." J. Prosth. Dent., 7, 804-813, 1957.

227. Wilson, C. "On the Influence of Surface Loading on the Flexure of Beams." Phil. Mag., 32, 481-494, 1891.

228. Wilson, W. H., and Lang, R. L. Practical Crown and Bridge Prosthodontics. New York, McGraw-Hill, 1962, 254 p. (p. 100-103).

229. Wing, George. "Pontic Design and Construction in Fixed Bridgework." Dent. Pract., 12, 390-391, 1962.

230. Wylie, W. L. "A Comparative Study of Slice and Box Preparations." Am. Dent. A. J., 21, 1391-1400, 1934.

231. Yajima, Tadao. "Photoelastic Tests of the Teeth, Sections of Anterior Teeth." Shikawa Gakuho, 54, 121-130, 1954.